AD_____

AWARD NUMBER: DAMD17-01-1-0806

TITLE: Bone Geometry as a Predictor of Tissue Fragility and Stress Fracture Risk

PRINCIPAL INVESTIGATOR: Karl J. Jepsen, Ph.D.

CONTRACTING ORGANIZATION: Mount Sinai School of Medicine
New York, New York 10029-6574

REPORT DATE: October 2006

TYPE OF REPORT: Final

PREPARED FOR: U.S. Army Medical Research and Materiel Command
Fort Detrick, Maryland 21702-5012

REPORT DOCUMENTATION PAGE

Form Approved
OMB No. 0704-0188

1. REPORT DATE *(DD-MM-YYYY)*	**2. REPORT TYPE**	**3. DATES COVERED** *(From - To)*
01-10-2006	Final	10 Sep 2001 – 10 Sep 2006

4. TITLE AND SUBTITLE

Bone Geometry as a Predictor of Tissue Fragility and Stress Fracture Risk

5a. CONTRACT NUMBER

5b. GRANT NUMBER
DAMD17-01-1-0806

5c. PROGRAM ELEMENT NUMBER

6. AUTHOR(S)

Karl J. Jepsen, Ph.D.

E-Mail: karl.jepsen@mssm.edu

5d. PROJECT NUMBER

5e. TASK NUMBER

5f. WORK UNIT NUMBER

7. PERFORMING ORGANIZATION NAME(S) AND ADDRESS(ES)

Mount Sinai School of Medicine
New York, New York 10029-6574

8. PERFORMING ORGANIZATION REPORT NUMBER

9. SPONSORING / MONITORING AGENCY NAME(S) AND ADDRESS(ES)
U.S. Army Medical Research and Materiel Command
Fort Detrick, Maryland 21702-5012

10. SPONSOR/MONITOR'S ACRONYM(S)

11. SPONSOR/MONITOR'S REPORT NUMBER(S)

12. DISTRIBUTION / AVAILABILITY STATEMENT
Approved for Public Release; Distribution Unlimited

13. SUPPLEMENTARY NOTES

14. ABSTRACT

Having a narrow tibia relative to body mass has been shown to be a major predictor of stress fracture risk and fragility. The reason for this phenomenon is not understood. Based on studies of genetically distinct inbred mouse strains, we found a reciprocal relationship between bone mass and bone quality, such that slender bones are associated with more damageable bone tissue. We postulate that a similar reciprocal relationship between bone mass and bone material properties exists in the human skeleton. The intriguing possibility that slender bones, like those we have demonstrated in animal models, may be composed of more damageable material than larger bones has not been considered. To test this hypothesis, we determined whether whole bone geometry is a predictor of tissue fragility in the tibia from young male donors. Tissue damageability was assessed from biomechanical testing of compact bone samples and correlated with measures of bone slenderness. Specimens were subjected to detailed analyses of bone microstructure, composition, and microdamage content. In the second set of experiments, these analyses were repeated for female donors to test for gender differences in tissue fragility. Further, we tested whether ultrasound measurements were sensitive enough to detect the presence of damage and could thus be used for early diagnosis of stress fractures.

15. SUBJECT TERMS
Stress fracture, Bone Mass, Bone Quality, Biomechanics, Damage, Fatigue, Ultrasound. Non-Invasive measures. Genetic background

16. SECURITY CLASSIFICATION OF:			**17. LIMITATION OF ABSTRACT**	**18. NUMBER OF PAGES**	**19a. NAME OF RESPONSIBLE PERSON**
a. REPORT	**b. ABSTRACT**	**c. THIS PAGE**			USAMRMC
U	U	U	UU	76	**19b. TELEPHONE NUMBER** *(include area code)*

Table of Contents

INTRODUCTION

Having a narrow tibia relative to body mass has been shown to be a major predictor of stress fracture risk and fragility (Giladi et al, 1987; Milgrom et al, 1989; Beck et al, 1996). The reason for this phenomenon is not fully understood. Based on studies of genetically distinct inbred mouse strains, we found a reciprocal relationship between femoral bone size (mid-diaphyseal cortical area) and tissue-level mechanical properties (bone quality). Specifically, we found that slender bones (small width to length ratio) were associated with more damageable bone tissue (Jepsen et al, 2001). *We postulate that a similar reciprocal relationship between bone size and bone material properties exists in the human skeleton. The intriguing possibility that slender bones, like those we have demonstrated in animal models, may be composed of more damageable material than larger bones has not been considered.* To test this hypothesis, we determined whether whole bone geometry is a predictor of tissue fragility in the tibiae from young male donors. Tissue damageability was assessed from biomechanical testing of compact bone samples and correlated with measures of bone size and slenderness. Specimens were subjected to detailed analyses of bone microstructure, composition, and microdamage content. In the second set of experiments, these analyses were repeated for female donors to test for gender differences in tissue fragility.

BODY

Major Outcome: Summary

All primary objectives of this grant have been successfully completed. We found that not all bones are constructed in the same manner. Bones that are more slender are comprised of material that is more damageable compared to bones that are more robust. The increased damageability appears to be a result of an increase in ash content. These results were consistent for both males and females. Thus, young adult males and females with small cross-sectional area relative to bone length show a coupled increase in tissue-level mineralization apparently in an attempt to increase tissue-stiffness and to compensate for the small bone geometry in order to achieve an adequate whole bone stiffness. The results of this study are entirely consistent with our investigations of the mouse skeleton.

Tissue-level mechanical properties, including measures of fragility and damageability, were assessed for cortical bone samples that were machined from the diaphyses of young, adult male and female tibiae. The data indicated that the tibial diaphyses of females and males were composed of material having similar tissue-level mechanical properties, and that the mechanical properties degraded with age at similar rates over the age range of 17-46 years. Further, females and males showed a similar relationship between tissue-level mechanical properties and cross-sectional morphology. These data suggested that the genetic {Iscan, 1984 #491; Turner, 1990 #492; Wiren, 2004 #284} and environmental {Gordon, 1994 #490} factors contributing to sex-specific growth patterns affected adult tibial cross-sectional size and shape, but did not affect bone matrix construction, mineralization, and organization in a way that significantly affected tissue-level mechanical properties. This analysis included mechanical properties like stiffness, which is important for day-to-day activities, as well strength, ductility, toughness, and damageability, which provide insight into the amount of damage accumulated during intense physical activity and the fracture resistance during an extreme load condition such as a fall.

Implications for Stress Fracture Risk in Military Recruits

The results of this study provide new insight into why bone size is a risk factor for stress fractures. Stress fractures are believed to be a consequence of excess damage accumulation following intense, repetitive activities. Biological processes that attempt to repair the damage may further weaken the tissue because the increased resorption results in increased tissue porosity (Schaffler and Burr, 1988). However, the actual contribution of biological repair processes to stress fracture risk remains unclear (Milgrom et al, 2004). Damage, in the form of microcracks, is the expected sequelae of repetitive

loading following normal, daily activities (Schaffler et al, 1990). Intense loading conditions, such as those associated with military training and long distance running, are expected to further increase in situ damage accumulation and degrade tissue-level mechanical properties (Mori et al, 1993). Therefore, under extreme loading conditions (e.g., military training), variation in bone quality, specifically tissue damageability, may be a contributing factor to the increased risk of stress fracture for individuals with more slender bones. The current data suggested that bone morphology could be used as a predictor of tissue fragility and stress fracture risk in the absence of available non-invasive imaging techniques that accurately measure bone damageability.

The results of this study provided additional insight into why female military recruits show a greater incidence of stress fractures compared to male military recruits (Friedl et al, 1992; Beck et al 1996). The undersized morphology of female tibiae combined with having similar tissue-level mechanical properties as males suggested that female tibiae may be overloaded during training compared to males. This overloading during intensive training would be expected to lead to increased tissue-stresses and strains, and subsequently increased *in situ* damage accumulation and greater risk of developing a stress fracture (Johnson et al, 1963; Burr et al, 1990; Martin et al, 1995). Taken together, these results suggested that one factor contributing to the discrepancy in stress fracture risk between females and males may be differences in the way bone size adapts to body size after longitudinal growth has ceased. Thus, fracture risk reduction would benefit from having a better understanding of the factors that promote or inhibit bone adaptation in the young adult skeleton (Lanyon et al, 2001; Milgrom et al, 2000; Warden et al, 2005).

Major Outcomes: Details

Sample Population

We successfully acquired tibiae from 14 young-adult female and 17 young-adult male donors. The major exclusion criteria for acceptance of tibia into our study was that the donors could have no medical history (disease, pharmaceutical use) that would have a major bone-effect. As shown in the Table 1, female donors were shorter than males (163 $\pm$ 6 cm vs. 178 $\pm$ 4cm; $p<0.0001$), but were not different in body weight (74 $\pm$ 21cm vs. 84 $\pm$ 25cm; $p<0.2$).

Table 1. Description of donor population

Trait	Females	Males
Number of samples	14	17
Average age	36.9 $\pm$ 8.1	32.9 $\pm$ 10.4
Age range	22 - 46	17 - 46
Weight (kg)	73.7 $\pm$ 21.1	83.8 $\pm$ 25.1
Height (cm)	163.5 $\pm$ 5.9	177.7 $\pm$ 4.3
BMI (kg/m^2)	27.4 $\pm$ 7.2	26.6 $\pm$ 8.0
Tibia Length (cm)	33.9 $\pm$ 2.8	38.1 $\pm$ 1.9

Monotonic properties

Tissue-level mechanical properties were assessed by loading four cortical bone samples from each tibia to failure in 4-point bending at 0.05mm/s (Fig. 2A) using a servohydraulic materials testing system (Instron model 8872, Instron Corp., Canton, MA, USA). Specimens were submerged in a PBS solution with added calcium (Gustafson et al, 1996) and maintained at 37°C throughout all tests. Load and deflection were converted to stress and strain using the following equations which take yielding into consideration (Nadai, 1950):

$$\sigma = 2[2M + \phi dM/d\phi]/bh^2 \quad (1)$$

$$\varepsilon = h\phi/2a = \tfrac{1}{2}\, h\Delta[(L - a)/(2a^3/3 - a^2L + L^3/3)] \quad (2)$$

where σ and ε are the stress and strain at the outer surface of the beam, M = applied moment, b = specimen width, h = specimen height, a = ½ the span between the upper two load points = 9mm, L = ½ the span between the two lower load points = 21mm, and ϕ = angle of inclination = a/ρ. The angle of inclination was written in terms of the measured deflection (Δ) by estimating the curvature (ρ) using standard beam equations. Mechanical properties were calculated from the stress-strain curves and these included modulus, strength, total energy, and post-yield strain. Modulus was calculated from a linear regression of the initial portion of the stress-strain curve. Yield was determined using the 0.2% offset method. Post-yield strain was defined as the strain at failure minus the strain at yield. All properties were averaged over the four samples tested for each tibia.

Females and males showed similar regressions for tissue modulus, strength, post-yield strain, and energy-to-failure versus age (Figure 1). No differences in the average tissue-level mechanical properties were observed between females and males (Table 2), even when corrected for differences in donor age. This included measures of stiffness (modulus), strength, ductility (failure strain, post-yield strain), and toughness (energy-to-failure). Thus, females and males show similar tissue-level monotonic properties.

Our data confirm that males and females achieve similar adult tissue-level mechanical properties, which has only been assumed in prior analyses (Ruff, 2000). Prior studies reported property values for this age-range, but did not directly compare data for males and females (Currey and Butler, 1975; Currey, 1979). The mechanical properties measured from the 4-point bending tests in this study were consistent with the mechanical properties of cortical bone measured previously in tension (Reilly and Burstein, 1975; Burstein et al, 1976; McCalden et al, 1993), which was expected given that failure in our bending tests occurred following fracture initiated within the tensile region. Further, the bending formula that was used to convert load and deflection to stress and strain, because it accounted for nonlinear effects (Nadai, 1950), provided a more appropriate estimate of bending strength compared to standard beam theory (Burstein et al, 1972). Because the bone samples used in this study were machined from within the middle of the cortex, the tissue that was added to the subperiosteal or subendosteal surfaces during and after puberty was likely not tested in our study. Thus, the current data could not be used to determine if sex-specific differences in tissue-quality exist following puberty. This data thus reflects the tissue properties established early in life, plus the modifications to these properties associated with osteonal-remodeling and cortical drift (Enlow, 1963) during the ensuing years.

The similarity in tissue-level mechanical properties for adult men and women may be explained based on early transverse bone-growth patterns. During pre-pubertal growth, the periosteal and endosteal surfaces of female and male long bone diaphyses follow nearly identical expansion rates (Garn, 1970). Despite the dimorphic transverse bone-growth patterns arising during puberty (Garn, 1970), the long bones of both sexes appear to be constructed in a way so that by 20 years of age bone size is properly adapted to satisfy loading demands associated with body weight (Sumner and Andriacchi, 1996; Moro et al, 1996; Ruff, 2003; Forwood et al, 2004). Whole bone stiffness and peak tissue strains are thus kept at proper levels (Frost, 1987) during growth simply by depositing enough tissue on the periosteal and endosteal surfaces to keep pace with weight gain. Thus, because there is no discrepancy in the relationship between bone size and body size during growth, males and females can construct the tibia with similar tissue-level mechanical properties without a loss in mechanical function.

Figure 1. Females show an age-related change in tissue-level a) modulus, b) strength, c) energy-to-failure, and d) damageability that is similar to males.

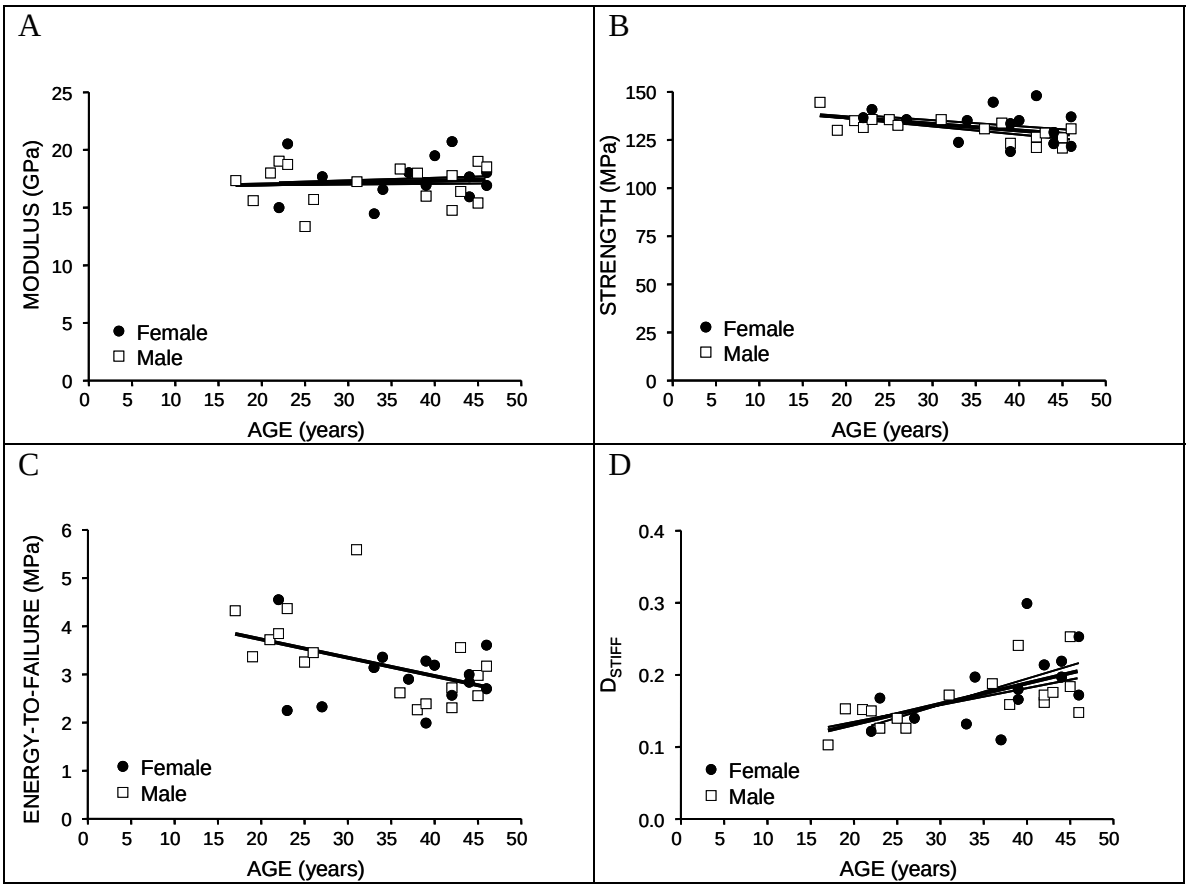

Table 2. Monotonic mechanical properties for young-adult females and males.

MECHANICAL PROPERTY	FEMALE	MALE	p-value
Modulus, GPa	17.5 ± 1.8	17.1 ± 1.7	0.5
Yield Strain	0.008 ± 0.0004	0.008 ± 0.0003	0.7
Yield Stress, MPa	106.2 ± 10.0	104.4 ± 7.8	0.6
Post-yield Strain	0.023 ± 0.006	0.025 ± 0.005	0.3
Failure Strain	0.031 ± 0.006	0.033 ± 0.005	0.3
Strength, MPa	133.8 ± 8.4	130.1 ± 4.2	0.2
Energy-to-Failure, MPa	3.1 ± 0.7	3.2 ± 0.7	0.3

Data was age-adjusted and shown as mean ± standard deviation.

Tissue-Level Damageability

Tissue damageability was assessed using a protocol designed to induce and accumulate cracks in cortical bone specimens. The accumulation of damage leads to measurable degradation of mechanical

properties (Lemaitre, 1992). Therefore, the degradation of mechanical properties can be used as an index of matrix damage. Four cortical bone samples from each tibia were subjected to a fifteen cycle damage accumulation protocol (Figure 2A) similar to that described previously (Jepsen and Davy, 1997). For this protocol, "diagnostic" cycles (1, 3, 5, 7, 9, 11, 13, and 15) were interposed between "damage" cycles (2, 4, 6, 8, 10, 12, and 14). For the diagnostic cycles, the specimens were loaded in four-point bending at 0.5mm/s to 50% of the average displacement at yield (determined from the monotonic tests), held for 60 seconds, and then unloaded at 0.5mm/s. Preliminary studies indicated that this load level provided information on tissue-level mechanical properties without inducing additional damage. For the damage cycles, the specimens were loaded at 0.5mm/s to 50, 75, 100, 125, 150, 175, and 200% of displacement at yield respectively, held for 60 seconds, and then unloaded at 0.5mm/sec. A 5-minute recovery period followed each damage cycle. Displacement at yield was used as a reference in the damage cycles because this parameter showed little variation among the test samples when subjected to monotonic four-point bending. The displacement at yield was 1.0mm for the samples with a height of 2.5mm and 1.07mm for the samples with a height of 2.2mm.

A mechanical measure of the amount of damage that accumulated within the test sample was quantified from the magnitude of stiffness degradation. For each diagnostic cycle, stiffness was calculated from a linear regression of the initial portion of the load-deformation curve. Specimen stiffness decreased non-uniformly with each cycle revealing increasing amounts of damage induced within each cycle and an overall damage accumulation by the end of the protocol (Figure 2B). At the end of the test sequence, the overall damage parameter, D, was calculated by comparing the stiffness of the first and last diagnostic tests such that:

$$D = 1 - S_{15}/S_0, \tag{3}$$

where S_{15} is the stiffness of the last diagnostic cycle and S_0 is the average stiffness of the first two diagnostic cycles (S_1, S_3) and the first damage cycle (S_2).

No differences in either total stiffness degradation or the total change in relaxation (Table 3) were observed between females and males. Further, the changes in stiffness and relaxation after each damage cycle were similar for females and males (Figure 3). These results indicated that the loading protocol introduced similar amounts of damage at each load step for females and males.

Table 3. Comparison of total damage accumulation parameters for female and male cortical bone.

DAMAGE PARAMETER	FEMALE	MALE	p-value
Stiffness Degradation	0.18 $\pm$ 0.04	0.17 $\pm$ 0.03	0.6
Relaxation Degradation	1.89 $\pm$ 0.08	1.91 $\pm$ 0.12	0.6

Data was age-adjusted and shown as mean $\pm$ standard deviation.

Figure 2. A) A fifteen-cycle loading protocol was used to induce damage within machined cortical bone specimens and to measure resultant stiffness degradation. Damage was induced during cycles 2, 4, 6, 8, 10, 12, and 14 by conducting relaxation tests at increasing levels of applied displacement (expressed below as a percentage of the displacement at yield). Diagnostic cycles were interposed between damaging cycles. Each damage cycle was preceded by a diagnostic cycle at 50% of displacement at yield. A 5-minute recovery period was introduced following the damage cycles to relieve residual internal stresses. B) The change in stiffness calculated between sequential diagnostic tests was plotted versus cycle number for the damage tests. The dashed curve represents a specimen showing little stiffness degradation (i.e., little damage accumulation). The solid line represents a specimen showing large stiffness degradation (i.e., more damage accumulation).

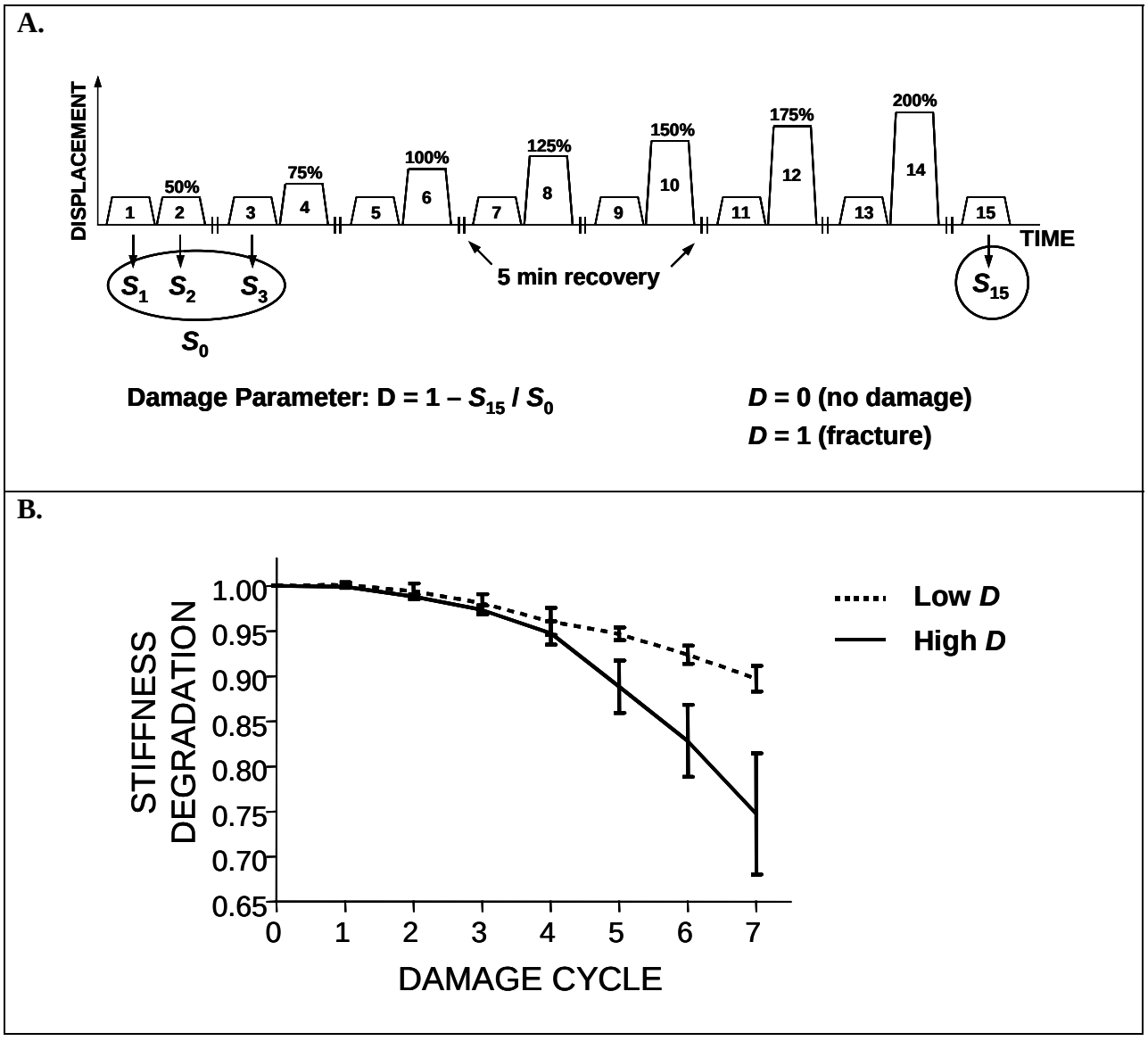

Figure 3. A plot of a) stiffness degradation, D_{STIFF}, and b) relaxation degradation, D_{RELAX}, for each cycle in the damage-accumulation protocol. Females and males show similar curves. Data was not age-corrected.

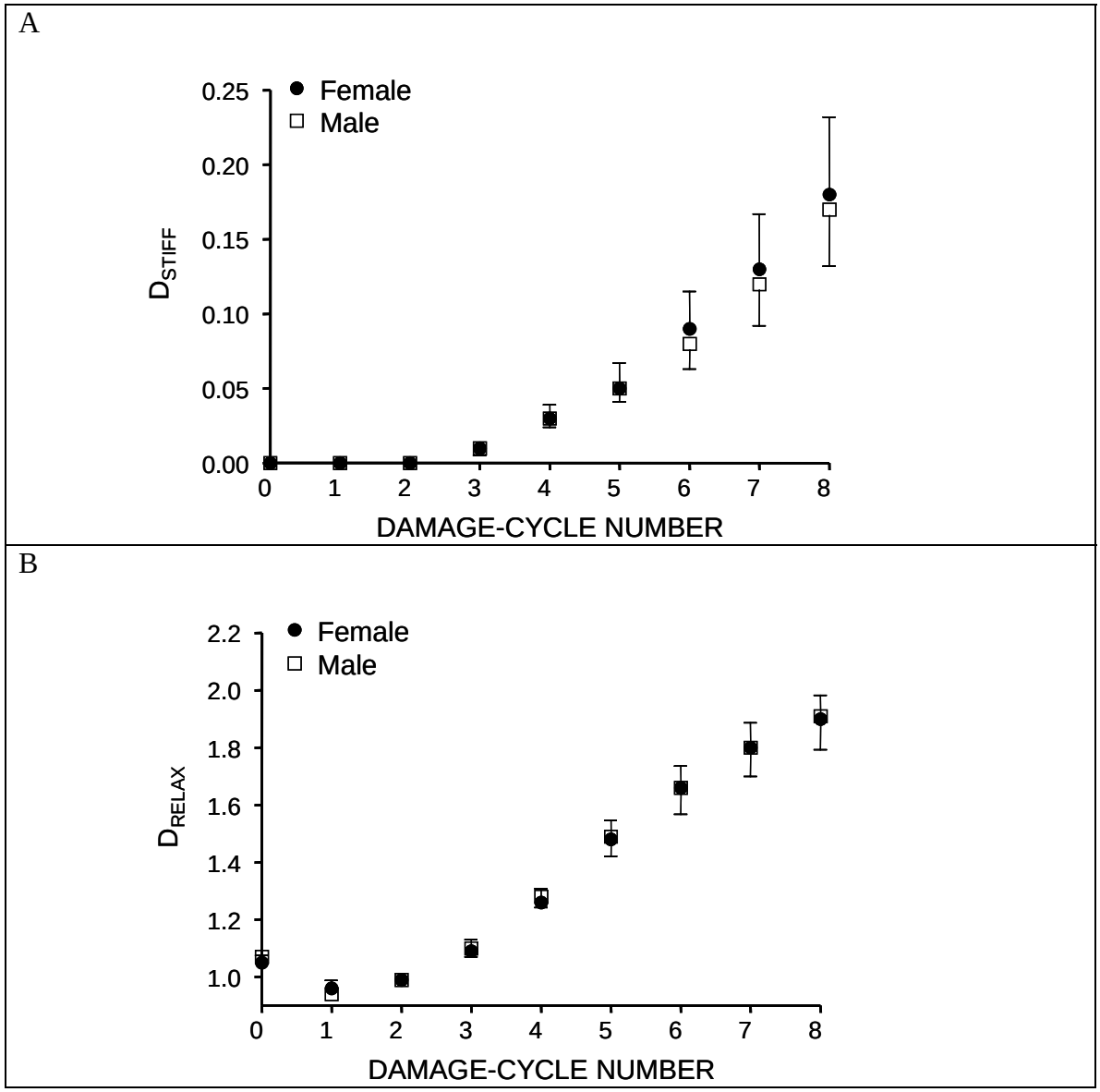

The Relationship Between Morphology and Tissue-level Mechanical Properties

Tibia length (L) was measured as the average distance between the middle of the talar trochlear facet and the medial and lateral proximal condyles (Ruff, 2000) using a large-capacity slide caliper with an accuracy of ±2.5mm (Mantex Precision, Haglöf Inc., Madison, MS, USA). Tibia widths in the antero-posterior ($Width_{AP}$) and medial-lateral ($Width_{ML}$) directions were measured using a 300mm vernier caliper with an accuracy of ±0.02mm (Fowler Company Inc., Newton, MA, USA). Measures were taken at 10% intervals from 30% to 70% of the total tibia length and averaged in order to assess the diaphyseal morphological traits (Miller and Purkey, 1980).

Cross-sectional morphological traits were quantified from 3-mm thick mid-diaphyseal cross-sections cut at 30, 50, and 70% of the total tibia length using a diamond coated metallurgical saw (Model 660, South Bay Technology Inc., San Clemente, CA, USA). Each cross-section was digitally imaged (0.024mm/pixel) and analyzed using IMAQ Vision Builder (version 6.0, National Instruments Corp., Austin, TX, USA). Morphological traits included cortical area (CtAr), the moments of inertia about the antero-posterior (I_{AP}) and medial-lateral (I_{ML}) axes, the polar moment of inertia ($J = I_{AP} + I_{ML}$), and the section modulus in the AP ($J/Width_{AP}/2$) and ML ($J/Width_{ML}/2$) directions. Moment of inertia and section modulus were assessed because these geometric measures are related to the bending and torsional stiffness of intact tibiae. A slenderness index (S) was calculated as the ratio of the AP and ML section modulus values, respectively, to tibia length and body weight:

$$S_{AP} = \frac{(L * BW)}{(J/(Width_{AP}/2))} \quad (4)$$

$$S_{ML} = \frac{(L * BW)}{(J/(Width_{ML}/2))} \quad (5)$$

where L = tibia length (mm) and BW = body weight (kg). For semantic reasons, the formulae are the inverse to that used previously (Selker and Carter, 1989), such that an increase in S_{AP} or S_{ML} indicates a more slender (gracile) bone. All morphological traits were averaged over the three cross-sections for each tibia.

None of the morphological traits showed a significant correlation with age for either males or females (data not shown). Adult females achieved a different bone size and shape compared to males: female tibiae were smaller (J, CtAr, Width), more slender (S_{AP}, S_{ML}, J/L), and showed a smaller J:A ratio compared to males (Table 4). Females and males showed similar slopes for the regression of $J/Width_{AP}$ versus body weight * tibial length ($p<0.17$, ANCOVA). However, females showed a significantly smaller intercept compared to males ($p<0.0001$, ANCOVA), indicating that female tibiae were not as well adapted to body weight (i.e., less robust) compared to males (Figure 4). Similar results were observed when using $J/Width_{ML}$.

The tissue-level mechanical properties were regressed against bone morphological traits and no significant differences in slopes were found for females and males. A correlation analysis (Table 5), which was conducted using the combined female and male data sets, showed that tissue-level modulus decreased with increasing bone section modulus ($J/Width_{AP}$, $J/Width_{ML}$), post-yield strain increased with increasing bone width ($Width_{AP}$), and tissue-damage (D_{stiff}) increased with increasing tibial slenderness (S_{AP}, S_{ML}). The significant regressions are shown in Figure 5. The amount of overlap between the female and male datasets depended on whether the bone morphology traits were adjusted for body size. For unadjusted traits like width and J/width, the female data simply extended the relationships observed for the males (Figures 5A, 5B). For the regression involving bone slenderness, which is adjusted for body weight and tibial length, the female data overlapped substantially with the male data (Figure 5C).

Although each of the tissue-level mechanical properties that we measured showed a small coefficient of variation for both sexes, approximately 20% of this variation was explained by the size of the tibia.

Female tibiae extended the correlations that were observed previously for males (Tommasini et al, 2005), and indicated that individuals with smaller cross-sectional size (i.e., more slender bones) showed a larger tissue-level stiffness. This relationship may be indicative of an inherent adaptive response of bone to modify tissue-level mechanical properties in order to compensate for the smaller size (Ferretti et al, 1993). This coupling suggested that osteoblasts and osteoclasts are capable of coordinately adapting bone morphology and tissue-level mechanical properties so that the combination of these traits satisfies mechanical demands. A more dramatic coordinated relationship among morphological traits, tissue-quality, and mechanical function has been observed previously across a large range of bones from many species (Currey, 1979) and for inbred mice (Jepsen et al, 2001; Tommasini et al, 2005; Price et al, 2005), bats (Swartz et al, 1992), gulls (Carrier and Leon, 1990), and polar bears (Brear et al, 1990). Although this coupling appears advantageous for ensuring that an adequate whole bone stiffness is achieved for day-to-day activity, the disadvantage is that the tissue-quality factors that tend to make bone stiff also tend to make bone less ductile, less tough, and more damageable (Currey, 1984). These latter tissue-quality factors are important during extreme loading conditions (Turner, 2002).

The relationship between bone size (section modulus) and body size (body weight * tibia length) was established previously by Ruff (Ruff, 2000) and was based on the resistance of bone to bending loads. The divergence between males and females suggested that the adaptive factors that match bone size to body size during growth (Sumner and Andriacchi, 1996; Moro et al, 1996; Ruff, 2003; Forwood et al, 2004) no longer work the same way when men and women reach adulthood. This latent difference in bone adaptation may be due to differences in post-pubescent endocrine factors that regulate the relative amounts of bone added to the periosteum versus the endosteum (Duan et al, 2003). Our data, and those of others (Geusens et al, 1991; Looker et al, 2001; Duan et al, 2003; Nieves et al, 2005), indicated that the relationship between bone size and body size diverges for females and males after 20 years of age (Figure 4), such that female long bones become progressively undersized relative to body size. Thus, adult females would be expected to accumulate more damage under intense loading compared to males and this may be a contributing factor to the larger stress fracture incidence for female military recruits (Friedl et al, 1992; Beck et al, 1996).

Table 4. Diaphyseal cross-sectional morphology for female and male tibiae.

MORPHOLOGICAL TRAIT	FEMALE	MALE	p-value
TIBIA LENGTH, mm	33.9 $\pm$ 2.8	38.1 $\pm$ 1.9	0.0001
$WIDTH_{AP}$, mm	26.5 $\pm$ 2.7	31.2 $\pm$ 2.5	0.0001
$WIDTH_{ML}$, mm	20.8 $\pm$ 2.4	24.3 $\pm$ 2.3	0.0001
CtAr, mm^2	249 $\pm$ 40	356 $\pm$ 55	0.0001
J, mm^4	24776 $\pm$ 7917	51640 $\pm$ 15886	0.0001
J / r_{AP}, m^3	1836 $\pm$ 473	3279 $\pm$ 819	0.0001
J / r_{ML}, m^3	2352 $\pm$ 613	4188 $\pm$ 907	0.0001
J / L, m^3	722 $\pm$ 194	1352 $\pm$ 405	0.0001
J / A, m^2	97.1 $\pm$ 18.5	142.7 $\pm$ 24.9	0.0001
S_{AP}, $1/mm^2/kg$	14.1 $\pm$ 4.1	9.9 $\pm$ 2.0	0.002
S_{ML}, $1/mm^2/kg$	11.1 $\pm$ 3.6	7.7 $\pm$ 1.5	0.004

Data was calculated over 30-70% of the total tibial length and shown as mean $\pm$ standard deviation.

Table 5. Correlation matrix between morphological traits and tissue-level mechanical properties.

	MODULUS	STRENGTH	PY STRAIN	ENERGY	DAMAGE
$WIDTH_{AP}$	-0.13 (0.5)	-0.15 (0.4)	**0.35** **(0.05)**	0.34 (0.06)	-0.12 (0.5)
$WIDTH_{ML}$	-0.13 (0.5)	-0.17 (0.4)	0.29 (0.12)	0.28 (0.13)	-0.03 (0.8)
CtAr	-0.25 (0.2)	-0.18 (0.3)	0.31 (0.09)	0.30 (0.1)	-0.24 (0.2)
J	-0.33 (0.07)	-0.25 (0.2)	0.27 (0.14)	0.24 (0.2)	-0.24 (0.2)
J / L	**-0.35** **(0.05)**	-0.26 (0.2)	0.26 (0.2)	0.22 (0.2)	-0.26 (0.2)
J / $Width_{AP}$	**-0.36** **(0.04)**	-0.25 (0.2)	0.22 (0.2)	0.18 (0.3)	-0.27 (0.1)
J / $Width_{ML}$	**-0.36** **(0.05)**	-0.26 (0.2)	0.24 (0.2)	0.20 (0.3)	-0.30 (0.1)
S_{AP}	0.25 (0.2)	-0.05 (0.8)	-0.10 (0.6)	-0.09 (0.7)	**0.43** **(0.02)**
S_{ML}	0.27 (0.1)	-0.04 (0.8)	-0.13 (0.56)	-0.11 (0.6)	**0.44** **(0.01)**

Combined male and female data sets.
First row = Pearson correlation coefficient. Second row = p-value.
Damage = stiffness degradation.

Figure 4. Variation in the section modulus (Polar moment of inertia, J / $Width_{AP}$) versus body size (body weight * tibial length) for adult female and male tibiae.

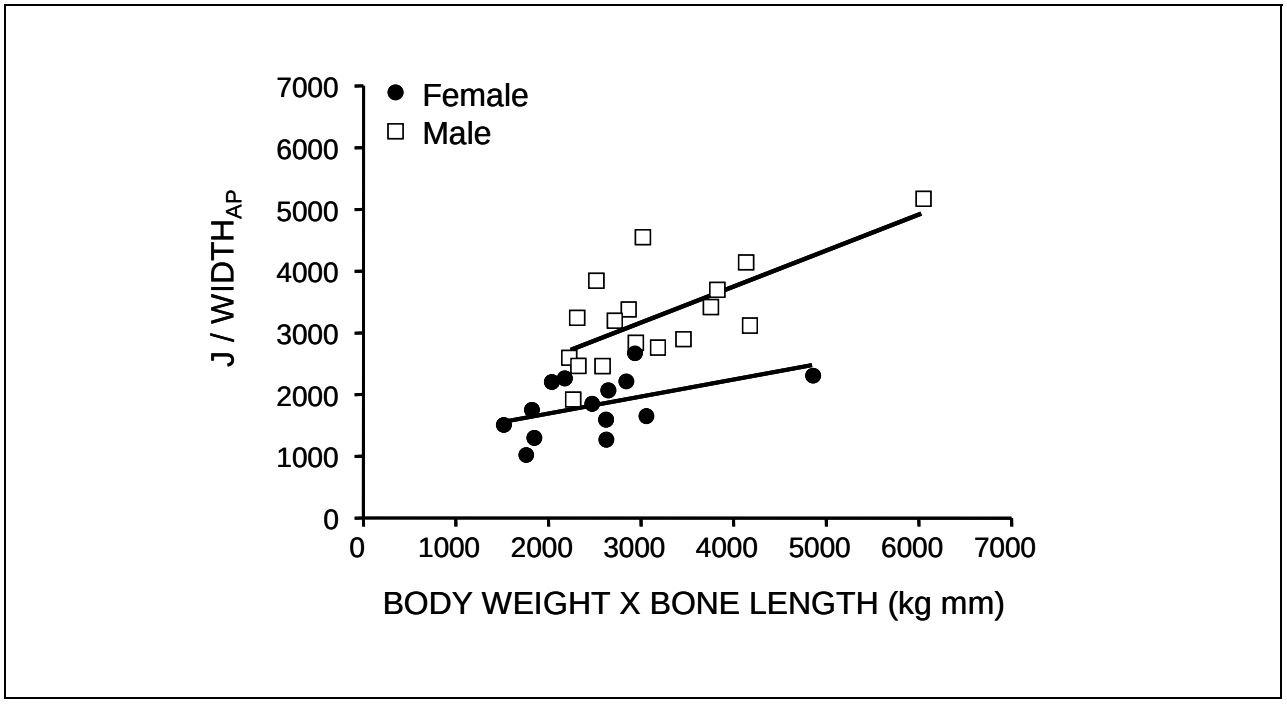

Figure 5. Variation in mechanical properties as a function of diaphyseal cross-sectional morphology. Solid lines represent the regression for the combined female and male datasets. Dashed lines represent the regressions for males and females separately.

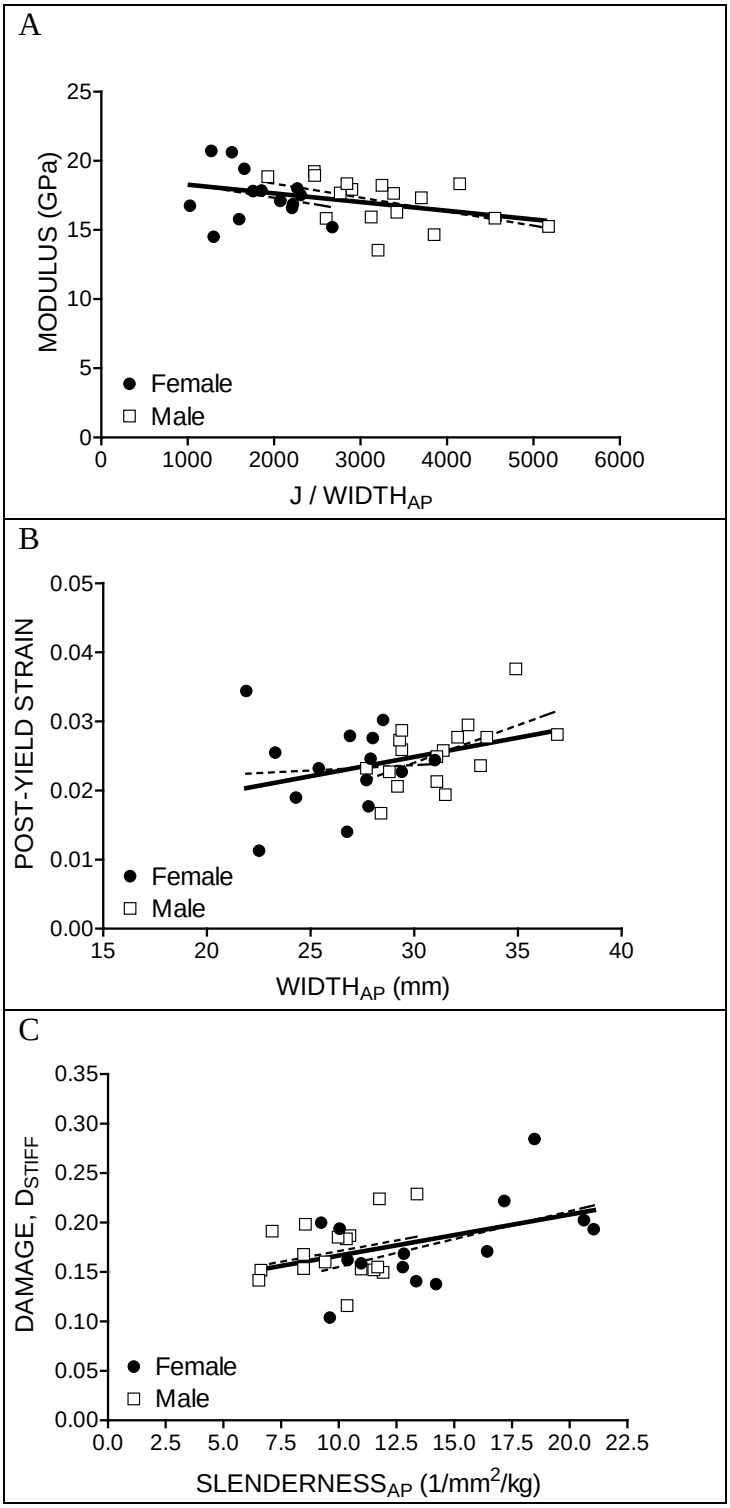

The Relationship Among Morphological, Tissue-level Mechanical Properties, Tissue Composition, and Matrix Architecture

The density, ash content, and water content were determined for each sample retrieved from the monotonic tests. Specimen volume was determined using Archimedes' principal. Submerged weight, hydrated weight, dry weight, and ash weights were measured. To test for variation in matrix organization in males and females, bone microstructure was assessed for each sample retrieved from the damageability tests. For each specimen, digital images of three transverse sections, 100μm in thickness, were taken at 10X, stitched together, and traced using a Tablet monitor (WACOM). Parameters measured include porosity and the area fractions of osteonal, interstitial (remodeled), and circumferential lamellar (unremodeled) tissues. Both vascular canals and resorption spaces were counted as pores. Osteonal tissue was defined as a lamellar region with a Haversian canal completely surrounded by a cement line. Data from individual test samples were averaged for each donor.

To determine if males and females show a similar relationship between tibia cross-sectional morphology, bone microstructure, and tissue-level mechanical properties, linear regressions were performed while taking age into consideration and slopes and intercepts between male and female regressions were compared (ANCOVA).

Since no differences were found between male and female regressions, combined male and female datasets were used to compare tissue-level mechanical properties, cross-sectional morphology, composition, and bone microstructure. The only significant correlations between compositional or architectural traits and tissue-level mechanical properties were observed between ash content and tissue modulus ($p < 0.003$), strength ($p < 0.02$), and post-yield strain ($p < 0.01$; Figure 6A). Measures of bone size (total cross-sectional area, cortical area, ML and AP width, cross-sectional polar moment of inertia) were negatively correlated with ash content ($p < 0.02$). Bone slenderness (polar moment of inertia normalized for width and polar moment of inertia normalized for tibia length) was also negatively correlated with ash content ($p < 0.02$; Figure 6B). Bone size and slenderness were positively correlated with the area fraction of remodeled tissue ($p < 0.05$). Thus, wider (more robust) tibiae had lower mineral content and increased amount of remodeled tissue and narrow (more slender) tibiae had increased mineral content and decreased amount of remodeled tissue.

The current study confirmed that, similar to inbred mice, the tibia diaphyses of young, adult females and males show a reciprocal relationship between bone morphology and tissue quality, as hypothesized. Tissue from more slender bones (narrow relative to tibia length) was composed of material having higher mineral content and, consequently, increased tissue stiffness and strength, but reduced ductility. Unlike the mouse model, this relationship was subtle and only observed when combining male and female datasets to expand the range of data. The current study revealed a general biological phenomenon that has only been observed previously by looking across a large range of bones from many species. Here, bone from the same species with similar function showed that more slender morphology might be compensated by increased ash content. Although this coupling appears advantageous for ensuring that an adequate whole bone stiffness is achieved for day-to-day activity, the disadvantage is that the tissue-quality factors that tend to make bone stiff also tend to make bone less ductile, less tough, and more damageable.

This is an intriguing finding because, despite dimorphic growth patterns, males and females have similar tissue-level mechanical properties. Thus, both sexes may share a common underlying biological (adaptive) mechanism. This data suggest that osteoblasts and osteoclasts are capable of not only adapting bone morphology, but also modulating tissue-level mechanical properties so that the combination of traits satisfies mechanical demands (Jepsen et al, 2001; Currey, 1979). Therefore, the phenomenon that slender bones are constructed differently with material level variation that ultimately

leads to more damageable material than larger bones may help explain why individuals with more slender bones are at increased risk of stress fractures early in life and fragility fractures later in life.

Figure 6. Correlation between ash content and (A) post-yield strain, PYε and (B) polar moment of inertia, J, normalized for tibia length, L.

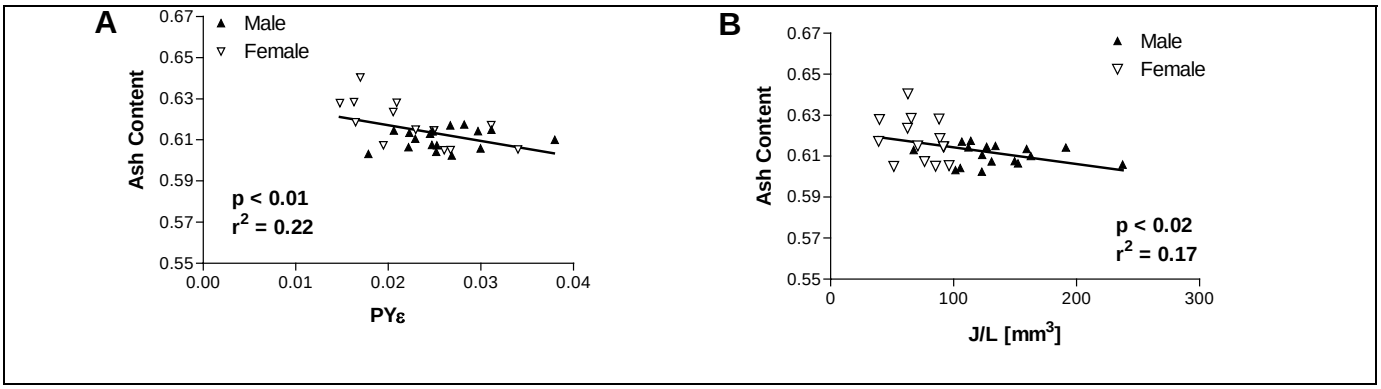

Ultrasound Studies

In year three, we conducted a series of experiments that examined whether ultrasound has the sensitivity to detect the presence of damage in bone. Most studies have found that ultrasound is insensitive to damage. We found that damage affects the viscoelastic properties of bone to a greater degree than the stiffness properties and we focused our attention on the attenuation of the ultrasound signal as this may be more sensitive to the presence of damage. A student for the City University of New York worked on this project and found that, like prior work, the velocity of the ultrasound signal was insensitive to the presence of damage. He examined the attenuation (a measure related to the viscoelastic properties of bone) following damage accumulation, however, could not make a reasonable conclusion because of difficulties in matching the size of the sample to the size of the ultrasound transducer (i.e., we would have to use samples machined from bovine bone to test this concept). Although viscous properties may be more sensitive to the presence of damage, we concluded from this study that it was not practical to reliably measure this parameter using machined bone samples from human tibiae. Thus, it is uncertain whether ultrasound would be a valuable measure to test for the presence of in situ damage accumulation engendered during basic training.

KEY RESEARCH ACCOMPLISHMENTS

The primary outcome of the grant is that the bone tissue for individuals with more slender bones are constructed in a fundamentally different way compared to individuals with more robust (wider) bones. With increasing slenderness, the material is more stiff, less ductile, and more damageable and this appears to be a consequence of higher matrix mineralization. These results support are central hypothesis and may help explain why individuals with smaller tibiae are at higher risk of stress fractures.

REPORTABLE OUTCOMES

Bouxsein ML, Jepsen KJ. Etiology and biomechanics of hip and vertebral fractures. *Atlas of Osteoporosis,* Second Edition. Current Medicine, Inc., Eds. Eric S. Orwoll, Stanley G. Korenman, 2003.

Jepsen K. The aging cortex: to crack or not to crack. *Osteoporos Int.* 2003 Sep;14 Suppl 5:57-66. 2003.

Tommasini SM, Nasser P, Jepsen KJ. Gender differences in bone slenderness are not related to material properties. Transactions Orthopaedic Research Society, 2002.

Tommasini SM, Morgan TG, van der Meulen MCH, Jepsen KJ. Genetic variation in vertebral mechanical properties determined by the relationship between morphological and compositional bone traits. Transactions Orthopaedic Research Society, 2003.

Jepsen KJ, Price C, Nadeau JH. Systems analysis of bone fragility. Pathways, Networks, and Systems: Theory and Experiments. Aegean Conference, Santorini, Greece, 2003.

Tommasini SM, Nasser P, Jepsen KJ. The relationship between bone morphology and bone quality: Implications for stress fracture risk in young adult male tibiae. Poster and podium presentations as the American Society of Bone and Mineral Research Annual meeting, Seattle, WA, 2004.

Bird JE, Nasser P, Tommasini S, Casagrande D, Jepsen KJ. The relationship between continued periosteal apposition and bone fragility. Poster presentation at the American Society of Bone and Mineral Research Annual meeting, Seattle, WA, 2004.

Tommasini SM, Nasser P, Schaffler MB, Jepsen KJ. The relationship between bone morphology and bone quality in male tibiae: Implications for stress fracture risk. *Journal of Bone and Mineral Research*, 20(8):1372-1380, 2005.

Price C, Herman BC, Lufkin T, Goldman HM, Jepsen KJ. Genetic variation in bone growth patterns defines adult mouse bone fragility. *Journal of Bone and Mineral Research,* 20(11): 1983-1991, 2005.

Jepsen, KJ. *Assessing the mechanical properties of mineralized tissues. Invited talk,* Advances in Mineral Metabolism (AIMM); Snowmass, CO, 2005.

Jepsen, KJ. *Using mice to understand structure-function relationships in the skeleton*. Invited talk, Bone Quality Meeting; Sponsored by the National Institutes of Arthritis and Musculoskeletal and Skin Diseases (NIAMS) and the American Society of Bone and Mineral Research; Bethesda MD May 2-3, 2005.

Jepsen, KJ. *Biomechanical insights into the components of bone strength. Invited talk,* Alliance for Better Bone Health Sponsored Symposium at the Second Joint Meeting of the European Calcified Tissue Society (ECTS) and the International Bone and Mineral Society (IBMS), Geneva, Switzerland, June, 2005.

Jepsen, KJ. *Can heritable aspects of bone quality be enhanced through intervention? Invited talk,* American Society of Bone and Mineral Research; Working group on Bone Remodeling and Stress Fracture, Nashville, TN, 2005.

Tommasini SM, Nasser P, Jepsen KJ. Sexual dimorphism affects tibial size and shape but not tissue-level mechanical properties. Selected as a Plenary Poster at the 2006 Annual Meeting of the American Society of Bone and Mineral Research, Philadelphia, PA, USA.

Tommasini SM, Nasser P, Jepsen KJ. Sexual dimorphism affects tibial size and shape but not tissue-level mechanical properties. *Bone,* in press, June 2006.

Tommasini SM, Nasser P, Hu B, Schaffler M B, Jepsen KJ. Of Mice, Men, and Women: The Relationship Between Bone Morphology and Tissue Quality. Submitted to the 2007 Annual Meeting of the Orthopaedic Research Society, San Diego, CA, USA.

Funding

The data generated by this grant provided evidence that the mouse represents an important model for understanding the genetic variability in the human skeleton. This data helped secure an RO1 grant from the NIH (AR44927) titled, "Genetic Determination of Skeletal Fragility".

The data generated by this grant was also used in the submission of two NIH grants titled, “Genetic regulation of bone growth and development” and “Age-changes in bone morphology as a predictor of fracture risk”. The goal of the first grant is to identify chromosomes harboring quantitative trait loci influencing bone growth patterns. The goal of the second grant is to determine if 25 year changes in moment of inertia predict fracture incidence. This latter grant utilizes information from the Framingham Heart Study and was written in collaboration with the Boston University School of Public Health and the Hebrew Rehabilitation Center for the Aged.

CONCLUSIONS

The results of this grant have revealed a novel relationship between bone morphology and tissue mechanical properties. The investigations of the mouse skeleton revealed that genetic variation in bone morphology strongly influence tissue mechanical properties through variations in matrix composition. The data from this DOD grant indicated that a similar relationship also exists in the human skeleton. Thus, individuals who have smaller (more narrow) tibia for their body size appear to compensate for the smaller geometry through variation in tissue-level mechanical properties. One of the side effects of this compensation is altered damageability which may be revealed under extreme physical activity such as that experienced during military training.

CITED REFERENCES

Beck TJ, Ruff CB, Mourtada FA, Shaffer RA, Maxwell-Williams K, Kao GL, Sartoris DJ, Brodine S. Dual-energy X-ray absorptiometry derived structural geometry for stress fracture prediction in male U.S. Marine Corps recruits. *J Bone Miner Res,* 11:645-653, 1996.

Brear K, Currey JD, Pond CM. Ontogenetic changes in the mechanical properties of the femur of the polar bear Ursus maritimus. *J Zool, London,* 222*:*49-58, 1990.

Burr DB, Milgrom C, Boyd RD, Higgins WL, Robin G, Radin EL. Experimental stress fractures of the tibia. Biological and mechanical aetiology in rabbits. *J Bone Joint Surg Br,* 72*:*370-375, 1990.

Burstein AH, Currey JD, Frankel VH, Reilly DT. The ultimate properties of bone tissue: the effects of yielding. *J Biomech,* 5:35-44, 1972.

Burstein AH, Reilly DT, Martens M. Aging of bone tissue: mechanical properties. *J Bone Joint Surg Am,* 58*:*82-86, 1976.

Carrier D, Leon LR. Skeletal growth and function in the California gull (Larus californicus). *J Zool, London,* 222*:*375-389, 1990.

Currey JD. Changes in the impact energy absorption of bone with age. *J Biomech,* 12*:*459-469, 1979.

Currey JD. Effects of differences in mineralization on the mechanical properties of bone. *Philos Trans R Soc Lond B Biol Sci,* 304:509-518, 1984.

Currey JD, Butler G. The mechanical properties of bone tissue in children. *J Bone Joint Surg Am,* 57*:*810-814, 1975.

Duan Y, Beck TJ, Wang XF, Seeman E. Structural and biomechanical basis of sexual dimorphism in femoral neck fragility has its origins in growth and aging. *J Bone Miner Res,* 18*:*1766-1774, 2003

Enlow DH. Principles of bone remodeling; an account of post-natal growth and remodeling processes in long bones and the mandible: Thomas; 1963.

Ferretti JL, Capozza RF, Mondelo N, Zanchetta JR. Interrelationships between densitometric, geometric, and mechanical properties of rat femora: inferences concerning mechanical regulation of bone modeling. *J Bone Miner Res,* 8*:*1389-1396, 1993.

Forwood MR, Bailey DA, Beck TJ, Mirwald RL, Baxter-Jones AD, Uusi-Rasi K. Sexual dimorphism of the femoral neck during the adolescent growth spurt: a structural analysis. *Bone,* 35*:*973-981, 2004.

Friedl KE, Nuovo JA, Patience TH, Dettori JR. Factors associated with stress fracture in young army women: indications for further research. *Mil Med,* 157*:*334-38, 1992.

Frost HM. Bone "mass" and the "mechanostat": a proposal. *Anat Rec,* 219*:*1-9, 1987.

Garn S. The earlier gain and the later loss of cortical bone. Springfield, IL: Charles C Thomas; 1970.

Geusens P, Cantatore F, Nijs J, Proesmans W, Emma F, Dequeker J. Heterogeneity of growth of bone in children at the spine, radius and total skeleton. *Growth Dev Aging,* 55*:*249-256, 1991.

Giladi M, Milgrom C, Simkin A, Stein M, Kashtan H, Margulies J, Rand N, Chisin R, Steinberg R, Aharonson Z, et al. Stress fractures and tibial bone width. A risk factor. *J Bone Jt Surg Br,* 69:326-329, 1987.

Gordon KR, Levy C, Perl M, Weeks OI. Experimental perturbation of the development of sexual size dimorphism in the mouse skeleton. *Growth Dev Aging,* 58*:*95-104, 1994.

Gustafson MB, Martin RB, Gibson V, Storms DH, Stover SM, Gibeling J, Griffin L 1996 Calcium buffering is required to maintain bone stiffness in saline solution. *J Biomech,* 29(9)**:**1191-4.

Iscan MY, Miller-Shaivitz P. Discriminant function sexing of the tibia. *J Forensic Sci,* 29*:*1087-1093, 1984.

Jepsen KJ, Akkus O, Majeska RJ, Nadeau JH. Hierarchical relationship between genetically determined bone traits and whole bone mechanical properties in inbred mice. *Mammalian Genome,* 14(2):97-104, 2003.

Jepsen KJ, Davy DT. Comparison of damage accumulation measures in human cortical bone. *J Biomech,* 30(9)**:**891-894, 1997.

Jepsen, KJ, Pennington, DE, Lee, Y-L, Warman, M, Nadeau, J. Bone brittleness varies with genetic background in A/J and C57BL/6J inbred mice. *J Bone Miner Res,* 16(10):1854-1862, 2001.

Johnson L, Stradford HT, Geis RW, Dineen JR. Histogenesis of stress fractures. *J Bone Joint Surg Am,* 45*:*1542, 1963.

Lanyon L, Skerry T. Postmenopausal osteoporosis as a failure of bone's adaptation to functional loading: a hypothesis. *J Bone Miner Res,* 16*:*1937-1947, 2001.

Lemaitre J. A course on damage mechanics. Springer-Verlag, Berlin; New York, 1992.

Looker AC, Beck TJ, Orwoll ES. Does body size account for gender differences in femur bone density and geometry? *J Bone Miner Res,* 16*:*1291-1299, 2001.

Martin R. Mathematical model for repair of fatigue damage and stress fracture in osteonal bone. *J Orthop Res,* 13*:*309-316, 1995.

McCalden RW, McGeough JA, Barker MB, Court-Brown CM. Age-related changes in the tensile properties of cortical bone. The relative importance of changes in porosity, mineralization, and microstructure. *J Bone Joint Surg Am,* 75*:*1193-1205, 1993.

Milgrom C, Finestone A, Novack V, Pereg D, Goldich Y, Kreiss Y, Zimlichman E, Kaufman S, Liebergall M, Burr D. The effect of prophylactic treatment with risedronate on stress fracture incidence among infantry recruits. *Bone,* 35(2)**:**418-24, 2004.

Milgrom C, Giladi M, Simkin A, Rand N, Kedem R, Kashtan H, Stein M, Gomori M. The area moment of inertia of the tibia: A risk factor for stress fractures. *J Biomech,* 22:1243-1248, 1989.

Milgrom C, Giladi M, Stein M, Kashtan H, Margulies JY, Chisin R, Steinberg R, Aharonson Z. Stress fractures in military recruits. A prospective study showing an unusually high incidence. *J Bone Joint Surg Br,* 67(5):732-735, 1985.

Milgrom C, Simkin A, Eldad A, Nyska M, Finestone A. Using bone's adaptation ability to lower the incidence of stress fractures. *Am J Sports Med,* 28*:*245-251, 2000.

Miller GJ, Purkey WW, Jr. The geometric properties of paired human tibiae. *J Biomech,* 13*:*1-8, 1980.

Mori S, Burr DB. Increased intracortical remodeling following fatigue damage. *Bone,* 14(2)**:**103-109, 1993.

Moro M, van der Meulen MC, Kiratli BJ, Marcus R, Bachrach LK, Carter DR. Body mass is the primary determinant of midfemoral bone acquisition during adolescent growth. *Bone,* 19*:*519-26, 1996.

Nádai A. Theory of flow and fracture of solids. Engineering societies monographs. McGraw-Hill, New York, 1950.

Nieves JW, Formica C, Ruffing J, Zion M, Garrett P, Lindsay R, Cosman F. Males have larger skeletal size and bone mass than females, despite comparable body size. *J Bone Miner Res,* 20*:*529-35, 2005.

Price C, Herman BC, Lufkin T, Goldman HM, Jepsen KJ. Genetic variation in bone growth patterns defines adult mouse bone fragility. *Journal of Bone and Mineral Research,* 20(11): 1983-1991, 2005.

Reilly DT, Burstein AH. The elastic and ultimate properties of compact bone tissue. *J Biomech,* 8*:*393-405, 1975.

Ruff CB. Body size, body shape, and long bone strength in modern humans. *J Hum Evol,* 38*:*269-290, 2000.

Ruff C. Growth in bone strength, body size, and muscle size in a juvenile longitudinal sample. *Bone,* 33*:*317-329, 2003.

Schaffler MB, Burr DB. Stiffness of compact bone: effects of porosity and density. *J Biomech,* 21(1)**:**13-6, 1988.

Schaffler MB, Radin EL, Burr DB. Long-term fatigue behavior of compact bone at low strain magnitude and rate. *Bone,* 11(5)**:**321-326, 1990.

Selker F, Carter DR. Scaling of long bone fracture strength with animal mass. *J Biomech,* 22*:*1175-1183, 1989.

Sumner DR, Andriacchi TP. Adaptation to differential loading: comparison of growth-related changes in cross-sectional properties of the human femur and humerus. *Bone,* 19*:*121-126, 1996.

Swartz SM, Bennett MB, Carrier DR. Wing bone stresses in free flying bats and the evolution of skeletal design for flight. *Nature,* 359*:*726-729, 1992.

Tommasini SM, Nasser P, Schaffler MB, Jepsen KJ. The relationship between bone morphology and bone quality in male tibiae: Implications for stress fracture risk. *Journal of Bone and Mineral Research,* 20(8):1372-1380, 2005.

Turner CH. Biomechanics of bone: determinants of skeletal fragility and bone quality. *Osteoporos Int,* 13*:*97-104, 2002.

Turner RT, Wakley GK, Hannon KS. Differential effects of androgens on cortical bone histomorphometry in gonadectomized male and female rats. *J Orthop Res,* 8*:*612-617, 1990.

Warden SJ, Hurst JA, Sanders MS, Turner CH, Burr DB, Li J. Bone adaptation to a mechanical loading program significantly increases skeletal fatigue resistance. *J Bone Miner Res,* 20*:*809-816, 2005.

Wiren KM, Zhang XW, Toombs AR, Kasparcova V, Gentile MA, Harada S, Jepsen KJ. Targeted overexpression of androgen receptor in osteoblasts: unexpected complex bone phenotype in growing animals. *Endocrinology,* 145*:*3507-3522, 2004.

Appendix 1

Tommasini SM, Nasser P, Schaffler MB, Jepsen KJ. The relationship between bone morphology and bone quality in male tibiae: Implications for stress fracture risk. *Journal of Bone and Mineral Research*, 20(8):1372-1380, 2005.

Appendix 2

Price C, Herman BC, Lufkin T, Goldman HM, Jepsen KJ. Genetic variation in bone growth patterns defines adult mouse bone fragility. *Journal of Bone and Mineral Research,* 20(11): 1983-1991, 2005.

Appendix 3

Tommasini SM, Nasser P, Jepsen KJ. Sexual dimorphism affects tibial size and shape but not tissue-level mechanical properties. *Bone*, in press, June 2006.

Appendix 4 (to be submitted as a manuscript to the Journal of Bone and Mineral Research, Dec. 2006)

Tommasini SM, Nasser P, Hu B, Schaffler M B, Jepsen KJ. Of Mice, Men, and Women: The Relationship Between Bone Morphology and Tissue Quality. Submitted to the 2007 Annual Meeting of the Orthopaedic Research Society, San Diego, CA, USA.

JOURNAL OF BONE AND MINERAL RESEARCH
Volume 20, Number 8, 2005
Published online on March 28, 2005; doi: 10.1359/JBMR.050326

Relationship Between Bone Morphology and Bone Quality in Male Tibias: Implications for Stress Fracture Risk

Steven M Tommasini,[1] Philip Nasser,[2] Mitchell B Schaffler,[2] and Karl J Jepsen[2]

ABSTRACT: Biomechanical properties were assessed from the tibias of 17 adult males 17–46 years of age. Tissue-level mechanical properties varied with bone size. Narrower tibias were comprised of tissue that was more brittle and more prone to accumulating damage compared with tissue from wider tibias.

Introduction: A better understanding of the factors contributing to stress fractures is needed to identify new prevention strategies that will reduce fracture incidence. Having a narrow (i.e., more slender) tibia relative to body mass has been shown to be a major predictor of stress fracture risk and fragility in male military recruits and male athletes. The intriguing possibility that slender bones, like those shown in animal models, may be composed of more damageable material has not been considered in the human skeleton.
Materials and Methods: Polar moment of inertia, section modulus, and antero-posterior (AP) and medial-lateral (ML) widths were determined for tibial diaphyses from 17 male donors 17–46 years of age. A slenderness index was defined as the inverse ratio of the section modulus to tibia length and body weight. Eight prismatic cortical bone samples were generated from each tibia, and tissue-level mechanical properties including modulus, strength, total energy, postyield strain, and tissue damageability were measured by four-point bending from monotonic (n = 4/tibia) and damage accumulation (n = 4/tibia) test methods. Partial correlation coefficients were determined between each geometrical parameter and each tissue-level mechanical property while taking age into consideration.
Results: Significant correlations were observed between tibial morphology and the mechanical properties that characterized tissue brittleness and damageability. Positive correlations were observed between measures of bone size (AP width) and measures of tissue ductility (postyield strain, total energy), and negative correlations were observed between bone size (moment of inertia, section modulus) and tissue modulus.
Conclusions: The correlation analysis suggested that bone morphology could be used as a predictor of tissue fragility and stress fracture risk. The average mechanical properties of cortical tissue varied as a function of the overall size of the bone. Therefore, under extreme loading conditions (e.g., military training), variation in bone quality parameters related to damageability may be a contributing factor to the increased risk of stress fracture for individuals with more slender bones.
J Bone Miner Res 2005;20:1372–1380. Published online on March 28, 2005; doi: 10.1359/JBMR.050326

Key words: bone biomechanics, stress fracture, bone quality, bone morphology, strength, damage, brittleness

INTRODUCTION

Stress fractures are overuse injuries of bone that are common among elite runners and military recruits.[1–3] Before injury, affected bones are typically normal with no acute injury. Morbidity from stress fractures ranges from minor pain to serious lifetime disability for the individual.[4] Stress fractures have been reported in the ribs, hip, spine, and metatarsals,[3,5] but vigorous weight-bearing activities, such as running and jogging, commonly lead to stress fractures of the lower extremities, especially the tibia.[3] During basic training, 1–5% of U.S. male military recruits sustain a stress fracture.[2] However, this incidence is two to five times higher in female recruits.[6] Stress fractures lead to loss of manpower, valuable loss of training time, expense of medical care, and discharge of affected soldiers.[7] A better understanding of the factors contributing to stress fractures is needed to identify new prevention strategies that will reduce fracture incidence.

A number of risk factors for stress fracture have been identified including physical fitness, external hip rotation, body height and weight, age, race, gender, muscle mass, motivation, footwear, smoking, and family history of osteoporosis.[1,4,8–10] One of the best predictors of stress fracture risk is bone geometry. Specifically, having a narrow (i.e., more slender) tibia relative to body mass has been shown to

The authors have no conflict of interest.

[1]New York Center for Biomedical Engineering, CUNY Graduate School, Department of Biomedical Engineering, City College of New York, New York, New York, USA; [2]Leni & Peter W. May Department of Orthopaedics, Mount Sinai School of Medicine, New York, New York, USA.

be a major predictor of stress fracture risk and fragility in male military recruits[1,2,11] and male athletes.[12] A stress fracture is thought to be a consequence of transiently reduced tissue strength arising from increased resorptive activity (i.e., increased porosity) that acts to repair damage induced by vigorous physical activity.[13] Thus, stress fractures may be pronounced in individuals with more slender bones because smaller bone size is thought to lead to higher tissue-level stresses and thus increased damage accumulation.[1,2] However, this postulate is based on the assumption that all bones are constructed in equivalent manners, and the contribution of variable tissue-level mechanical properties to stress fracture incidence has not been explored.

An examination of inbred mouse strains may help explain why bone size is a risk factor for stress fractures in the human skeleton. A comparison of adult A/J and C57BL/6J inbred mouse strains revealed that the bone slenderness was inversely related to mineral content (as measured by ash content) and, by correlation, tissue modulus and strength.[14] Mineral content has been shown to be positively correlated with tissue stiffness and strength.[15] These results suggested that bone morphology and mineral content were coordinately regulated so whole bone stiffness appropriately matched the mechanical demands imposed by weight bearing. However, the downside of regulating mineral content to match bone size was that mineral content was also negatively correlated with tissue ductility.[14,15] We postulate that a similar reciprocal relationship between bone size and bone quality exists in the human skeleton. The intriguing possibility that slender bones, like those shown in animal models, may be composed of more damageable material has not yet been considered in the human skeleton.

The goal of this study was to determine whether tissue-level mechanical properties vary with bone size in the human skeleton. This was tested by assessing the biomechanical properties of tibias from young adult males. Understanding why bone morphology is a risk factor for stress fractures should lead to better identification of those at risk and, ultimately, to early diagnosis, treatment, and modification of training regimens.

MATERIALS AND METHODS

Sample population

Tibias of 17 male donors (15 white, 1 Hispanic, 1 black) 32.9 ± 10.4 years of age (range, 17–46 years) were acquired from the Musculoskeletal Transplant Foundation (Edison, NJ, USA). Donor body weight and height were obtained from the source. Only donors with no known skeletal pathology were included in the study. The tibias were freshly harvested, wrapped in wet gauze, and stored in plastic bags at –40°C.

Whole bone morphology

Tibia length (L) was measured as the average distance between the distal articular center (the middle of the talar trochlear facet) and the two proximal articular centers (medial and lateral condyles)[16] using a large-capacity slide caliper with an accuracy of ±2.54 mm (Mantex Precision; Haglöf, Madison, MS, USA). Tibia width was measured in the antero-posterior (AP) and medial-lateral (ML) directions at 10% intervals from 30–70% of the total tibia length using a 300-mm vernier caliper with an accuracy of ±0.02 mm (Fowler Company, Newton, MA, USA).

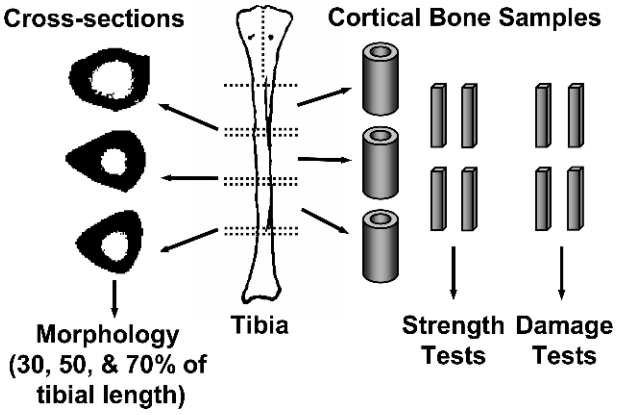

FIG. 1. Schematic of how whole tibias were sectioned to produce the 3-mm-thick sections used for cross-sectional morphology and cortical bone samples for biomechanical testing from three diaphyseal cylindrical sections (monotonic, $n = 4$/tibia; damage accumulation, $n = 4$/tibia).

Cross-sectional morphology was determined from 3-mm-thick middiaphyseal cross-sections cut at 30%, 50%, and 70% of the total tibia length (Fig. 1) using a diamond coated metallurgical saw (Model 660; South Bay Technology, San Clemente, CA, USA). A calibrated image of each cross-section was obtained using a digital camera at a 0.024 mm/pixel resolution. Image analysis software (IMAQ Vision Builder 6.0; National Instruments, Austin, TX, USA) was used to threshold each image and quantify cortical area (CtAr), the moments of inertia about the AP (I_{AP}) and ML (I_{ML}) axes, the polar moment of inertia ($J = I_{AP} + I_{ML}$), and the section modulus in the AP (J/APwidth/2) and ML (J/MLwidth/2) directions. Moment of inertia and section modulus were assessed because these geometric measures are related to the bending and torsional stiffness of intact tibias. A slenderness index (S) was calculated in the AP and ML directions as the ratio of the AP and ML section modulus values, respectively, to tibia length and body weight[17]:

$$S = 1/\{[J/(\text{width}/2)]/(L \times BW)\} \quad (1)$$

where L = tibia length (mm) and BW = body weight (kg). The section modulus has been shown to scale linearly with body mass.[17] The inverse ratio was used so that a tibia with a large slenderness value is one that is thinner or gracile for the weight and height of an individual. A small slenderness value reflects a stocky or robust tibia. All morphological traits were averaged over the three cross-sections for each tibia.

Bone sample generation

Cortical bone samples were prepared from the diaphysis of each tibia for biomechanical testing (Fig. 1). The three diaphyseal cylindrical sections were rough-cut into antero-

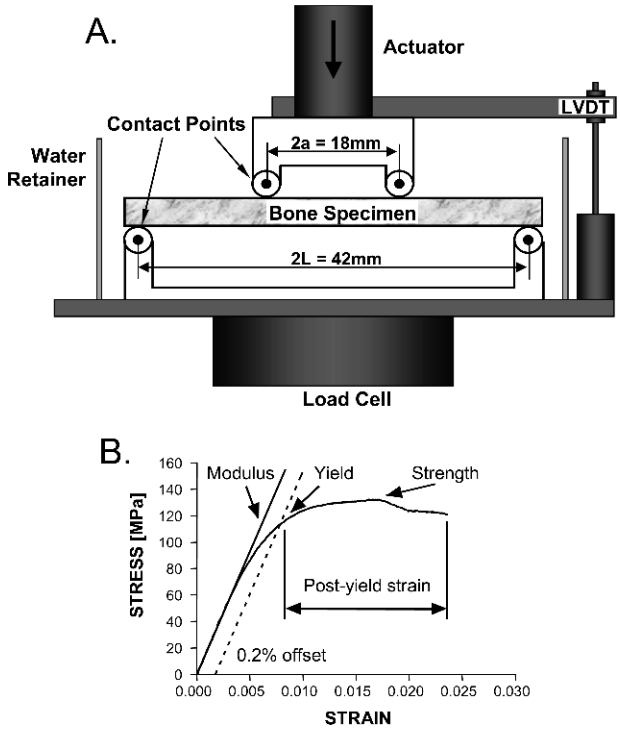

FIG. 2. (A) Schematic of the four-point bending device shows how cortical bone samples were tested. The span between the upper contact points is 2a = 18 mm, and the span between the lower contact points is 2L = 42 mm. (B) Typical stress-strain curve from the four-point bending monotonic tests shows how modulus, strength, postyield strain, and total energy were calculated.

lateral, antero-medial, and posterior regions. From each of these regions, one to three prismatic beams were cut using a diamond-coated metallurgical saw (Isomet; Buehler, Lake Bluff, IL, USA). The beams were machined to regular test samples using an automated CNC milling machine under constant irrigation (Modela MDX-20; Roland DGA, Irvine, CA, USA). Sample width (circumferential direction) was machined to 5 mm and length (longitudinal direction) was machined to 55 mm for all samples. Sample height (radial direction) was 2.5 mm except for four tibias with thin cortices, which were machined to 2.2 mm. A total of eight samples were generated from each tibia and randomly distributed to monotonic ($n = 4$) and damage accumulation ($n = 4$) test groups. All samples were stored at –40°C in gauze saturated with PBS with added calcium[18] and placed individually in airtight bags.

Monotonic failure properties

Tissue-level mechanical properties were assessed by loading four cortical bone samples from each tibia to failure in four-point bending at 0.05 mm/s (Fig. 2A) using a servohydraulic materials testing system (Instron model 8872; Instron, Canton, MA, USA). Specimens were submerged in a PBS solution with added calcium[18] and maintained at 37°C throughout all tests. Load and deflection were converted to stress and strain using the following equations, which take yielding into consideration[19]:

$$\sigma = 2[2M + \phi(dM/d\phi)]/bh^2 \quad (2)$$

$$\varepsilon = h\phi/2a = \tfrac{1}{2}h\Delta[(L - a)/(2a^3/3 - a^2L + L^3/3)] \quad (3)$$

where σ and ε are the stress and strain at the outer surface of the beam, M = applied moment, b = specimen width, h = specimen height, a = ½ the span between the upper two load points = 9 mm, L = ½ the span between the two lower load points = 21 mm, ϕ = angle of inclination = a/ρ, and d/dϕ is the derivative with respect to ϕ. The angle of inclination was written in terms of the measured deflection (Δ) by estimating the curvature (ρ) using standard beam equations. Mechanical properties were calculated from the stress-strain curves, and these included modulus, strength, total energy, and postyield strain (Fig. 2B). Modulus was calculated from a linear regression of the initial portion of the stress-strain curve. Yield was determined using the 0.2% offset method. Postyield strain was defined as the strain at failure minus the strain at yield. All properties were averaged over the four samples tested for each tibia.

Damage accumulation tests

Tissue damageability was assessed using a protocol designed to induce and accumulate cracks in cortical bone specimens. The accumulation of damage leads to measurable degradation of mechanical properties.[20] Therefore, the degradation of mechanical properties can be used as an index of matrix damage. Four cortical bone samples from each tibia were subjected to a fifteen cycle damage accumulation protocol (Fig. 3A) similar to that described previously.[21] For this protocol, "diagnostic" cycles (1, 3, 5, 7, 9, 11, 13, and 15) were interposed between "damage" cycles (2, 4, 6, 8, 10, 12, and 14). For the diagnostic cycles, the specimens were loaded in four-point bending at 0.5 mm/s to 50% of the average displacement at yield (determined from the monotonic tests), held for 60 s, and unloaded at 0.5 mm/s. Preliminary studies indicated that this load level provided information on tissue-level mechanical properties without inducing additional damage. For the damage cycles, the specimens were loaded at 0.5 mm/s to 50%, 75%, 100%, 125%, 150%, 175%, and 200% of displacement at yield, respectively, held for 60 s, and unloaded at 0.5 mm/s. A 5-minute recovery period followed each damage cycle. Displacement at yield was used as a reference in the damage cycles because this parameter showed little variation among the test samples when subjected to monotonic four-point bending. The displacement at yield was 1.0 mm for the samples with a height of 2.5 mm and 1.07 mm for the samples with a height of 2.2 mm.

A mechanical measure of the amount of damage that accumulated within the test sample was quantified from the magnitude of stiffness degradation. For each diagnostic cycle, stiffness was calculated from a linear regression of the initial portion of the load-deformation curve. Specimen stiffness decreased nonuniformly with each cycle revealing increasing amounts of damage induced within each cycle and an overall damage accumulation by the end of the protocol (Fig. 3B). At the end of the test sequence, the overall

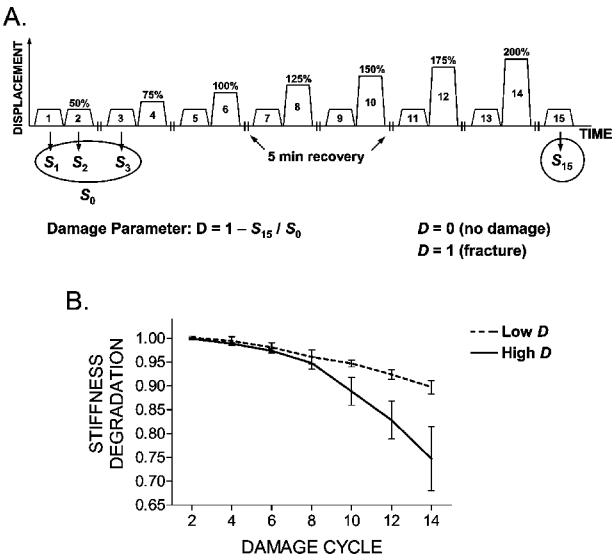

FIG. 3. (A) A 15-cycle loading protocol was used to induce damage within machined cortical bone specimens and to measure resultant stiffness degradation. Damage was induced during cycles 2, 4, 6, 8, 10, 12, and 14 by conducting relaxation tests at increasing levels of applied displacement (expressed as a percentage of the displacement at yield). Diagnostic cycles were interposed between damaging cycles. Each damage cycle was preceded by a diagnostic cycle at 50% of displacement at yield. A 5-minute recovery period was introduced after the damage cycles to relieve residual internal stresses. (B) The change in stiffness calculated between sequential diagnostic tests was plotted vs. cycle number for the damage tests. The dashed curve represents a specimen showing little stiffness degradation (i.e., little damage accumulation). The solid line represents a specimen showing large stiffness degradation (i.e., more damage accumulation).

damage parameter, D, was calculated by comparing the stiffness of the first and last diagnostic tests such that:

$$D = 1 - S_{15}/S_0, \quad (4)$$

where S_{15} is the stiffness of the last diagnostic cycle and S_0 is the average stiffness of the first two diagnostic cycles (S_1, S_3) and the first damage cycle (S_2).

Statistical analysis

All data were regressed against age using linear regression analysis to identify the properties that varied significantly with age (GraphPad Prism, San Diego, CA, USA). To determine whether bone morphology was related to tissue level material properties, partial correlation coefficients were determined between each geometrical parameter (e.g., I_{AP}, I_{ML}, J, S) and each tissue level mechanical property (modulus, strength, total energy, postyield strain, damageability) while taking age into consideration (Minitab, State College, PA, USA).[22]

RESULTS

The sample population showed broad ranges of body size, body stature, and bone morphology values (Table 1). Modulus and strength showed little variation among individuals (CV = 9.73% and 4.62%, respectively). However,

TABLE 1. VARIATION IN PROPERTIES AMONG YOUNG ADULT MALE TIBIAS

Property	*Mean ± SD*	*Range*
Age (years)	32.9 ± 10.4	17–46
Body weight (kg)	83.8 ± 25.1	57.2–158.8
Body height (cm)	177.7 ± 4.3	170.2–182.9
Body mass index (kg/m^2)	26.7 ± 8.0	17.1–51.7
Tibia length (cm)	38.1 ± 1.9	34.4–40.4
Cortical area (mm^2)	355.9 ± 55.2	268.3–511.1
AP width (mm)	31.2 ± 2.5	28.4–36.9
ML width (mm)	24.3 ± 2.3	19.9–30.6
AP moment of inertia (mm^4)	34,390 ± 10,149	19,466–60,698
ML moment of inertia (mm^4)	17,250 ± 5,945	8,246–34,734
Polar moment of inertia (mm^4)	51,640 ± 15,886	27,713–95,432
AP section modulus (mm^3)	3,279 ± 819	1,925–5,172
ML section modulus (mm^3)	4,188 ± 907	2,785–6,237
AP slenderness (1/mm^2/kg)	9.9 ± 2.0	6.5–13.4
ML slenderness (1/mm^2/kg)	7.7 ± 1.5	5.4–10.2
Modulus (GPa)	17.0 ± 1.7	13.4–19.0
Strength (MPa)	130.7 ± 6.1	120.8–144.5
Total energy (MPa)	3.3 ± 0.9	2.3–5.6
Post-yield strain	0.026 ± 0.006	0.016–0.039
Damage parameter (D)	0.165 ± 0.038	0.103–0.253

AP, antero-posterior direction; ML, medial-lateral direction.

postyield strain (CV = 24.0%), total energy (CV = 26.4%), and the damage parameter (CV = 23.0%) all showed large variability among the samples. Morphological measures such as AP width, section modulus, and the polar moment of inertia, J (Fig. 4), increased linearly with body weight ($R^2 = 0.59$, $p < 0.003$) and body mass index (BMI; $R^2 = 0.57$, $p < 0.004$), but were independent of body height ($R^2 = 0.01$, $p < 0.7$). These relationships did not change when the body weight values were corrected for age (data not shown). Body height was uncorrelated with body weight ($R^2 = 0.01$, $p < 0.8$), indicating that the sample population consisted of individuals with similar heights but widely varying body weights.

Significant age-related changes were observed for the tissue-level mechanical properties and the size of the tibia. A significant, positive correlation was observed between tibia slenderness in the AP ($R^2 = 0.31$, $p < 0.02$) and ML ($R^2 = 0.24$, $p < 0.05$) directions and age. However, I_{AP}, I_{ML}, and J did not vary with age, suggesting that the variation in slenderness with age was due largely to higher body weight and BMI ($R^2 = 0.29$–0.32, $p < 0.03$) values for the older individuals. Although tissue modulus did not vary significantly with age, tissue strength ($R^2 = 0.53$, $p < 0.001$), postyield strain ($R^2 = 0.44$, $p < 0.004$), and total energy ($R^2 = 0.32$, $p < 0.002$) were significantly lower for the older individuals. Furthermore, a significant, negative correlation was observed between the damage parameter and age ($R^2 = 0.41$, $p < 0.006$). This data suggested that, whereas the tibia became more slender relative to body size with age, the cortical tissue became progressively less strong and less ductile (i.e., more brittle) with age.

The correlation analysis showed significant correlations between tibial morphology and the mechanical properties that characterized tissue brittleness and damageability (Table 2). The relationships among tissue-level mechanical

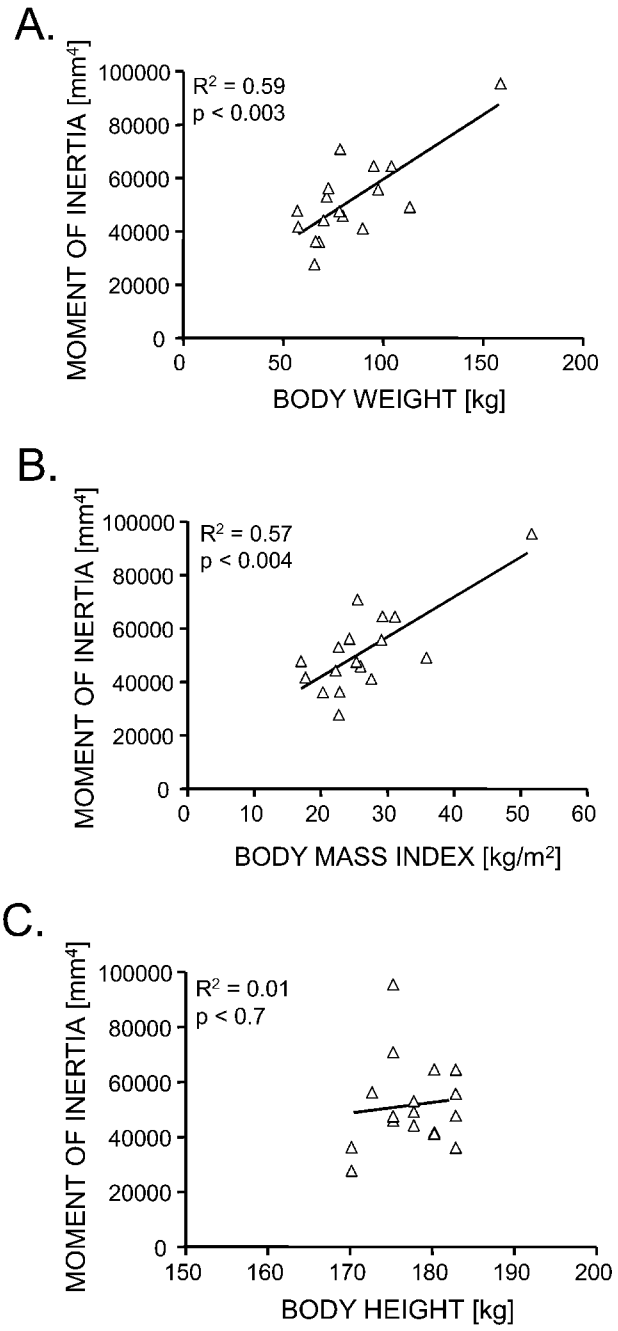

FIG. 4. The average cross-sectional polar moment of inertia of the tibia from males increased with (A) body weight and (B) body mass index but not with (C) body height. Removing the outlier changed the R^2 values to 0.24 ($p < 0.05$) for A and 0.20 ($p < 0.09$) for B.

properties and cross-sectional morphology were linear. Postyield strain and total energy increased significantly with AP width (Figs. 5A and 5B). Modulus decreased with I_{AP} ($p < 0.07$), J ($p < 0.08$), AP section modulus ($p < 0.05$), and ML section modulus (Figs. 5C–5F). Tissue damageability increased with tibia slenderness in the AP ($p < 0.05$; Fig. 6) and ML ($p < 0.09$) directions. These correlations, which were independent of age, indicated that a narrower bone was comprised of tissue that failed in a more brittle manner and accumulated more damage.

DISCUSSION

The results of this study revealed that the tissue-level mechanical properties of cortical bone varied with the size of the tibia. Positive correlations were observed between measures of bone size (AP width) and measures of tissue ductility (postyield strain, total energy), and negative correlations were observed between bone size (moment of inertia, section modulus) and tissue modulus. Many of these correlations were significant. The lack of significant correlation with all measures of bone size can be attributed largely to the complex shape of the tibia. The tibia has a triangular cross-section and, consequently, measures of width correlated significantly with mechanically relevant traits like cortical area and moment of inertia but explained only 50–80% of the variability in these measures (data not shown). These correlations would be greater if the cross-section had a circular shape. The variability in these correlations was sufficiently large that neither the linear (width) traits nor the integrated traits like area and moment of inertia correlated significantly with a particular tissue-level mechanical property simultaneously. Nevertheless, the data indicated that bones with smaller width were comprised of stiffer and less ductile (i.e., more brittle) material compared with larger, more robust bones. The correlation between tissue ductility and bone size may help explain why male military recruits[1,2,11] and male athletes[12] with narrow bones show a higher incidence of stress fractures compared with individuals with wide bones.

The development of the slenderness index[17] was for a "normal" range in height and weight and is probably not useful beyond this range. However, the morphological variation observed in our sample population was consistent with that reported for military recruits[1,2] and runners,[12] and height and weight were consistent with recent national averages.[23] As expected, bone size varied with body weight,[17] but did not vary with height (Fig. 4).[24] Thus, narrow bones came from less heavy individuals who were of similar height as those with wide tibias. Weight varied more than height for our sample population similar to that observed for the aged-matched national data. Furthermore, the variability in weight, specifically inclusion of one outlier (Fig. 4), did not affect the results (i.e., the heaviest person did not have an unusual slenderness value). Thus, the bones used in this study seem to be an appropriate size relative to body type.

The variation in long bone slenderness has been attributed to genetic and environmental factors influencing growth and development[25] and has been implicated as a risk factor for osteoporotic fracture.[26] To be relevant for military recruits, the sample population should have ranged in age between 18 and 25 years. However, for the age range in this study, the tissue-level mechanical properties varied linearly with age and were easily corrected using a linear regression method.[22] Consequently, the correlation analysis presented here provides relevant insight into the relationship observed between bone size and stress fracture risk

TABLE 2. PARTIAL CORRELATION COEFFICIENTS TAKING AGE INTO CONSIDERATION

	Modulus	*Strength*	*Total energy*	*PY strain*	*Damageability*
Cortical area	–0.24	0.03	0.37	0.40	–0.23
	(0.35)	(0.90)	(0.14)	(0.11)	(0.37)
AP width	–0.09	–0.03	**0.57**	**0.70**	–0.16
	(0.74)	(0.90)	**(0.02)**	**(0.002)**	(0.55)
ML width	–0.32	–0.22	0.34	0.41	–0.19
	(0.21)	(0.39)	(0.18)	(0.11)	(0.45)
AP moment of inertia	**–0.45**	–0.10	0.25	0.32	–0.27
	(0.07)	(0.70)	(0.34)	(0.21)	(0.29)
ML moment of inertia	–0.39	–0.18	0.22	0.28	–0.25
	(0.12)	(0.50)	(0.39)	(0.28)	(0.32)
Polar moment of inertia	**–0.43**	–0.13	0.24	0.31	–0.27
	(0.08)	(0.61)	(0.35)	(0.23)	(0.30)
AP section modulus	**–0.50**	–0.13	0.10	0.14	–0.30
	(0.04)	(0.62)	(0.70)	(0.60)	(0.25)
ML section modulus	**–0.47**	–0.05	0.18	0.23	–0.33
	(0.06)	(0.84)	(0.49)	(0.38)	(0.20)
Ap slenderness	0.36	0.10	0.09	0.03	**0.48**
	(0.15)	(0.69)	(0.72)	(0.92)	**(0.05)**
ML slenderness	0.23	–0.01	0.04	–0.05	0.41
	(0.39)	(0.96)	(0.89)	(0.84)	(0.10)

Pearson correlation coefficients are shown with p values in parentheses. Significant correlations are shown in bold. Abbreviations are as shown in Table 1.

for young adult males. Further studies are needed to determine if this relationship holds over a wider (older) age range.

The data provide a new paradigm that may explain how variation in bone slenderness contributes to stress fracture risk. Individuals with narrow tibias were previously thought to show increased fatigue damage during intense training because the smaller bone size would lead to an overload situation (i.e., higher tissue level stresses).[1,2,12] This interpretation was based on the assumption that tissue mechanical properties did not vary among individuals. However, the current results indicated that tissue-level mechanical properties do vary among individuals. Specifically, the data suggest that there are at least two important tissue-level mechanical property variations that need to be considered to understand why bone size is a risk factor for stress fractures. Narrower tibias were comprised of tissue that was more brittle (low total energy) and was prone to accumulate more damage compared with tissue from wider tibia. Having tissue that is more or less damageable may be inconsequential during day-to-day activities. However, tissue-level mechanical properties like total energy and ductility become particularly important in defining the response of bone to an extreme loading condition, such as that expected during military training or during a fall. Total energy defines the amount of energy required to break a bone (important during a fall) and ductility and damageability define the amount of damage accumulated under overload or repetitive loading (important during military training). Furthermore, tissue stresses would be expected to remain higher for narrow tibias loaded in bending or torsion. Moment of inertia is related to the external diameter raised to the fourth power. Because whole bone stiffness and strength are correlated with moment of inertia,[17,27] a bone with a large external diameter should also show large overall stiffness and strength values. However, the ~30% variation in tissue modulus (Table 1) did not fully compensate for the ~100% variation in the moment of inertia or the section modulus (Table 1).[27] Thus, in situ damage accumulation may elicit a biological response (remodeling) that, coupled with the higher tissue stresses, exacerbates the fatigue process.[13,28] Consequently, individuals with narrow tibia may be at higher risk of stress fractures because of higher in vivo tissue stresses (overloading) coupled with tissue that is more prone to accumulating damage.

The data may also help explain why age is another risk factor for stress fractures.[7,29] Bone strength, postyield strain, and total energy decreased over the 17- to 46-year-old age range. This was consistent with previous studies[30–32] and indicated that cortical bone becomes less ductile (i.e., more brittle) and weaker with age and that these changes began early in life. This age-related decline in strength and ductility is thought to be a result of increased mineralization and remodeling.[33,34] Thus, even in the young adult age range, the amount of damage accumulated under vigorous loading regimens would be expected to increase with age. This variation in tissue ductility may increase the susceptibility of stress fracture risk for recruits that enter into military training at an older age.

These results, and those of others, indicated that not all cortical tissue was constructed in the same manner. The mechanical properties of cortical tissue vary with age,[30–32,35] across species,[35] among bones of the same individual,[36] and among anatomical sites within the same bone.[37,38] Here we showed that the average mechanical properties of cortical tissue also varied as a function of the overall size of the bone. This coupling between bone morphology and tissue-level mechanical properties has been attributed to an adaptive response of bone.[14,35,39] In this study, smaller tibia bone size was coupled with an increase

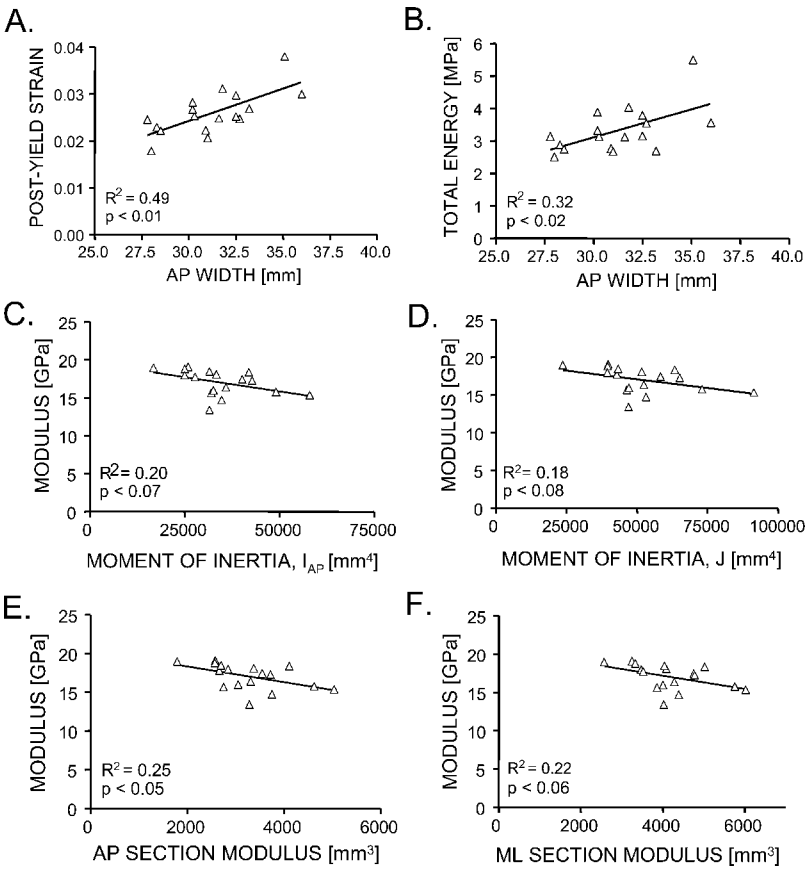

FIG. 5. (A) Postyield strain and (B) total energy correlated with AP width. Modulus decreased with (C) I_{AP}, (D) J, (E) AP section modulus, and (F) ML section modulus. Data were age-corrected based on a linear regression method.[22]

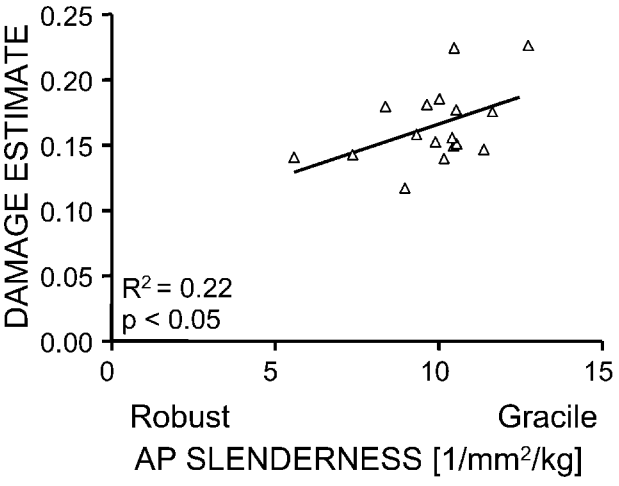

FIG. 6. Damageability correlated with AP slenderness suggesting that tibias that were more slender relative to body size and stature were comprised of tissue that accumulated more damage. Data were age-corrected based on a linear regression method.[22]

in tissue modulus. The goal of this adaptive response is to ensure that morphology and quality together meet mechanical demands. This coupling was observed when comparing bones subjected to widely varying mechanical demands from different species[35] and has also been used to explain the maturation of bone during growth.[40–43] Our current results suggested that this coupling might also exist for a particular bone (tibia) within the same species (human). Additional studies are needed to determine if similar relationships between morphology and quality exist for other long bones (femur, humerus, radius).

The relationship between morphology and tissue-level mechanical properties observed in the human skeleton was consistent with that observed for the mouse skeleton.[14] In both the mouse and human skeletons, genetic heterogeneity leads to variability in adult bone morphology and tissue level mechanical properties. A comparison of femurs from A/J and C57/BL6 (B6) inbred strains showed that A/J femurs were more slender than B6 as a result of the two strains having similar bone lengths, but A/J having a significantly smaller cross-sectional size and shape.[14] Despite the difference in bone size, the two strains showed similar whole bone stiffness values. The variability in bone slenderness was inversely related to mineral content, suggesting that bone morphology and mineral content were coordinately regulated so whole bone stiffness appropriately matched the mechanical demands imposed by weight bearing. However, as a result of regulating mineral content to match bone size, A/J femurs failed in a brittle manner and showed poor fatigue properties. In the human skeleton, smaller bones were stiffer and less ductile. Thus, a reciprocal relationship was observed between bone stiffness and ductility for both skeleton systems. This reciprocal relationship has been extensively reported for cortical bone,[15] and

it is thought to be a result of the nature of the compositional and structural factors that can be modulated on a biological level.[44–47] Although variation in mineral content may have explained the differences in brittleness for the mouse skeleton, we expect that the human skeleton will be more complex and that the variation in tissue-level mechanical properties will be a consequence of variable composition (mineral, collagen, water) as well as microarchitecture (lamellae, osteon size, porosity).

The calculated bending modulus and strength values, which were determined from machined bone samples and were thus quantified in a manner that was independent of bone size, were consistent with bone tensile properties,[30] as expected. Test samples were randomly selected to obtain representative mean values for each tibia and the variation in mechanical properties within each tibia was similar to the variability observed across tibias. Thus, we believe that the mean values reported here represent the generalized tissue-level mechanical behavior for each tibia.

Compared with back-calculating tissue-level mechanical properties from whole bone failure tests, the current method of measuring tissue-level mechanical properties directly from machined samples provided a broader range of mechanical properties that were needed to better understand why bone size is a risk factor for stress fractures. The mechanical properties included measures of ductility (i.e., postyield strain, total energy) as well as an independent measure of damageability (i.e., the damage parameter). These properties were chosen because they were relevant for understanding the material response of bones subjected to the vigorous, repetitive loading associated with military training and running. Postyield strain and total energy represent measures of tissue ductility and were assessed to discriminate between ductile and brittle failure modes. Materials that fail in a brittle manner show low postyield strain and total energy values. Variation in the ductility of cortical bone arises from differences in the initiation, accumulation, propagation, and coalescence of damage in the form of microcracks.[48,49] Variation in the damage parameter reflected differences in the amount of damage accumulated within the tissue and/or differences in the way damage degraded tissue stiffness. The damage parameter correlated negatively with postyield strain and total energy (R^2 = 0.22–0.25, $p < 0.05$) indicating that cortical tissue that failed in a brittle manner also tended to have higher tissue damageability or, accumulate more damage. Although the ex vivo bending tests do not necessarily reflect the in vivo loads imposed on the tibia,[17,50–52] the bending loads were expected to induce a combination of tensile, compressive, and shear damage[53] that may be sufficiently complex to represent a generalized variation in bone quality among human tibias.

The results of this study provide new insight into why bone size is a risk factor for stress fractures. Stress fractures are believed to be a consequence of excess damage accumulation following intense, repetitive activities. Biological processes that attempt to repair the damage may further weaken the tissue because the increased resorption results in increased tissue porosity.[54] However, the actual contribution of biological repair processes to stress fracture risk remains unclear.[55] Damage, in the form of microcracks, is the expected sequelae of repetitive loading following normal, daily activities.[56] Intense loading conditions, such as those associated with military training and long distance running, are expected to further increase in situ damage accumulation and degrade tissue-level mechanical properties.[13] Therefore, under extreme loading conditions (e.g., military training), variation in bone quality, specifically tissue damageability, may be a contributing factor to the increased risk of stress fracture for individuals with more slender bones. The current data suggested that bone morphology could be used as a predictor of tissue fragility and stress fracture risk in the absence of available noninvasive imaging techniques that accurately measure bone damageability.

ACKNOWLEDGMENTS

The authors thank the U.S. Department of Defense (DAMD17-01-1-0806; DAMD17-98-1-8515) and the Musculoskeletal Transplant Foundation for their support of this research.

REFERENCES

1. Milgrom C, Giladi M, Simkin A, Rand N, Kedem R, Kashtan H, Stein M, Gomori M 1989 The area moment of inertia of the tibia: A risk factor for stress fractures. J Biomech **22:**1243–1248.
2. Beck TJ, Ruff CB, Mourtada FA, Shaffer RA, Maxwell-Williams K, Kao GL, Sartoris DJ, Brodine S 1996 Dual-energy X-ray absorptiometry derived structural geometry for stress fracture prediction in male U.S. Marine Corps recruits. J Bone Miner Res **11:**645–653.
3. Milgrom C, Giladi M, Stein M, Kashtan H, Margulies JY, Chisin R, Steinberg R, Aharonson Z 1985 Stress fractures in military recruits. A prospective study showing an unusually high incidence. J Bone Joint Surg Br **67:**732–735.
4. Lappe JM, Stegman MR, Recker RR 2001 The impact of lifestyle factors on stress fractures in female Army recruits. Osteoporos Int **12:**35–42.
5. Milgrom C, Finestone A, Sharkey N, Hamel A, Mandes V, Burr D, Arndt A, Ekenman I 2002 Metatarsal strains are sufficient to cause fatigue fracture during cyclic overloading. Foot Ankle Int **23:**230–235.
6. Friedl KE, Nuovo JA, Patience TH, Dettori JR 1992 Factors associated with stress fracture in young army women: Indications for further research. Mil Med **157:**334–338.
7. Brudvig TJ, Gudger TD, Obermeyer L 1983 Stress fractures in 295 trainees: A one-year study of incidence as related to age, sex, and race. Mil Med **148:**666–667.
8. Bennell K, Matheson G, Meeuwisse W, Brukner P 1999 Risk factors for stress fractures. Sports Med **28:**91–122.
9. Jones BH, Thacker SB, Gilchrist J, Kimsey CD Jr, Sosin DM 2002 Prevention of lower extremity stress fractures in athletes and soldiers: A systematic review. Epidemiol Rev **24:**228–247.
10. Giladi M, Milgrom C, Simkin A, Danon Y 1991 Stress fractures. Identifiable risk factors. Am J Sports Med **19:**647–652.
11. Giladi M, Milgrom C, Simkin A, Stein M, Kashtan H, Margulies J, Rand N, Chisin R, Steinberg R, Aharonson Z 1987 Stress fractures and tibial bone width. A risk factor. J Bone Joint Surg Br **69:**326–329.
12. Crossley K, Bennell KL, Wrigley T, Oakes BW 1999 Ground reaction forces, bone characteristics, and tibial stress fracture in male runners. Med Sci Sports Exerc **31:**1088–1093.
13. Mori S, Burr DB 1993 Increased intracortical remodeling following fatigue damage. Bone **14:**103–109.

14. Jepsen KJ, Pennington DE, Lee YL, Warman M, Nadeau J 2001 Bone brittleness varies with genetic background in A/J and C57BL/6J inbred mice. J Bone Miner Res **16:**1854–1862.
15. Currey JD 1984 Effects of differences in mineralization on the mechanical properties of bone. Philos Trans R Soc Lond B Biol Sci **304:**509–518.
16. Ruff CB 2000 Body size, body shape, and long bone strength in modern humans. J Hum Evol **38:**269–290.
17. Selker F, Carter DR 1989 Scaling of long bone fracture strength with animal mass. J Biomech **22:**1175–1183.
18. Gustafson MB, Martin RB, Gibson V, Storms DH, Stover SM, Gibeling J, Griffin L 1996 Calcium buffering is required to maintain bone stiffness in saline solution. J Biomech **29:**1191–1194.
19. Nádai A 1950 Theory of Flow and Fracture of Solids. Engineering Societies Monographs. McGraw-Hill, New York, New York, USA.
20. Lemaitre J 1992 A Course on Damage Mechanics. Springer-Verlag, Berlin, New York.
21. Jepsen KJ, Davy DT 1997 Comparison of damage accumulation measures in human cortical bone. J Biomech **30:**891–894.
22. Di Masso RJ, Font MT, Capozza RF, Detarsio G, Sosa F, Ferretti JL 1997 Long-bone biomechanics in mice selected for body conformation. Bone **20:**539–545.
23. Ogden CL, Fryar CD, Carroll MD, Flegal KM 2004 Mean body weight, height, and body mass index, United States 1960-2002. Adv Data **347:**1–17.
24. Miller GJ, Purkey WW Jr 1980 The geometric properties of paired human tibiae. J Biomech **13:**1–8.
25. Christian JC, Yu PL, Slemenda CW, Johnston CC Jr 1989 Heritability of bone mass: A longitudinal study in aging male twins. Am J Hum Genet **44:**429–433.
26. Kiel DP, Hannan MT, Broe KE, Felson DT, Cupples LA 2001 Can metacarpal cortical area predict the occurrence of hip fracture in women and men over 3 decades of follow-up? Results from the Framingham Osteoporosis Study. J Bone Miner Res **16:**2260–2266.
27. van der Meulen MC, Jepsen KJ, Mikic B 2001 Understanding bone strength: Size isn't everything. Bone **29:**101–104.
28. Burr DB, Forwood MR, Fyhrie DP, Martin RB, Schaffler MB, Turner CH 1997 Bone microdamage and skeletal fragility in osteoporotic and stress fractures. J Bone Miner Res **12:**6–15.
29. Shaffer RA, Brodine SK, Almeida SA, Williams KM, Ronaghy S 1999 Use of simple measures of physical activity to predict stress fractures in young men undergoing a rigorous physical training program. Am J Epidemiol **149:**236–242.
30. Burstein AH, Reilly DT, Martens M 1976 Aging of bone tissue: Mechanical properties. J Bone Joint Surg Am **58:**82–86.
31. McCalden RW, McGeough JA, Barker MB, Court-Brown CM 1993 Age-related changes in the tensile properties of cortical bone. The relative importance of changes in porosity, mineralization, and microstructure. J Bone Joint Surg Am **75:**1193–1205.
32. Currey JD, Butler G 1975 The mechanical properties of bone tissue in children. J Bone Joint Surg Am **57:**810–814.
33. Evans FG 1976 Age changes in mechanical properties and histology of human compact bone. Yearb Phys Anthropol **20:**1361–1372.
34. Currey JD, Brear K, Zioupos P 1996 The effects of ageing and changes in mineral content in degrading the toughness of human femora. J Biomech **29:**257–260.
35. Currey JD 1979 Mechanical properties of bone tissues with greatly differing functions. J Biomech **12:**313–319.
36. Papadimitriou HM, Swartz SM, Kunz TH 1996 Ontogenetic and anatomic variation in mineralization of the wing skeleton of the Mexican free-tailed bat, *Tadarida brasiliensis*. J Zool **240:**411–426.
37. Riggs CM, Vaughan LC, Evans GP, Lanyon LE, Boyde A 1993 Mechanical implications of collagen fibre orientation in cortical bone of the equine radius. Anat Embryol (Berl) **187:**239–248.
38. Skedros JG, Dayton MR, Sybrowsky CL, Bloebaum RD, Bachus KN 2003 Are uniform regional safety factors an objective of adaptive modeling/remodeling in cortical bone? J Exp Biol **206:**2431–2439.
39. Ferretti JL, Capozza RF, Mondelo N, Zanchetta JR 1993 Interrelationships between densitometric, geometric, and mechanical properties of rat femora: Inferences concerning mechanical regulation of bone modeling. J Bone Miner Res **8:**1389–1396.
40. Ferretti JL, Cointry GR, Capozza RF, Frost HM 2003 Bone mass, bone strength, muscle-bone interactions, osteopenias and osteoporoses. Mech Ageing Dev **124:**269–279.
41. Heinrich RE 1999 Ontogenetic changes in mineralization and bone geometry in the femur of muskoxen (Ovibos moschatus). J Zool **247:**215–223.
42. Brear K, Currey JD, Pond CM 1990 Ontogenetic changes in the mechanical properties of the femur of the polar bear Ursus maritimus. J Zool **222:**49–58.
43. Carrier D, Leon LR 1990 Skeletal growth and function in the California gull (*Larus californicus*). J Zool **222:**375–389.
44. Martin RB, Boardman DL 1993 The effects of collagen fiber orientation, porosity, density, and mineralization on bovine cortical bone bending properties. J Biomech **26:**1047–1054.
45. Portigliatti Barbos M, Bianco P, Ascenzi A, Boyde A 1984 Collagen orientation in compact bone: II. Distribution of lamellae in the whole of the human femoral shaft with reference to its mechanical properties. Metab Bone Dis Relat Res **5:**309–315.
46. Skedros JG, Sybrowsky CL, Parry TR, Bloebaum RD 2003 Regional differences in cortical bone organization and microdamage prevalence in Rocky Mountain mule deer. Anat Rec **274A:**837–850.
47. Skedros JG, Hunt KJ 2004 Does the degree of laminarity correlate with site-specific differences in collagen fibre orientation in primary bone? An evaluation in the turkey ulna diaphysis. J Anat **205:**121–134.
48. Jepsen KJ, Davy DT, Akkus O 2001 Observations of damage in bone. In: Cowin SC (ed.) Bone Mechanics Handbook, 2nd ed. CRC Press, Boca Raton, FL, USA, pp. 17.1–17.18.
49. Currey JD, Brear K 1992 Fractal analysis of compact bone and antler fracture surfaces. Biomimetics **1:**103–118.
50. Ruff CB 1984 Allometry between length and cross-sectional dimensions of the femur and tibia in Homo sapiens sapiens. Am J Phys Anthropol **65:**347–358.
51. Lanyon LE, Hampson WG, Goodship AE, Shah JS 1975 Bone deformation recorded in vivo from strain gauges attached to the human tibial shaft. Acta Orthop Scand **46:**256–268.
52. Burr DB, Milgrom C, Fyhrie D, Forwood M, Nyska M, Finestone A, Hoshaw S, Saiag E, Simkin A 1996 In vivo measurement of human tibial strains during vigorous activity. Bone **18:**405–410.
53. Boyce TM, Fyhrie DP, Glotkowski MC, Radin EL, Schaffler MB 1998 Damage type and strain mode associations in human compact bone bending fatigue. J Orthop Res **16:**322–329.
54. Schaffler MB, Burr DB 1988 Stiffness of compact bone: Effects of porosity and density. J Biomech **21:**13–16.
55. Milgrom C, Finestone A, Novack V, Pereg D, Goldich Y, Kreiss Y, Zimlichman E, Kaufman S, Liebergall M, Burr D 2004 The effect of prophylactic treatment with risedronate on stress fracture incidence among infantry recruits. Bone **35:**418–424.
56. Schaffler MB, Radin EL, Burr DB 1990 Long-term fatigue behavior of compact bone at low strain magnitude and rate. Bone **11:**321–326.

Address reprint requests to:
Karl J Jepsen, PhD
Department of Orthopaedics
Mount Sinai School of Medicine
Box 1188, One Gustave L. Levy Place
New York, NY 10029, USA
E-mail: karl.jepsen@mssm.edu

Received in original form November 12, 2004; revised form March 16, 2005; accepted March 28, 2005.

JOURNAL OF BONE AND MINERAL RESEARCH
Volume 20, Number 11, 2005
Published online on July 11, 2005; doi: 10.1359/JBMR.050707

Genetic Variation in Bone Growth Patterns Defines Adult Mouse Bone Fragility

Christopher Price,[1] Brad C Herman,[1] Thomas Lufkin,[2] Haviva M Goldman,[3] and Karl J Jepsen[1]

ABSTRACT: Femoral morphology and composition were determined for three inbred mouse strains between ages E18.5 and 1 year. Genotype-specific variation in postnatal, pubertal, and postpubertal growth patterns and mineral accrual explained differences in adult bone trait combinations and thus bone fragility.

Introduction: Fracture risk is strongly regulated by genetic factors. However, this regulation is generally considered complex and polygenic. Therefore, the development of effective genetic-based diagnostic and treatment tools hinges on understanding how multiple genes and multiple cell types interact to create mechanically functional structures. The goal of this study was to connect variability in whole bone mechanical function, including measures of fragility, to variability in the biological processes underlying skeletal development. We accomplished this by testing for variation in bone morphology and composition among three inbred mouse strains from E18.5 to 1 year of age.
Materials and Methods: Mid-diaphyseal cross-sectional areas, diameters, moments of inertia, and ash content were determined for three strains of mice with widely differing adult whole bone femoral mechanical properties (A/J, C57BL/6J, and C3H/HeJ) at E18.5 and postnatal days 1, 7, 14, 28, 56, 112, 182, and 365 (n = 5–15 mice/strain/age).
Results: Significant differences in the magnitude and rate of change in morphological and compositional bone traits were observed among the three strains at each phase of growth, including prenatal, postnatal, pubertal, and adult ages. These genotype-specific variations in growth patterns mathematically determined how variation in adult bone trait combinations and mechanical properties arose. Furthermore, six bone traits were identified that characterize phenotypic variability in femoral growth. These include (1) bone size and shape at postnatal day 1, (2) periosteal and (3) endosteal expansion during early growth, (4) periosteal expansion and (5) endosteal contraction in later growth, and (6) ash content. These results show that genetic variability in adult bone traits arises from variation in biological processes at each phase of growth.
Conclusions: Inbred mice achieve different combinations of adult bone traits through genotype-specific regulation of bone surface activity, growth patterns, and whole bone mineral accrual throughout femoral development. This study provides a systematic approach, which can be applied to the human skeleton, to uncover genetic control mechanisms influencing bone fragility.
J Bone Miner Res 2005;20:1983–1991. Published online on July 11, 2005; doi: 10.1359/JBMR.050707

Key words: genetics, inbred mice, growth and development, bone biomechanics, bone fragility, morphology, ash content

INTRODUCTION

Genetic factors are generally acknowledged to play an important role in the determination of skeletal fragility. Clinically, genetic variability in BMD,[1] bone quality,[2] adult bone morphology,[3] and the kinetics of bone loss[4,5] all contribute to the variation in fracture risk.[6] Therefore, genetic-based screening tools that identify an individual's skeletal growth potential and/or potential for bone loss could be used for the early diagnosis of osteoporotic fracture risk and for tailored treatment regimens thereafter.[7] However, these genetic factors are not completely understood. Additionally, the processes of bone growth and bone loss are genetically complex, such that the modeling and remodeling of complex structures involves the coordinated expression of many genes by multiple cell types (osteoblasts, osteoclasts, and osteocytes).[7] Therefore, a primary challenge for developing effective genetic-based diagnostic tools for fracture risk will be to understand how multiple genes, in multiple cell types, interact throughout life to create and maintain structures that are mechanically and biologically functional.[8]

To study the functional connections between genotype and skeletal fragility, we adopted a top-down approach that

The authors have no conflict of interest.

[1]Leni & Peter W. May Department of Orthopaedics, Mount Sinai School of Medicine, New York, New York, USA; [2]Stem Cell and Developmental Biology, Genome Institute of Singapore, Singapore; [3]Department of Neurobiology and Anatomy, Drexel University College of Medicine, Philadelphia, Pennsylvania, USA.

reveals the functional connections between genotype and skeletal fragility.[9] Our approach uses long bones from inbred mouse strains to relate genetic variability in whole bone mechanical properties to the underlying biological processes regulating bone growth and loss in a systematic and hierarchical manner. Previous research using inbred mice has shown genotype-specific variability in skeletal morphology,[10–12] BMD,[13] mechanical properties,[14,15] bone formation rates,[16,17] and responsiveness to mechanical stimulation.[18,19] Previously, we showed that individual inbred mouse strains exhibited a particular combination of cortical area (Ct.Ar), polar moment of inertia (J_o), and mineral content (ash content) that together explained 66–88% of the genetic variability in adult whole bone mechanical properties.[9] These results indicated that the combination of transverse bone size, shape, and material quality was responsible for the particular repertoire of stiffness, strength, and toughness that characterized each strain. The next step in our systematic approach was to determine how genetic variability in these three physical bone traits (Ct.Ar, J_o, and ash content) arises during the growth process.

Bone traits are influenced by both genetic and environmental factors during growth, and specific combinations of bone traits are established to satisfy the mechanical demands associated with weight bearing.[20] Long bone diaphyses are hollow cylinders whose size and shape can be mathematically determined by the relative amounts of bone apposition and resorption on the periosteal and endosteal surfaces.[21–24] We hypothesize that genetic variability in the rates of periosteal and endosteal expansion throughout life (i.e., growth patterns) defines genotype-specific combinations of adult bone traits. To test this hypothesis, we compared changes in femoral morphology (Ct.Ar and J_o) and composition (ash content) across development (from embryonic day 18.5 [E18.5] to 1 year). Transverse growth was studied because these traits contribute predominantly to the resistance of in vivo loads.[25] Three genetically distinct inbred mouse strains, A/J (A), C57BL/6J (B6), and C3H/HeJ (C3H), with widely differing adult bone trait magnitudes, were examined to better understand the expansive growth of bone surfaces and how this growth leads to unique combinations of adult morphological (Ct.Ar, Tt.Ar, Ma.Ar, and J_o) and compositional (ash content) trait values.[9] We show that variability in skeletal growth patterns reveals the biological and genetic control mechanisms that define adult physical bone traits and, consequently, bone fragility.

MATERIALS AND METHODS

Animals

Female (n = 20/strain) and male (n = 10/strain) A/J (A), C57BL/6J (B6), and C3H/HeJ (C3H) mice were purchased from Jackson Laboratory (Bar Harbor, ME, USA) at 6–8 weeks of age and used to establish breeding colonies. Mice were fed a standard mouse chow (Purina Laboratory Chow 5001; Purina Mills) and water ad libitum and kept on a 12-h light:dark cycle. Matings were monitored, and after 4 weeks of weaning, the offspring were separated by sex and housed with four to five mice per cage. Female offspring were killed at selected time-points for analysis: these included E18.5, postnatal day 1, 7, 14, 28, 56, 112, 182, and 365 (Table 1). For the E18.5 age group, pregnant females were identified by the first appearance of a vaginal plug (designated as day E0.5). The pups were extracted 18 days later through caesarian section and killed by decapitation. All mice 1 day of age and older were killed by carbon dioxide asphyxiation and decapitation. The Mount Sinai Institutional Animal Care and Use Committee approved all procedures for the treatment of mice.

Morphological traits

Right femurs were harvested and embedded in polymethylmethacrylate as described previously.[14] Transverse sections of the femoral diaphyses (150 μm in thickness) were obtained using a low-speed diamond-coated wafering saw (Buehler, Lake Bluff, IL, USA) from a site immediately distal to the third trochanter. The sections were affixed to acrylic slides, polished to 1-μm finish, and stained using von Kossa's method.[26] The sections were imaged with a digital camera (Sony Exwave HAD, 3CCD Camera; Sony) attached to a visible light microscope (Zeiss Axioplan2; Zeiss). The pixel resolution of this optical imaging system was 2.1 μm. An advanced image analysis software package (IMAQ Vision Builder 6.0; National Instruments Corp., Austin, TX, USA) was used to quantify the cross-sectional areas (total area [Tt.Ar], cortical area [Ct.Ar], and marrow area [Ma.Ar]), cortical thickness (Ct.Th), and the polar moment of inertia (J_o). Young bones (ages E18.5 through 2 weeks of age) had a predominantly woven appearance with considerable cortical porosity. Therefore, at these time-points, morphometric measurements included all porosities within the cortical shell and were considered apparent traits. Three cross-sections were analyzed per bone, and the values were averaged. To establish rates of surface growth, the time normalized change in Tt.Ar and Ma.Ar during the early phase of growth (1–28 days of age) and the later phase of growth (28–112 days of age) were obtained from the following equations for all strains:

$$\Delta Tt.Ar_{1-28} = [Tt.Ar_{28} - avg(Tt.Ar_1)]/28 \text{ days} \quad (1)$$

$$\Delta Tt.Ar_{28-112} = [Tt.Ar_{112} - avg(Tt.Ar_{28})]/84 \text{ days} \quad (2)$$

$$\Delta Ma.Ar_{1-28} = [Ma.Ar_{28} - avg(Ma.Ar_1)]/28 \text{ days} \quad (3)$$

$$\Delta Ma.Ar_{Ma.ArMax-112} = [Ma.Ar_{112} - avg(Ma.Ar_{Ma.ArMax})]/(112 - Ma.ArMax) \text{ days} \quad (4)$$

The subscript refers to the age(s) over which the rate was determined. Ma.ArMax corresponds to the age at which maximum Ma.Ar was obtained for a given strain. This age was used as the initial time-point to calculate the rate of marrow infilling during later growth. avg($Tt.Ar_i$) and avg($Ma.Ar_i$) refers to the strain average Tt.Ar and Ma.Ar value at time-point i.

Table 1. Body Weight and Morphological Traits for Femoral Diaphyses of Three Inbred Mouse Strains Between Embryonic Day 18.5 (E18.5) and 1 Year of Age

Strain (age)	*N*	*Weight (g)*	*Cortical area (mm^2)*	*Total area (mm^2)*	*Marrow area (mm^2)*	*J_o (mm^4)*	*Average cortical thickness (mm)*
A							
E18.5	5	—	0.11 ± 0.02†	0.16 ± 0.02†,‡	0.05 ± 0.01†,‡	0.004 ± 0.001†	0.10 ± 0.02
1d	15	1.3 ± 0.1	0.13 ± 0.02†	0.30 ± 0.05†	0.17 ± 0.03	0.010 ± 0.004†	0.08 ± 0.01
7d	12	2.8 ± 0.5‡	0.22 ± 0.02	0.50 ± 0.05†,‡	0.28 ± 0.04†,‡	0.028 ± 0.005	0.11 ± 0.01†
14d	8	6.0 ± 0.4	0.23 ± 0.05‡	0.59 ± 0.08†,‡	0.35 ± 0.05†,‡	0.035 ± 0.011†,‡	0.10 ± 0.02†
28d	8	10.8 ± 1.6	0.37 ± 0.03‡	0.82 ± 0.06†,‡	0.45 ± 0.04†,‡	0.076 ± 0.012†,‡	0.13 ± 0.01†
56d	9	16.4 ± 2.3	0.51 ± 0.09‡	0.97 ± 0.10†,‡	0.46 ± 0.03†	0.119 ± 0.027†,‡	0.18 ± 0.03
112d	13	22.9 ± 3.0†	0.74 ± 0.04‡	1.15 ± 0.8†,‡	0.41 ± 0.05†,‡	0.189 ± 0.023†,‡	0.25 ± 0.02†,‡
182d	12	23.2 ± 1.6†,‡	0.79 ± 0.04‡	1.25 ± 0.06†,‡	0.46 ± 0.03†,‡	0.224 ± 0.024†,‡	0.26 ± 0.02†,‡
365d	9	24.7 ± 2.4	0.79 ± 0.06‡	1.28 ± 0.11†,‡	0.49 ± 0.07†	0.228 ± 0.037†,‡	0.25 ± 0.02‡
B6							
E18.5	10	—	0.17 ± 0.04*,‡	0.33 ± 0.04*,‡	0.16 ± 0.04*,‡	0.014 ± 0.004*,‡	0.10 ± 0.03
1d	15	1.3 ± 0.1	0.16 ± 0.03*	0.35 ± 0.03*	0.19 ± 0.04	0.014 ± 0.003*	0.09 ± 0.02
7d	12	3.1 ± 0.3‡	0.19 ± 0.05	0.61 ± 0.05*	0.41 ± 0.05*,‡	0.032 ± 0.008	0.08 ± 0.02*
14d	12	6.4 ± 0.5‡	0.24 ± 0.04‡	0.90 ± 0.08*,‡	0.66 ± 0.06*,‡	0.061 ± 0.012*	0.08 ± 0.01*,‡
28d	6	10.9 ± 1.0	0.39 ± 0.05	1.24 ± 0.09*,‡	0.85 ± 0.06*,‡	0.133 ± 0.023*,‡	0.11 ± 0.01*,‡
56d	11	16.8 ± 0.8	0.57 ± 0.03‡	1.47 ± 0.07*,‡	0.90 ± 0.05*,‡	0.226 ± 0.022*,‡	0.16 ± 0.01‡
112d	10	20.9 ± 0.6*	0.75 ± 0.03‡	1.55 ± 0.06*,‡	0.80 ± 0.04*,‡	0.297 ± 0.026*	0.21 ± 0.03*,‡
182d	9	21.7 ± 0.9*	0.76 ± 0.05‡	1.48 ± 0.09*,‡	0.72 ± 0.06*,‡	0.283 ± 0.029*	0.20 ± 0.04*,‡
365d	10	25.2 ± 1.8	0.82 ± 0.06‡	1.82 ± 0.10*	1.00 ± 0.07*,‡	0.387 ± 0.044*	0.20 ± 0.02‡
C3H							
E18.5	8	—	0.13 ± 0.01†	0.24 ± 0.03*,†	0.11 ± 0.02*,†	0.007 ± 0.001†	0.10 ± 0.01
1d	15	1.4 ± 0.1	0.15 ± 0.03	0.32 ± 0.03	0.16 ± 0.02	0.012 ± 0.002	0.09 ± 0.02
7d	9	4.4 ± 0.5*,†	0.23 ± 0.06	0.56 ± 0.07*	0.33 ± 0.04*,†	0.032 ± 0.010	0.10 ± 0.02
14d	10	5.7 ± 0.4†	0.31 ± 0.03*,†	0.77 ± 0.11*,†	0.46 ± 0.10*,†	0.059 ± 0.015*	0.12 ± 0.01†
28d	8	10.4 ± 1.5	0.43 ± 0.05*	0.97 ± 0.7*,†	0.54 ± 0.04*,†	0.107 ± 0.017*,†	0.14 ± 0.01†
56d	10	15.6 ± 2.2	0.67 ± 0.07*,†	1.11 ± 0.09*,†	0.44 ± 0.04†	0.174 ± 0.029*,†	0.21 ± 0.04†
112d	11	22.4 ± 1.3	1.08 ± 0.04*,†	1.41 ± 0.06*,†	0.34 ± 0.03*,†	0.310 ± 0.025*	0.34 ± 0.01*,†
182d	9	20.9 ± 0.9*	1.08 ± 0.05*,†	1.35 ± 0.05*,†	0.26 ± 0.04*,†	0.285 ± 0.024*	0.37 ± 0.03*,†
365d	7	23.7 ± 1.8	1.29 ± 0.17*,†	1.71 ± 0.23†	0.42 ± 0.10†	0.448 ± 0.115*	0.35 ± 0.04*,†

* Significantly different from A, ANOVA $p < 0.05$.
† Significantly different from B6, ANOVA $p < 0.05$.
‡ Significantly different from C3H, ANOVA $p < 0.05$.

Compositional traits

Ash content was assessed for the left femurs of all mice 2 weeks of age and older. These femurs had previously been loaded to failure in four-point bending (data not included). The diaphyseal pieces were retrieved and cleaned of all soft tissues under a stereomicroscope. The hydrated, dried, and ashed weights were determined as described previously.[9] Water content was defined as the hydrated weight minus dried weight and expressed as a percentage of hydrated weight. Ash content was determined as the ash weight normalized for hydrated weight.

Statistics

All results are expressed as mean ± SD. Differences in trait values among the three genotypes at each time-point were determined with a one-way ANOVA and a Tukey's posthoc test. A p value less than 0.05 was considered significant (GraphPad Software, San Diego, CA, USA).

RESULTS

Overall changes in femoral diaphyseal structure

All three strains underwent qualitatively similar changes in bone architecture, size, and shape of the mid-diaphyseal cortex as a function of age (Fig. 1). For example, each strain exhibited an entirely woven or porous tissue microstructure at E18.5. However, by 14 days of age, the woven tissue was located only in the posterior-lateral quadrant, and by 28 days of age, the entire mid-diaphysis exhibited a solid, compact, lamellar tissue structure. However, despite similar overall growth patterns, significant variation in bone size, shape, and composition were observed among the strains throughout growth (Table 1).

Prenatal bone growth

Significant differences in total area (Tt.Ar), cortical area (Ct.Ar), and polar moment of inertia (J_o) were observed as early as E18.5 (Fig. 2A; ANOVA, $p < 0.05$). B6 mice showed the largest Ct.Ar, Tt.Ar, and J_o, whereas A mice showed the smallest. C3H mice more closely resembled A mice at E18.5. Between E18.5 and 1 day of age none of the morphological traits changed in B6 mice. In contrast, A and C3H mice showed increases in all three traits, so that by 1 day of age only A mice showed significantly smaller Tt.Ar, Ct.Ar, and J_o values compared with B6 (Fig. 2B; $p < 0.05$).

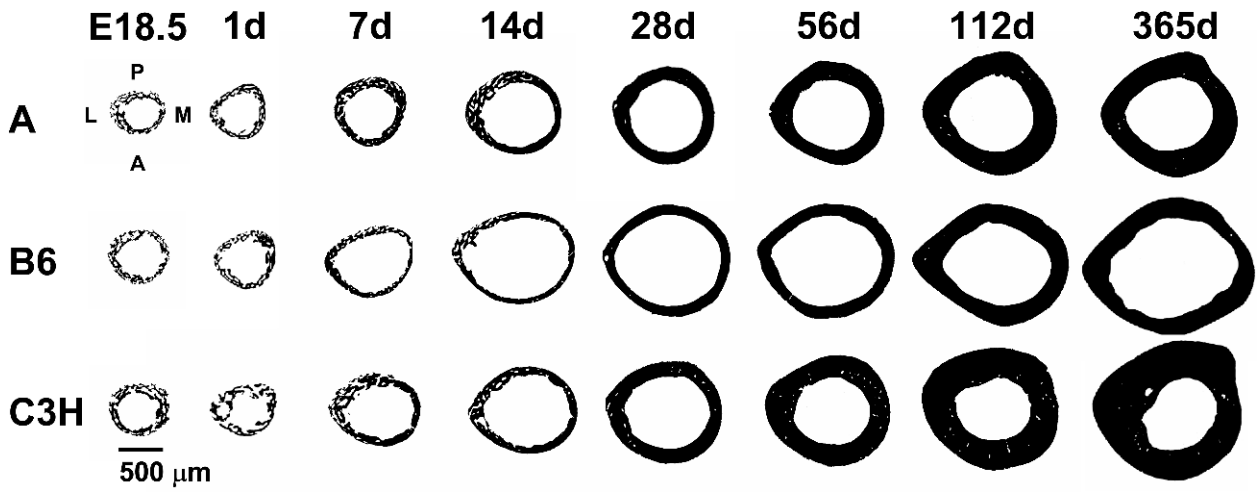

FIG. 1. Variation in femoral cross-sectional morphology across development for female A, B6, and C3H mice. Sections represent equivalent locations within the femoral diaphysis taken immediately distal to the third trochanter. Note change from a porous, woven structure to a compact, lamellar structure between P1 and P28 days of age. Scale bar shown applies to all images.

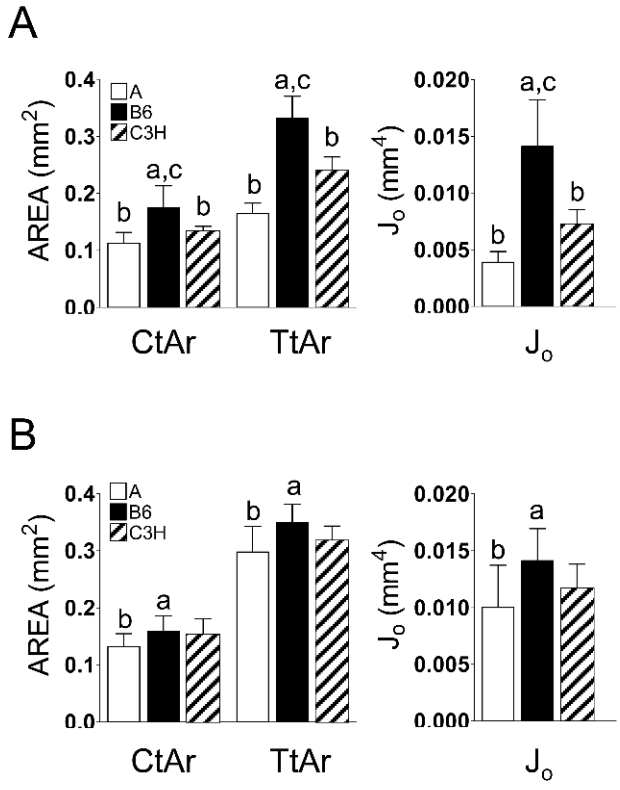

FIG. 2. Variation in femoral cortical area (Ct.Ar), total area (Tt.Ar), and polar moment of inertia (J_o) among A, B6, and C3H mice at (A) embryonic day 18.5 (E18.5) and (B) postnatal day 1. a, b, and c indicates a significant difference from A, B6, and C3H mice, respectively (ANOVA, $p < 0.05$).

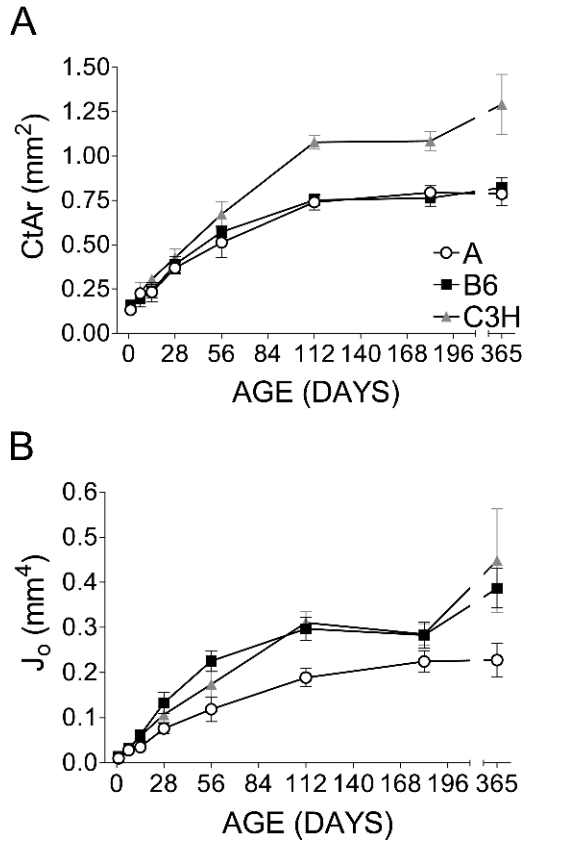

FIG. 3. Variation in (A) cortical area (Ct.Ar), (B) polar moment of inertia (J_o), and (C) ash content across development for A, B6, and C3H femurs. Significant differences among strains in Ct.Ar, J_o, and ash content are indicated in Table 1.

Postnatal changes in Ct.Ar and J_o

After birth, Ct.Ar and J_o increased nonlinearly to 112 days of age (Figs. 3A and 3B). Significant differences in Ct.Ar and J_o values were observed among the strains throughout development (Table 1); however, these differences became more prominent at 56 days of age. For Ct.Ar, A and B6 mice showed similar values beyond 7 days of age, whereas C3H mice showed larger Ct.Ar than both A and

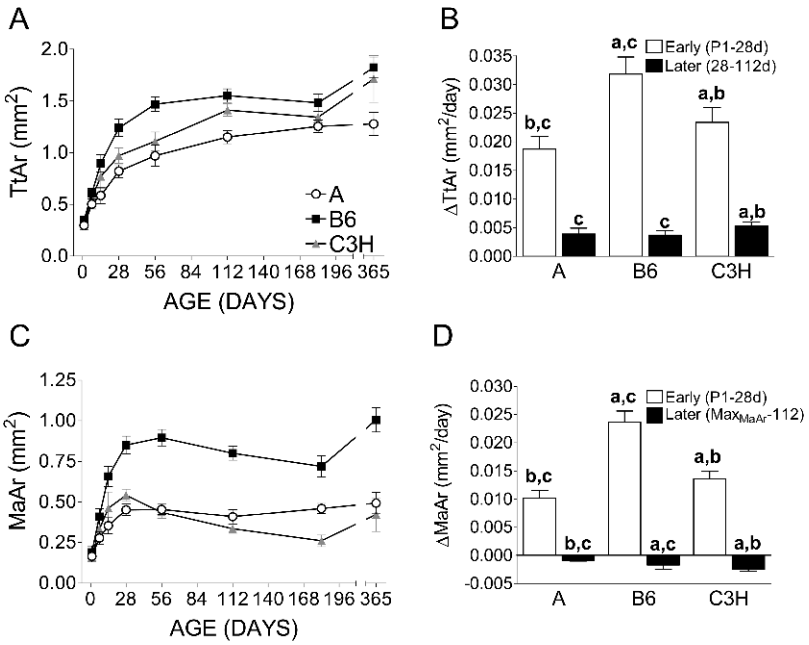

FIG. 4. Variation in femoral total area (Tt.Ar) and marrow area (Ma.Ar) among A, B6, and C3H female mouse strains. (A) Changes in total area across development. (B) Rate of change in total area during early growth (P1–P28 days of age) and later growth (28–112 days of age). (C) Changes in marrow area across development. (D) Rate of change in marrow area during early growth (P1–P28 days of age) and growth after maximum marrow area was achieved ($Ma.Ar_{Max}$–112 days of age). Significant differences among strains in Tt.Ar and Ma.Ar are indicated in Table 1. a, b, and c indicates a significant difference from A, B6, and C3H mice, respectively, at the indicated timepoint.

B6 after 14 days of age (ANOVA, $p < 0.05$). For J_o, B6 and C3H mice showed similar values beyond 56 days of age, whereas A mice showed smaller values compared with B6 and C3H beyond 14 days of age ($p < 0.05$). These differences in physical bone traits were accompanied by nearly identical age-related increases in body weight among all strains (Table 1).

Postnatal expansion of the periosteal surface

Tt.Ar increased nonuniformly with age in a genotype-dependent manner (Fig. 4A). Each strain achieved 80–90% of adult Tt.Ar and periosteal diameter by 28 days of age. In contrast, all three strains achieved only 40–50% of adult weight, Ct.Ar, and J_o by this age. These data indicated that the periosteum expanded rapidly for all strains early in life. However, the rate of expansion at the periosteum (i.e., increase in Tt.Ar per day) during early growth, and the size of Tt.Ar at 28 days of age differed significantly among the strains (B6 > C3H > A; ANOVA, $p < 0.05$; Fig. 4B; Table 1). Between 28 and 112 days of age, the average rate of increase in Tt.Ar was reduced by ~80% compared with the rates observed between P1 and P28 days of age. During the later phase of growth (28–112 days), the rate of Tt.Ar expansion was greatest in C3H mice, whereas A and B6 mice showed similarly lower rates of expansion ($p < 0.05$). Age-related changes in periosteal diameter mirrored the changes in Tt.Ar, as expected (data not shown).

Postnatal expansion of the endosteal surface

Like Tt.Ar, marrow area (Ma.Ar) also changed nonuniformly with age and in a genotype-dependent manner (Fig. 4C). All mouse strains exhibited similar Ma.Ar values at birth and exhibited rapid postnatal marrow expansion between P1 and P28 days of age. During this early growth phase, B6 femurs exhibited the greatest rate of endosteal expansion (resorption), followed by C3H mice, and then A mice, resulting in significant differences in Ma.Ar size at 28 days of age (A < B6 < C3H; ANOVA, $p < 0.05$; Fig. 4D). Maximum Ma.Ar values were achieved for A and C3H mice at ~28 days of age, whereas this did not occur until 56 days of age for B6 mice. After reaching maximal Ma.Ar values, all strains exhibited decreases in Ma.Ar, indicating that the endosteal surface underwent a reversal in biological activity from net resorption to net apposition (i.e., infilling). During the period between the time of maximal Ma.Ar and 112 days of age, the three strains of mice showed significantly different rates of endosteal contraction (apposition; A < B6 < C3H; $p < 0.05$). As a result, adult Ma.Ar at 112 days of age was largest in B6 mice because of the early rapid expansion of the marrow cavity and smallest in C3H mice because of its slower marrow excavation and larger fractional infilling. Age-related changes in endosteal diameter were similar to those observed for Ma.Ar, as expected (data not shown).

Age-related changes in cortical thickness

Changes in cortical thickness (Ct.Th) reflected the relative rate of expansion of the periosteal and endosteal surfaces. The average cortical thickness increased nonlinearly between birth and 1 year of age in all three strains (Fig. 5). Between E18.5 and 7 days of age, the average cortical thickness did not change significantly for any of the strains indicating that expansion of the marrow cavity kept pace with expansion of the periosteum. However, beyond 14 days of age, cortical thickness increased linearly until peak values were obtained at 112 days of age. After 14 days of age, C3H femurs exhibited cortices with the largest average thickness, A femurs exhibited intermediate cortical thickness, and B6 the smallest (ANOVA, $p < 0.05$).

Postnatal changes in ash content

In all three strains, ash content increased with age to 112 days (Fig. 6). Genotype-specific variation in ash content

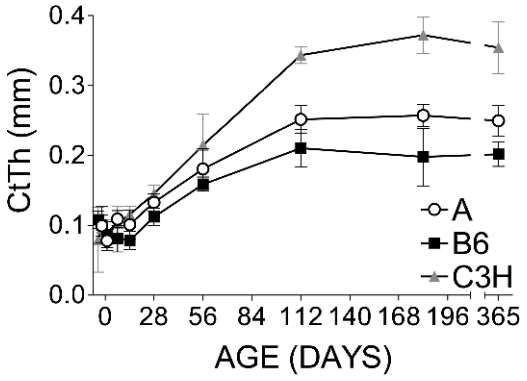

FIG. 5. Variation in femoral cortical thickness (Ct.Th) among A, B6, and C3H mice across development. Significant differences in Ct.Th among strains are indicated in Table 1.

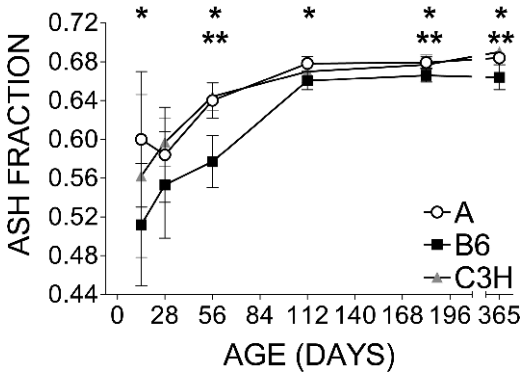

FIG. 6. Variation in femoral ash content across development for A, B6, and C3H femurs. *B6 < A (ANOVA; $p < 0.05$); **B6 < C3H (ANOVA; $p < 0.05$).

was observed at the earliest time-point assayed (2 weeks of age), and these relationships persisted throughout the remainder of the study.

DISCUSSION

This study showed that genetic variability in inbred mouse adult bone traits (Ct.Ar, J_o, and ash content) results directly from genotype-specific differences in periosteal and endosteal expansion and whole bone mineral accrual, as hypothesized. Previous studies comparing B6 and C3H mouse growth suggested that genetic variation in adult bone mass could be explained by prepubertal and pubertal growth patterns[27] and by different rates of bone formation during adolescent growth.[16] Additional studies examined B6 skeletal development alone.[28,29] However, these studies did not include prenatal and immediate postnatal growth (<7 days). Therefore, it remained unclear how in utero growth, early bone cell (osteoblast and osteoclast) activities, and peripubertal/adolescent growth contributed to genetic variability in adult trait magnitudes. By looking across growth, including several time-points not previously studied, we were able to connect early and later bone development. Thus, this work filled in gaps from previous studies and provided new insight into the genetic regulation of adult bone traits. Furthermore, we studied both the spatial distribution of bone (J_o) and matrix mineralization (ash content). Previous work from our laboratory has shown that these traits in combination with tissue amount (Ct.Ar) are important in the determination of whole bone strength and brittleness, respectively.[9] Last, we included a third strain (A), which was previously shown to have a small adult bone morphology and high adult ash content,[9,14] to further generalize how genetic background influences adult bone traits.

Our examination of bone morphology from E18.5 to 365 days of age revealed that A, B6, and C3H inbred mouse strains showed qualitatively similar transverse femoral growth patterns. The early rapid expansion of the periosteal and endosteal surfaces followed by marrow infilling observed for the mouse was consistent with that observed for human long bones.[21] As such, studying the genetic regulatory pathways controlling murine long bone growth and the attainment of peak bone properties should prove valuable in understanding similar processes in the human skeleton.

The attainment of a particular combination of Ct.Ar and J_o in adult inbred mice can be explained in mathematical terms based on variability in the relative expansion of the periosteal and endosteal surfaces during growth when the femoral diaphysis is modeled as a simple hollow cylinder.[20–22] Because Ct.Ar and J_o are related to periosteal and endosteal diameters differently,

$$\text{Ct.Ar} = \text{Tt.Ar} - \text{Ma.Ar} \propto \text{Dia}_{\text{Peri}}^2 - \text{Dia}_{\text{Endo}}^2 \quad (5)$$

$$J_o \propto \text{Tt.Ar}^2 - \text{Ma.Ar}^2 \propto \text{Dia}_{\text{Peri}}^4 - \text{Dia}_{\text{Endo}}^4 \quad (6)$$

cylinders of different diameters will necessarily have different combinations of Ct.Ar and J_o values. Thus, variability in adult Ct.Ar and J_o arise during growth necessarily because differences in the relative expansion of the periosteal and endosteal surface (i.e., growth patterns) lead to different periosteal and endosteal diameters.

We found that the unique pattern of periosteal and endosteal growth exhibited throughout life by each genotype could indeed explain, in mathematical terms, how variability in adult morphological trait combinations (Ct.Ar and J_o) arises. For B6 mice, the large J_o and small Ct.Ar observed in adulthood resulted primarily from a large periosteal and endosteal expansion during early growth (before puberty). For C3H mice, an intermediate rate of periosteal and endosteal expansion during early growth (compared with A and B6) and a significantly greater periosteal expansion and marrow infilling after puberty led to the large Ct.Ar and J_o values of adult C3H mice. As a result, Ct.Ar and J_o increased at a faster rate in C3H mice and led to a higher Ct.Ar relative to J_o because a larger proportion of new bone was added, in a less mechanically efficient manner, to the endosteum. It is noteworthy that B6 and C3H mice achieved similar adult J_o values. However, this occurred through very different growth patterns and, presumably, different biological control mechanisms. For A mice, the small adult Ct.Ar and J_o were a result of having the smallest periosteal and endosteal expansion both before and after

puberty. Interestingly, A and B6 mice achieved similar adult Ct.Ar values, but this occurred through very different growth patterns, suggesting that A and B6 mice achieve similar adult Ct.Ar through different biological control mechanisms. Together these results show that inbred mice build morphologically distinct femurs by regulating bone surface activity in a genotype-specific manner.

From these data, we identified six bone traits that helped characterize the variability in transverse femoral development among three strains of inbred mice and that provided additional insight into the biological control mechanisms underlying variability in adult bone traits. The six traits included (1) the initial size of the bone at 1 day of age, (2) periosteal expansion during the early (prepubertal), rapid growth phase, (3) endosteal expansion during the early growth phase, (4) periosteal expansion during the later (peri- to postpubertal) growth phase, (5) marrow infilling during the later growth phase, and (6) ash content (material composition) throughout growth. Interstrain variability in the first five indices reflects differences in bone cell activity during different growth phases, and the last index reflects variation in the tissue mineralization process. Together, these bone traits represent phenotypic indices that will be useful for identifying the biological (and genetic) mechanisms that influence adult whole bone mechanical properties.

Variability in bone size and shape (Ct.Ar, J_o, and TAr) at E18.5 and 1 day of age show that these inbred mice begin postnatal skeletal development with different initial morphologies. These results suggest that bone growth and adult bone mass might be related to allelic variability in the factors involved in in utero development. Differences in tissue patterning and condensation have been observed in the cranio-facial development of B6 and C3H mice,[30] and similar variability in tissue patterning and condensation, cartilage formation, or initial bone formation could influence long bone morphology at birth. Research in humans has identified correlations between in utero growth, postnatal growth, and adult bone mass that support the idea that pre- and postnatal growth influence adult skeletal properties.[31–33] Additional studies in mice may be useful in establishing the relationship between prenatal morphology and growth and adult bone trait values.

Investigation of early growth (1–28 days of age) revealed that prepubertal growth played a critical role in defining adult trait values. Strain specific differences in adult external size were established during early growth, suggesting that variation in Tt.Ar, bone width, and maximal Ma.Ar are likely the result of allelic variations influencing the processes controlling rapid surface expansion before puberty. Measures of adult bone morphology, which have been correlated with fracture risk,[3,34] are also largely determined before puberty in humans.[21] Therefore, the mouse may provide a useful model for studying how fracture risk is associated with the biology of early bone growth and the establishment of external size.

Variability in ash content was also established at the earliest time-point studied (2 weeks of age) and was consistent with the variability observed in adulthood. This suggested that differences in mineralization and material composition among the strains might be observed even earlier in life, possibly before birth, or within the first few days of postnatal growth. We previously showed that a 4.0% variation in ash content among inbred strains was correlated with a ~3.4- and ~1.9-fold variation in whole bone ductility and toughness, respectively.[14] Therefore, the consistently lower B6 femoral ash content, compared with A and C3H mice, implied that B6 femurs were constructed of bone tissue with a lower material stiffness but greater ductility[35] throughout life. Together, these results suggest that different strains of inbred mice might harbor allelic variations in the genetic factors inherent to or governing mineral accrual.

The rate and extent of periosteal and endosteal expansion during early growth appeared to be well matched to ash content values, suggesting that material composition may be functionally coupled to bone growth patterns. B6 mice, with the most rapid prepubertal surface expansions and largest Tt.Ar and J_o values at 28 days of age, showed small ash values. In contrast, the slower expanding bones of A and C3H mice showed larger ash values. From a mechanical basis, these results are not entirely surprising because the addition of an equivalent amount of tissue on the outer surface of a large bone will result in a greater increase in J_o, and therefore bone stiffness,[29,35] compared with a similar addition on a smaller bone. Thus, the rapid expansion of the periosteum and endosteum in B6 mice established a more efficient growth pattern compared with A and C3H mice. This greater structural efficiency would substantially increase whole bone stiffness and presumably afford B6 mice the ability to reach a mechanically functional end state with material of reduced ash content and thus reduced tissue level stiffness.

The variability in femoral growth patterns observed after the onset of puberty were entirely consistent with previously reported data.[16,27,29] Furthermore, our comparison of early and later growth suggests that female C3H mice might harbor allelic variations that significantly alter their growth patterns after puberty and predispose them to drastically increased bone growth in association with sexual maturation. Additional studies are required to test if pubertal maturation and sex hormones differentially affect the biological processes of skeletal growth and contribute to the variability in adult bone traits among these strains.

Significant variation in the aging of the inbred mouse skeleton was also observed. A mice showed no changes in Tt.Ar and Ma.Ar values between 182 and 365 days of age, suggesting little periosteal expansion and endosteal expansion during this time, whereas B6 and C3H mice showed large increases in Tt.Ar and Ma.Ar. The age-related expansion of B6 and C3H femurs is similar to that observed for the human skeleton.[21,36] These results suggest that the biological processes associated with skeletal aging vary with genetic background.

Although female A, B6, and C3H mice exhibited a wide range of skeletal phenotypes, further studies are warranted to test how growth patterns vary among other strains of mice, how growth patterns vary between male and females,[21,23,24] and how each phase of growth is related to biomechanical properties. In a standard cylindrical model of growth, measures of Tt.Ar and Ma.Ar are sufficient to

describe how a single species of bone cells (osteoblasts or osteoclast) influence surface changes. However, the transverse growth of the femoral mid-diaphysis occurs through both surface expansion and cortical drift.[37,38] In regions of long bones exhibiting drift, both apposition and resorption occur at different locations along each surface; therefore, the relative contribution of osteoblasts and osteoclasts working on both the periosteum and endosteum must be considered in the analysis of Tt.Ar and Ma.Ar, respectively.

From this study, we conclude that different strains of inbred mice build distinct, yet mechanically functional, femurs by regulating bone surface activity and mineral accrual in a genotype-specific manner. These genotype-specific growth patterns led directly to particular combinations of adult bone traits, and thus, specific repertoires of whole bone mechanical properties. By looking across all ages of growth, from prenatal development to adulthood, we identified six bone traits that can be used to explain, in a systematic manner, the differences in femoral growth patterns among inbred mice. This characterization of femoral growth for A, B6, and C3H mice throughout life revealed how and when specific combinations of adult bone traits arise in genetically distinct animals. Thus, the inbred mouse provides a valuable model to determine how genetic background influences the biological processes involved in establishing variability in adult bone traits, and thus, whole bone mechanical properties.

ACKNOWLEDGMENTS

The authors thank the National Institutes of Health (AR44927), and the Department of Defense (DAMD 17-01-1-0806) for support.

REFERENCES

1. Fox KM, Cummings SR, Powell-Threets K, Stone K 1998 Family history and risk of osteoporotic fracture. Study of Osteoporotic Fractures Research Group. Osteoporos Int **8:**557–562.
2. Howard GM, Nguyen TV, Harris M, Kelly PJ, Eisman JA 1998 Genetic and environmental contributions to the association between quantitative ultrasound and bone mineral density measurements: A twin study. J Bone Miner Res **13:**1318–1327.
3. Nelson DA, Barondess DA, Hendrix SL, Beck TJ 2000 Cross-sectional geometry, bone strength, and bone mass in the proximal femur in black and white postmenopausal women. J Bone Miner Res **15:**1992–1997.
4. Kelly PJ, Hopper JL, Macaskill GT, Pocock NA, Sambrook PN, Eisman JA 1991 Genetic factors in bone turnover. J Clin Endocrinol Metab **72:**808–813.
5. Kelly PJ, Nguyen T, Hopper J, Pocock N, Sambrook P, Eisman J 1993 Changes in axial bone density with age: A twin study. J Bone Miner Res **8:**11–17.
6. Bouxsein ML 2003 Bone quality: Where do we go from here? Osteoporos Int **14**(Suppl 5)**:**118–127.
7. Huang QY, Recker RR, Deng HW 2003 Searching for osteoporosis genes in the post-genome era: Progress and challenges. Osteoporos Int **14:**701–715.
8. Nadeau JH, Burrage LC, Restivo J, Pao YH, Churchill G, Hoit BD 2003 Pleiotropy, homeostasis, and functional networks based on assays of cardiovascular traits in genetically randomized populations. Genome Res **13:**2082–2091.
9. Jepsen KJ, Akkus OJ, Majeska RJ, Nadeau JH 2003 Hierarchical relationship between bone traits and mechanical properties in inbred mice. Mamm Genome **14:**97–104.
10. Stein K 1957 Genetical studies on the skeleton of the mouse XXI. The girdles and the long bones. J Genet **55:**313–324.
11. Lovell D, Johnson F 1983 Quantitative genetic variation in the skeleton of the mouse. Genet Res **42:**169–182.
12. Lovell D, Johnson F, Willis D 1986 Quantitative genetic variation in the skeleton of the mouse: II Description of variation within and between inbred strains. Am J Anat **176:**287–303.
13. Beamer WG, Donahue LR, Rosen CJ, Baylink DJ 1996 Genetic variability in adult bone density among inbred strains of mice. Bone **18:**397–403.
14. Jepsen KJ, Pennington DE, Lee YL, Warman M, Nadeau J 2001 Bone brittleness varies with genetic background in A/J and C57BL/6J inbred mice. J Bone Miner Res **16:**1854–1862.
15. Akhter MP, Fan Z, Rho JY 2004 Bone intrinsic material properties in three inbred mouse strains. Calcif Tissue Int **75:**416–420.
16. Sheng MH, Baylink DJ, Beamer WG, Donahue LR, Rosen CJ, Lau KH, Wergedal JE 1999 Histomorphometric studies show that bone formation and bone mineral apposition rates are greater in C3H/HeJ (high-density) than C57BL/6J (low-density) mice during growth. Bone **25:**421–429.
17. Akhter MP, Iwaniec UT, Covey MA, Cullen DM, Kimmel DB, Recker RR 2000 Genetic variations in bone density, histomorphometry, and strength in mice. Calcif Tissue Int **67:**337–344.
18. Akhter MP, Cullen DM, Pedersen EA, Kimmel DB, Recker RR 1998 Bone response to in vivo mechanical loading in two breeds of mice. Calcif Tissue Int **63:**442–449.
19. Amblard D, Lafage-Proust MH, Laib A, Thomas T, Ruegsegger P, Alexandre C, Vico L 2003 Tail suspension induces bone loss in skeletally mature mice in the C57BL/6J strain but not in the C3H/HeJ strain. J Bone Miner Res **18:**561–569.
20. Sumner DR, Andriacchi TP 1996 Adaptation to differential loading: Comparison of growth-related changes in cross-sectional properties of the human femur and humerus. Bone **19:**121–126.
21. Garn SM 1970 The Earlier Gain and the Later Loss of Cortical Bone, in Nutritional Perspective. Thomas, Springfield, IL, USA.
22. van der Meulen MC, Beaupre GS, Carter DR 1993 Mechanobiologic influences in long bone cross-sectional growth. Bone **14:**635–642.
23. Duan Y, Beck TJ, Wang XF, Seeman E 2003 Structural and biomechanical basis of sexual dimorphism in femoral neck fragility has its origins in growth and aging. J Bone Miner Res **18:**1766–1774.
24. Seeman E 1997 From density to structure: Growing up and growing old on the surfaces of bone. J Bone Miner Res **12:**509–521.
25. Selker F, Carter DR 1989 Scaling of long bone fracture strength with animal mass. J Biomech **22:**1175–1183.
26. Johnson FB 1992 Von Kossa method for minerals. In: Prophet EB (ed.) Laboratory Methods in Histotechnology. American Registry of Pathology, Washington, DC, USA, p. 197.
27. Richman C, Kutilek S, Miyakoshi N, Srivastava AK, Beamer WG, Donahue LR, Rosen CJ, Wergedal JE, Baylink DJ, Mohan S 2001 Postnatal and pubertal skeletal changes contribute predominantly to the differences in peak bone density between C3H/HeJ and C57BL/6J mice. J Bone Miner Res **16:**386–397.
28. Ferguson VL, Ayers RA, Bateman TA, Simske SJ 2003 Bone development and age-related bone loss in male C57BL/6J mice. Bone **33:**387–398.
29. Brodt MD, Ellis CB, Silva MJ 1999 Growing C57Bl/6 mice increase whole bone mechanical properties by increasing geometric and material properties. J Bone Miner Res **14:**2159–2166.
30. Miyake T, Cameron AM, Hall BK 1997 Variability of embryonic development among three inbred strains of mice. Growth Dev Aging **61:**141–155.
31. Gale CR, Martyn CN, Kellingray S, Eastell R, Cooper C 2001 Intrauterine programming of adult body composition. J Clin Endocrinol Metab **86:**267–272.

32. Cooper C, Fall C, Egger P, Hobbs R, Eastell R, Barker D 1997 Growth in infancy and bone mass in later life. Ann Rheum Dis **56:**17–21.
33. Loro ML, Sayre J, Roe TF, Goran MI, Kaufman FR, Gilsanz V 2000 Early identification of children predisposed to low peak bone mass and osteoporosis later in life. J Clin Endocrinol Metab **85:**3908–3918.
34. Giladi M, Milgrom C, Simkin A, Stein M, Kashtan H, Margulies J, Rand N, Chisin R, Steinberg R, Aharonson Z 1987 Stress fractures and tibial bone width. A risk factor. J Bone Joint Surg Br **69:**326–329.
35. Currey JD 2004 Tensile yield in compact bone is determined by strain, post-yield behaviour by mineral content. J Biomech **37:**549–556.
36. Lazenby RA 1990 Continuing periosteal apposition. I: Documentation, hypotheses, and interpretation. Am J Phys Anthropol **82:**451–472.
37. Sontag W 1986 Quantitative measurement of periosteal and cortical-endosteal bone formation and resorption in the midshaft of female rat femur. Bone **7:**55–62.
38. Enlow DH 1962 A study of the post-natal growth and remodeling of bone. Am J Anat **110:**79–101.

Address reprint requests to:
Karl J Jepsen, PhD
Department of Orthopaedics
Mount Sinai School of Medicine
Box 1188, One Gustave L. Levy Place
New York, NY 10029, USA
E-mail: karl.jepsen@mssm.edu

Received in original form May 13, 2005; revised form June 16, 2005; accepted July 5, 2005.

Elsevier Editorial System(tm) for Bone

Manuscript Draft

Manuscript Number:

Title: Sexual Dimorphism Affects Tibia Size and Shape but not Tissue-Level Mechanical Properties

Article Type: Full Length Article

Section/Category:

Keywords: dimorphism; gender/sex; strength; morphology; bone quality.

Corresponding Author: Dr. Karl J Jepsen,

Corresponding Author's Institution: Leni & Peter W. May Department of Orthopaedics, Mount Sinai School of Medicine, New York, NY USA

First Author: Steven M Tommasini

Order of Authors: Steven M Tommasini; Philip Nasser; Karl J Jepsen

Manuscript Region of Origin:

Abstract: Understanding how growth influences adult bone morphology and tissue-quality should provide important insight into why females show a greater incidence of stress fractures early in life and fragility fractures later in life compared to males. The objective of this study was to test whether females acquire similar tissue-level mechanical properties as males by the time peak bone properties are established. Standardized beams of bone were machined from the tibial diaphyses of 14 young, adult females ranging in age from 22-46 years. Data for males (n=17, age=17-46 years) were taken from a prior study. Measures of tissue-level mechanical properties, including stiffness, strength, ductility, toughness, and damageability, were compared between sexes using t-tests. The relationship between cross-sectional morphology and tissue-level mechanical properties was also examined. Males and females showed nearly identical tissue-level mechanical properties. Both sexes also showed similar age-related degradation of mechanical

properties and a similar relationship between cross-sectional morphology and tissue-quality. However, for all body sizes, female tibiae were smaller relative to body size (i.e., less robust) compared to males. The results indicated that sex-specific growth patterns affected transverse bone size, but did not affect tissue level mechanical properties. This, combined with the observation that young, adult female long bones are undersized relative to body size, suggests that adult females would be expected to accumulate more damage under intense loading compared to males. This may be a contributing factor to the greater incidence of stress fractures observed for female military recruits.

June 12, 2006

Dr. Steven A. Goldstein
Orthopaedic Research Laboratories
Orthopaedic Surgery
The University of Michigan
Ann Arbor, MI 48109-0486

Dear Dr. Goldstein,

Attached please find a manuscript, which is being submitted to Bone for review. If you have any questions, please do not hesitate to contact me. None of the authors have any financial interests that would affect the outcome of this study.

Regards,

Karl J. Jepsen, Ph.D.
Department of Orthopaedics
Mount Sinai School of Medicine
Box 1188
One Gustave L. Levy Place
New York, NY 10029
Voice: 212-241-6610
FAX: 212-876-3168
email: karl.jepsen@mssm.edu

Title: **Sexual Dimorphism Affects Tibia Size and Shape but not Tissue-Level Mechanical Properties**

Authors: Steven M. Tommasini[1], Philip Nasser[2], Karl J. Jepsen[2]

[1]New York Center for Biomedical Engineering, CUNY Graduate School, Department of Biomedical Engineering, City College of New York, New York, NY USA.

[2]Leni & Peter W. May Department of Orthopaedics, Mount Sinai School of Medicine, New York, NY USA.

Correspondence:

Karl J. Jepsen, Ph.D.
Department of Orthopaedics
Mount Sinai School of Medicine
Box 1188
One Gustave L. Levy Place
New York, NY 10029
Voice: 212-241-6610
Fax: 212-876-3168
Email: karl.jepsen@mssm.edu

Abstract

Understanding how growth influences adult bone morphology and tissue-quality should provide important insight into why females show a greater incidence of stress fractures early in life and fragility fractures later in life compared to males. The objective of this study was to test whether females acquire similar tissue-level mechanical properties as males by the time peak bone properties are established. Standardized beams of bone were machined from the tibial diaphyses of 14 young, adult females ranging in age from 22-46 years. Data for males (n=17, age=17-46 years) were taken from a prior study. Measures of tissue-level mechanical properties, including stiffness, strength, ductility, toughness, and damageability, were compared between sexes using t-tests. The relationship between cross-sectional morphology and tissue-level mechanical properties was also examined. Males and females showed nearly identical tissue-level mechanical properties. Both sexes also showed similar age-related degradation of mechanical properties and a similar relationship between cross-sectional morphology and tissue-quality. However, for all body sizes, female tibiae were smaller relative to body size (i.e., less robust) compared to males. The results indicated that sex-specific growth patterns affected transverse bone size, but did not affect tissue level mechanical properties. This, combined with the observation that young, adult female long bones are undersized relative to body size, suggests that adult females would be expected to accumulate more damage under intense loading compared to males. This may be a contributing factor to the greater incidence of stress fractures observed for female military recruits.

Key Words: biomechanics; stress fracture; dimorphism; gender/sex; strength; morphology; bone quality.

Introduction

Understanding why females show a greater incidence of stress fractures early in life [1, 2] and fragility fractures later in life [3-5] compared to males may provide important insight into the biological [6] and mechanical [7] mechanisms underlying fracture risk. Sexual dimorphism is one factor that may contribute to this discrepancy [6, 8], because bone size and shape are known determinants of bone strength [9]. Importantly, fracture also depends on tissue-level mechanical properties. Although it is known that sex-specific growth patterns influence bone structure, it is unclear whether variable growth patterns affect the construction of bone matrix in a way that leads to differences in tissue-level mechanical properties. The few studies that examined tissue-level mechanical properties of long bones from adult males and females never directly tested for sex-specific differences [10, 11]. The objective of this study was to test whether females acquire similar tissue-level mechanical properties as males by the time peak bone properties are established. In addition to tissue-level stiffness and strength, we also quantified tissue-damageability, toughness, and ductility, because these latter mechanical properties provide insight into the material response of bone when subjected to extreme load conditions such as during a fall, as well as the amount of damage accumulated within the bone when subjected to intense physical activity. We also tested whether females show a correlation between cross-sectional morphology and tissue-level mechanical properties similar to that previously observed for males [12].

Materials and methods

Sample population

Tibiae of 14 female donors (12 Caucasian, 1 African-American, 1 unknown) aged 22 - 46

years (average age = 36.9 $\pm$ 8.1 years) were acquired from the Musculoskeletal Transplant Foundation (Edison, NJ, USA) and the National Disease Research Interchange (Philadelphia, PA, USA). Donor body weight and height were obtained from the source. Only tibiae from donors with no known skeletal pathology were included in the study. The tibiae were freshly harvested, wrapped in wet gauze, and stored in plastic bags at –40°C. Data for male tibiae (n=17, average age = 32.9 $\pm$ 10.4, age range = 17-46 years) were taken from a previous publication [12].

Whole bone morphology

Tibia length (L) was measured as the average distance between the middle of the talar trochlear facet and the medial and lateral proximal condyles[13] using a large-capacity slide caliper with an accuracy of $\pm$2.5mm (Mantex Precision, Haglöf Inc., Madison, MS, USA). Tibia widths in the antero-posterior ($Width_{AP}$) and medial-lateral ($Width_{ML}$) directions were measured using a 300mm vernier caliper with an accuracy of $\pm$0.02mm (Fowler Company Inc., Newton, MA, USA). Measurements were taken at 10% intervals from 30% to 70% of the total tibia length and averaged in order to assess the diaphyseal morphological traits [14].

Cross-sectional morphological traits were quantified from 3-mm thick mid-diaphyseal cross-sections cut at 30, 50, and 70% of the total tibia length using a diamond coated metallurgical saw (Model 660, South Bay Technology Inc., San Clemente, CA, USA). Each cross-section was digitally imaged (0.024mm/pixel) and analyzed using IMAQ Vision Builder (version 6.0, National Instruments Corp., Austin, TX, USA). Morphological traits included cortical area (CtAr), the moments of inertia about the antero-posterior (I_{AP}) and medial-lateral (I_{ML}) axes, the polar moment of inertia ($J = I_{AP} + I_{ML}$), and the section modulus in the AP ($J/Width_{AP}/2$) and ML ($J/Width_{ML}/2$) directions. Moment of inertia and section modulus were assessed because these

geometric measures are related to the bending and torsional stiffness of intact tibiae. A slenderness index (S) was calculated as the ratio of the AP and ML section modulus values, respectively, to tibia length and body weight:

$$S_{AP} = (1/J/(Width_{AP}/2))/(L*BW) \quad (1)$$

$$S_{ML} = (1/J/(Width_{ML}/2))/(L*BW) \quad (2)$$

where L = tibia length (mm) and BW = body weight (kg). For semantic reasons, the formulae are the inverse to that used previously [15], such that an increase in S_{AP} or S_{ML} indicates a more slender (gracile) bone. All morphological traits were averaged over the three cross-sections for each tibia.

Bone sample generation

Cortical bone samples were prepared for biomechanical testing by machining beams with a rectangular cross-section from the diaphysis of each tibia using an automated CNC milling machine under constant irrigation (Modela MDX-20, Roland DGA Corp., Irvine, CA, USA). Sample width (circumferential direction of tibia) was machined to 5mm and length (longitudinal direction) was machined to 55mm for all samples. Sample height (radial direction) was either 2.2 or 2.5mm, depending on the cortical thickness of the tibia. A total of eight samples were generated from each tibia and randomly distributed to monotonic (n = 4) and damage accumulation (n = 4) test groups. All samples were stored at –40°C in gauze saturated with phosphate buffered saline (PBS) with added calcium [16] and placed individually in airtight bags.

Monotonic failure properties

Tissue-level mechanical properties were assessed by loading four cortical bone samples from each tibia to failure in 4-point bending at 0.05mm/s using a servohydraulic materials testing system (Instron model 8872, Instron Corp., Canton, MA, USA). Specimens were submerged in a PBS solution with added calcium and maintained at 37°C throughout all tests. Load and deflection were converted to stress and strain as described previously [12]. These bending equations take yielding into consideration [17], and thus provide an estimate of tissue strength that is consistent with tensile mechanical properties [18]. All properties were averaged over the four samples tested for each tibia.

Damageability

Tissue damageability was assessed using the same protocol described previously [12]. This protocol was designed to induce and accumulate cracks in cortical bone specimens and to measure the degradation of stiffness and relaxation as surrogate measures of damage accumulation [19]. Four cortical bone samples from each tibia were subjected to a fifteen-cycle damage accumulation protocol. For this protocol, diagnostic cycles were interposed between damage cycles to assess damage-associated degradation at each load level. For the diagnostic cycles, the specimens were loaded in four-point bending at 0.5mm/s to 50% of the average displacement at yield (determined from the monotonic tests), held for 60 seconds, and then unloaded at 0.5mm/s. For the damage cycles, the specimens were loaded at 0.5mm/s to 50, 75, 100, 125, 150, 175, and 200% of displacement at yield respectively, held for 60 seconds, and then unloaded at 0.5mm/sec. A 5-minute recovery period followed each damage cycle. Displacement at yield was used as a reference in the damage cycles because this parameter

showed little variation among the test samples when subjected to monotonic four-point bending. The displacement at yield was 1.0mm for the samples with a height of 2.5mm and 1.07mm for the samples with a height of 2.2 mm.

Damage accumulation within the test sample was quantified by calculating the stiffness degradation and the change in relaxation. We included measures of relaxation in this analysis because prior research showed that damage accumulation affects viscoelastic behavior more dramatically compared to stiffness [19-22] and thus would provide a more sensitive assay to assess variation in tissue damageability. For each diagnostic cycle, i, stiffness (S_i) was calculated from a linear regression of the initial portion of the load-deformation curve and relaxation (R_i) was defined as the decrease in load over the 60-second hold period. The total amount of damage induced in each sample was calculated by comparing the stiffness and relaxation values measured at the end of the entire test sequence (S_{15}, R_{15}) to those before (S_0, R_0). To test if the damage accumulation process was altered, degradation measures were also calculated after each damage cycle. The general equations for degradation measures are as follows:

$$D_{\mathrm{STIFF}_i} = 1 - S_i/S_0 \tag{4}$$

$$D_{\mathrm{RELAX}_i} = R_i/R_0 \tag{5}$$

where S_i and R_i are the stiffness and total relaxation, respectively, of the cycle i, and S_0 and R_0 are the average stiffness and total relaxation, respectively, of the first two diagnostic cycles and the first damage cycle.

Statistical analysis

Mechanical properties and morphological traits that changed significantly with age were corrected by regression analysis [23]. Differences between females and males were determined

using a Student's t-test with corrections applied for unequal variances (GraphPad Software, Inc; San Diego, CA USA). To determine if female and male tibiae were similarly adapted to body size, the section modulus (cross-sectional moment of inertia/bone width) was regressed against the product of body weight and tibia length [13] and the slopes were compared between sexes (ANCOVA). To determine if males and females show a similar relationship between tibial cross-sectional morphology and tissue-level mechanical properties [12], linear regressions were performed and differences in slopes and intercepts between female and male regressions were determined using a method equivalent to an Analysis of Covariance (GraphPad Software, Inc; San Diego, CA USA). Since no differences were found between male and female regressions, a matrix of Pearson correlation coefficients was constructed using the combined female and male datasets to identify the morphology-tissue quality relationships that were significant.

Results

Sample Population

Female donors were shorter than males (163 $\pm$ 6 cm vs. 178 $\pm$ 4cm; $p<0.0001$), but were not different in body weight (74 $\pm$ 21kg vs. 84 $\pm$ 25kg; $p<0.2$).

Monotonic properties

Females and males showed similar regressions for tissue modulus, strength, post-yield strain, and energy-to-failure versus age (Fig. 1). No differences in the average tissue-level mechanical properties were observed between females and males (Table 1), even when corrected for differences in donor age. This included measures of stiffness (modulus), strength, ductility (failure strain, post-yield strain), and toughness (energy-to-failure). Thus, males and females

showed similar tissue-level monotonic properties.

Damageability

No differences in either total stiffness degradation or the total change in relaxation (Table 2) were observed between females and males. Further, the changes in stiffness and relaxation after each damage cycle were similar for males and females (Fig. 2). These results indicated that the loading protocol induced similar amounts of damage at each load step for females and males.

Morphology-Tissue Quality Relationships

None of the morphological traits showed a significant correlation with age for either males or females (data not shown). Adult females achieved a different bone size and shape compared to males: female tibiae were smaller (J, CtAr, Width), more slender (S_{AP}, S_{ML}, J/L), and showed a smaller J:A ratio compared to males (Table 3). Females and males showed similar slopes for the regression of $J/Width_{AP}$ versus the product of body weight and tibial length ($p<0.17$, ANCOVA). However, females showed a significantly smaller intercept compared to males ($p<0.0001$, ANCOVA), indicating that, for all body sizes, female tibiae were smaller relative to body size (i.e., less robust) compared to males (Fig. 3). Similar results were observed when using $J/Width_{ML}$.

The tissue-level mechanical properties were regressed against bone morphological traits and no significant differences in slopes were found for females and males. A correlation analysis (Table 4), which was conducted using the combined male and female data sets, showed that tissue-level modulus decreased with increasing bone section modulus ($J/Width_{AP}$, $J/Width_{ML}$), post-yield strain increased with increasing bone width ($Width_{AP}$), and tissue-damage (D_{STIFF})

increased with increasing tibial slenderness (S_{AP}, S_{ML}). The significant regressions are shown in Figure 4. The amount of overlap between the female and male datasets depended on whether the bone morphology traits were adjusted for body size. For unadjusted traits like width and J/width, the female data simply extended the relationships observed for the males (Fig. 4A,B). For the regression involving bone slenderness, which is adjusted for body weight and tibial length, the female data overlapped substantially with the male data (Fig. 4C).

Discussion

Tissue-level mechanical properties, including measures of fragility and damageability, were assessed for cortical bone samples that were machined from the diaphyses of young, adult male and female tibiae. The data indicated that the tibial diaphyses of females and males were composed of material having similar tissue-level mechanical properties, and that the mechanical properties degraded with age at similar rates over the age range of 17-46 years. Further, males and females showed a similar relationship between tissue-level mechanical properties and cross-sectional morphology. These data suggested that the genetic [24-26] and environmental [27] factors contributing to sex-specific growth patterns affected adult tibial cross-sectional size and shape, but did not affect bone matrix construction, mineralization, and organization in a way that significantly affected tissue-level mechanical properties. This analysis included mechanical properties like stiffness, which is important for day-to-day activities, as well strength, ductility, toughness, and damageability, which provide insight into the amount of damage accumulated during intense physical activity and the fracture resistance during an extreme load condition such as a fall.

Our data confirm that males and females achieve similar adult tissue-level mechanical

properties, which has only been assumed in prior analyses [13]. Prior studies reported property values for this age-range, but did not directly compare data for females and males [10, 11]. The mechanical properties measured from the 4-point bending tests in this study were consistent with the mechanical properties of cortical bone measured previously in tension [28-30], which was expected given that failure in our bending tests occurred following fracture initiated within the tensile region. Further, the bending formula that was used to convert load and deflection to stress and strain, because it accounted for nonlinear effects [17], provided a more appropriate estimate of bending strength compared to standard beam theory [18]. Because the bone samples used in this study were machined from within the middle of the cortex, the tissue that was added to the subperiosteal or subendosteal surfaces during and after puberty was likely not tested in our study. Thus, the current data could not be used to determine if sex-specific differences in tissue-quality exist following puberty. This data thus reflects the tissue properties established early in life, plus the modifications to these properties associated with osteonal-remodeling and cortical drift [31] during the ensuing years.

Although the current data were collected by cross-sectional means, the mechanical property versus age regressions implied that *in situ* tissue-level mechanical properties begin to decline early in adulthood for males and females, even before bone loss becomes measurable [32]. Similar regressions were observed previously for data that included a much broader age range (19-90 years) [10, 29, 30, 33]. Stiffness and strength typically increase until about 30 years of age and then decline slowly thereafter [10]. In contrast, the post-yield behavior of bone degrades rapidly with age, and this loss in ductility is a primary reason why bone tissue becomes progressively more brittle [30] and shows lower impact strength [11]. The decline in tissue-level strength, ductility, and damageability have been attributed to age-related changes in ash content

[11], osteonal remodeling [34], collagen quality [35, 36], mineral density distribution [37], and porosity [11, 30]. Beyond 50 years of age, the mechanical properties of females and males may follow different degradation pathways associated with sex-specific bone loss patterns [30].

The similarity in tissue-level mechanical properties for adult men and women may be explained based on early transverse bone-growth patterns. During pre-pubertal growth, the periosteal and endosteal surfaces of female and male long bone diaphyses follow nearly identical expansion rates [38]. Despite the dimorphic transverse bone-growth patterns arising during puberty [38], the long bones of both sexes appear to be constructed in a way so that by 20 years of age bone size is properly adapted to satisfy loading demands associated with body weight [39-42]. Whole bone stiffness and peak tissue strains are thus kept at proper levels [43] during growth simply by depositing enough tissue on the periosteal and endosteal surfaces to keep pace with weight gain. Thus, because there is no discrepancy in the relationship between bone size and body size during growth, males and females can construct the tibia with similar tissue-level mechanical properties without a loss in mechanical function.

Although each of the tissue-level mechanical properties that we measured showed a small coefficient of variation for both sexes, approximately 20% of this variation was explained by the size of the tibia. Female tibiae extended the correlations that were observed previously for males [12], and indicated that individuals with smaller cross-sectional size (i.e., more slender bones) showed a larger tissue-level stiffness. This relationship may be indicative of an inherent adaptive response of bone to modify tissue-level mechanical properties in order to compensate for the smaller size [44]. This coupling suggested that osteoblasts and osteoclasts are capable of coordinately adapting bone morphology and tissue-level mechanical properties so that the combination of these traits satisfies mechanical demands. A more dramatic coordinated

relationship among morphological traits, tissue-quality, and mechanical function has been observed previously across a large range of bones from many species [45] and for inbred mice [46-48], bats [49], gulls [50], and polar bears [51]. Although this coupling appears advantageous for ensuring that an adequate whole bone stiffness is achieved for day-to-day activity, the disadvantage is that the tissue-quality factors that tend to make bone stiff also tend to make bone less ductile, less tough, and more damageable [52]. These latter tissue-quality factors are important during extreme loading conditions [53].

The relationship between bone size (section modulus) and body size (body weight x tibia length), which was established previously by Ruff [13] and was based on the resistance of bone to bending loads, was significantly different between males and females (Table 3, Fig. 3). Similar differences were observed by others [6, 54-56]. Given that adaptive factors appear to match bone size to body size during growth [39-42], this difference suggests that these adaptive factors no longer work the same way when men and women reach adulthood. This latent difference in bone adaptation may be due to differences in post-pubescent endocrine factors that regulate the relative amounts of bone added to the periosteum versus the endosteum [6]. Thus, adult females would be expected to accumulate more damage under intense loading compared to males and this may be a contributing factor to the larger stress fracture incidence for female athletes and military recruits [57, 58].

There are several limitations worth addressing. First, the difficulty in acquiring tibiae from healthy men and women in the 20-40 year age range limited the number of samples for this study. Nevertheless, this did not affect the comparison of mechanical and morphological properties between sexes, but it may have resulted in not seeing more significant correlations between morphology and tissue-quality (Table 4). Second, we presented only measures of

mechanical properties, and have not explained how variability in these mechanical properties arises from variability in matrix composition and/or micro-architecture. Third, tissue-damageability was based on measures of degradation of stiffness and relaxation. Future work will determine if the type, distribution, and quantity of damage is different for females and males. In addition, our measure of tissue-damageability relates to the progressive accumulation of damage prior to failure [19, 20], and may not reflect how damage accumulates under long-term fatigue loading. Fourth, the relationship between the cross-sectional size of the tibia and body size did not take into account load sharing between the tibia and the fibula. Fifth, our analysis does not take into consideration differences in the amount or type of loading, which have been shown to play important roles in the development of bone size and shape [59]. Finally, our analysis, which assumes that randomly acquired tibial samples provide a representative view into bone biology, does not take into account lean muscle mass, which has been shown to be better correlated with bone size and shape than overall body weight [60]. However, these limitations should not affect the similarity in mechanical properties between males and females, or the correlation between bone size and tissue-quality.

The results of this study provided additional insight into why female military recruits show a greater incidence of stress fractures compared to male military recruits [57, 58]. The undersized morphology of female tibiae combined with having similar tissue-level mechanical properties as males suggested that female tibiae are overloaded compared to males. This overloading during intensive training would be expected to lead to increased tissue-stresses and strains, and subsequently increased *in situ* damage accumulation and greater risk of developing a stress fracture [61-63]. Taken together, these results suggested that one factor contributing to the discrepancy in stress fracture risk between males and females may be differences in the way

bone size is adapted to body size after longitudinal growth has ceased. Thus, fracture risk reduction would benefit from having a better understanding of the factors that promote or inhibit bone adaptation [64-66].

Acknowledgments

The authors thank the U.S. Department of Defense (DAMD17-01-1-0806) for their support of this research. Samples were acquired through the Musculoskeletal Transplant Foundation (Edison, NJ, USA) and the National Disease Research Interchange (Philadelphia, PA, USA).

References

[1] Jones, B. H., Bovee, M. W., Harris, J. M., 3rd, and Cowan, D. N. Intrinsic risk factors for exercise-related injuries among male and female army trainees. Am J Sports Med 1993; 21:705-10.

[2] Beck, T. J., Ruff, C. B., Shaffer, R. A., Betsinger, K., Trone, D. W., and Brodine, S. K. Stress fracture in military recruits: gender differences in muscle and bone susceptibility factors. Bone 2000; 27:437-44.

[3] Gallagher, J. C., Melton, L. J., Riggs, B. L., and Bergstrath, E. Epidemiology of fractures of the proximal femur in Rochester, Minnesota. Clin Orthop Relat Res 1980:163-71.

[4] Cooper, C., Campion, G., and Melton, L. J., 3rd Hip fractures in the elderly: a world-wide projection. Osteoporos Int 1992; 2:285-9.

[5] Cummings, S. R., and Melton, L. J. Epidemiology and outcomes of osteoporotic fractures. Lancet 2002; 359:1761-1767.

[6] Duan, Y., Beck, T. J., Wang, X. F., and Seeman, E. Structural and biomechanical basis of sexual dimorphism in femoral neck fragility has its origins in growth and aging. J Bone Miner Res 2003; 18:1766-74.

[7] Winner, S. J., Morgan, C. A., and Evans, J. G. Perimenopausal risk of falling and incidence of distal forearm fracture. Bmj 1989; 298:1486-8.

[8] Seeman, E. The structural basis of bone fragility in men. Bone 1999; 25:143-7.

[9] van der Meulen, M. C., Jepsen, K. J., and Mikic, B. Understanding bone strength: size isn't everything. Bone 2001; 29:101-4.

[10] Currey, J. D., and Butler, G. The mechanical properties of bone tissue in children. J Bone Joint Surg Am 1975; 57:810-4.

[11] Currey, J. D. Changes in the impact energy absorption of bone with age. J Biomech 1979; 12:459-69.

[12] Tommasini, S. M., Nasser, P., Schaffler, M. B., and Jepsen, K. J. Relationship between bone morphology and bone quality in male tibias: implications for stress fracture risk. J Bone Miner Res 2005; 20:1372-80.

[13] Ruff, C. B. Body size, body shape, and long bone strength in modern humans. J Hum Evol 2000; 38:269-90.

[14] Miller, G. J., and Purkey, W. W., Jr. The geometric properties of paired human tibiae. J Biomech 1980; 13:1-8.

[15] Selker, F., and Carter, D. R. Scaling of long bone fracture strength with animal mass. J Biomech 1989; 22:1175-83.

[16] Gustafson, M. B., Martin, R. B., Gibson, V., Storms, D. H., Stover, S. M., Gibeling, J., and Griffin, L. Calcium buffering is required to maintain bone stiffness in saline solution. J Biomech 1996; 29:1191-4.

[17] Nadai, A. Theory of flow and fracture of solids. Engineering societies monographs. New York, NY: McGraw-Hill; 1950.

[18] Burstein, A. H., Currey, J. D., Frankel, V. H., and Reilly, D. T. The ultimate properties of bone tissue: the effects of yielding. J Biomech 1972; 5:35-44.

[19] Jepsen, K. J., and Davy, D. T. Comparison of damage accumulation measures in human cortical bone. J Biomech 1997; 30:891-4.

[20] Jepsen, K. J., Davy, D. T., and Krzypow, D. J. The role of the lamellar interface during torsional yielding of human cortical bone. J Biomech 1999; 32:303-10.

[21] Yeni, Y. N., Christopherson, G. T., Turner, A. S., Les, C. M., and Fyhrie, D. P. Apparent viscoelastic anisotropy as measured from nondestructive oscillatory tests can reflect the presence of a flaw in cortical bone. J Biomed Mater Res A 2004; 69*:*124-30.
[22] Morgan, E. F., Lee, J. J., and Keaveny, T. M. Sensitivity of multiple damage parameters to compressive overload in cortical bone. J Biomech Eng 2005; 127*:*557-62.
[23] Di Masso, R. J., Font, M. T., Capozza, R. F., Detarsio, G., Sosa, F., and Ferretti, J. L. Long-bone biomechanics in mice selected for body conformation. Bone 1997; 20*:*539-45.
[24] Iscan, M. Y., and Miller-Shaivitz, P. Discriminant function sexing of the tibia. J Forensic Sci 1984; 29*:*1087-93.
[25] Turner, R. T., Wakley, G. K., and Hannon, K. S. Differential effects of androgens on cortical bone histomorphometry in gonadectomized male and female rats. J Orthop Res 1990; 8*:*612-7.
[26] Wiren, K. M., Zhang, X. W., Toombs, A. R., Kasparcova, V., Gentile, M. A., Harada, S., and Jepsen, K. J. Targeted overexpression of androgen receptor in osteoblasts: unexpected complex bone phenotype in growing animals. Endocrinology 2004; 145*:*3507-22.
[27] Gordon, K. R., Levy, C., Perl, M., and Weeks, O. I. Experimental perturbation of the development of sexual size dimorphism in the mouse skeleton. Growth Dev Aging 1994; 58*:*95-104.
[28] Reilly, D. T., and Burstein, A. H. The elastic and ultimate properties of compact bone tissue. J Biomech 1975; 8*:*393-405.
[29] Burstein, A. H., Reilly, D. T., and Martens, M. Aging of bone tissue: mechanical properties. J Bone Joint Surg Am 1976; 58*:*82-86.
[30] McCalden, R. W., McGeough, J. A., Barker, M. B., and Court-Brown, C. M. Age-related changes in the tensile properties of cortical bone. The relative importance of changes in porosity, mineralization, and microstructure. J Bone Joint Surg Am 1993; 75*:*1193-205.
[31] Enlow, D. H. Principles of bone remodeling; an account of post-natal growth and remodeling processes in long bones and the mandible: Thomas; 1963.
[32] Parfitt, A. M. Age-related structural changes in trabecular and cortical bone: cellular mechanisms and biomechanical consequences. Calcified Tissue International 1984; 36*:*S123-8.
[33] Melick, R. A., and Miller, D. R. Variations of tensile strength of human cortical bone with age. Clin Sci 1966; 30*:*243-8.
[34] Evans, F. G., and Riolo, M. L. Relations between the fatigue life and histology of adult human cortical bone. J Bone Joint Surg Am 1970; 52*:*1579-86.
[35] Wang, X., Shen, X., Li, X., and Agrawal, C. M. Age-related changes in the collagen network and toughness of bone. Bone 2002; 31*:*1-7.
[36] Wang, X., Li, X., Shen, X., and Agrawal, C. M. Age-related changes of noncalcified collagen in human cortical bone. Ann Biomed Eng 2003; 31*:*1365-71.
[37] Reid, S. A., and Boyde, A. Changes in the mineral density distribution in human bone with age: image analysis using backscattered electrons in the SEM. J Bone Miner Res 1987; 2*:*13-22.
[38] Garn, S. The earlier gain and the later loss of cortical bone. Springfield, IL: Charles C Thomas; 1970.

[39] Sumner, D. R., and Andriacchi, T. P. Adaptation to differential loading: comparison of growth-related changes in cross-sectional properties of the human femur and humerus. Bone 1996; 19*:*121-6.
[40] Moro, M., van der Meulen, M. C., Kiratli, B. J., Marcus, R., Bachrach, L. K., and Carter, D. R. Body mass is the primary determinant of midfemoral bone acquisition during adolescent growth. Bone 1996; 19*:*519-26.
[41] Ruff, C. Growth in bone strength, body size, and muscle size in a juvenile longitudinal sample. Bone 2003; 33*:*317-29.
[42] Forwood, M. R., Bailey, D. A., Beck, T. J., Mirwald, R. L., Baxter-Jones, A. D., and Uusi-Rasi, K. Sexual dimorphism of the femoral neck during the adolescent growth spurt: a structural analysis. Bone 2004; 35*:*973-81.
[43] Frost, H. M. Bone "mass" and the "mechanostat": a proposal. Anat Rec 1987; 219*:*1-9.
[44] Ferretti, J. L., Capozza, R. F., Mondelo, N., and Zanchetta, J. R. Interrelationships between densitometric, geometric, and mechanical properties of rat femora: inferences concerning mechanical regulation of bone modeling. J Bone Miner Res 1993; 8*:*1389-96.
[45] Currey, J. D. Mechanical properties of bone tissues with greatly differing functions. J Biomech 1979; 12*:*313-9.
[46] Jepsen, K. J., Pennington, D. E., Lee, Y. L., Warman, M., and Nadeau, J. Bone brittleness varies with genetic background in A/J and C57BL/6J inbred mice. J Bone Miner Res 2001; 16*:*1854-62.
[47] Tommasini, S. M., Morgan, T. G., van der Meulen, M., and Jepsen, K. J. Genetic variation in structure-function relationships for the inbred mouse lumbar vertebral body. J Bone Miner Res 2005; 20*:*817-27.
[48] Price, C. P., Herman, B. C., Lufkin, T., Goldman, H. M., and Jepsen, K. J. Genetic variation in bone growth patterns defines adult mouse bone fragility. J Bone Miner Res 2005; 20*:*1983-91.
[49] Swartz, S. M., Bennett, M. B., and Carrier, D. R. Wing bone stresses in free flying bats and the evolution of skeletal design for flight. Nature 1992; 359*:*726-9.
[50] Carrier, D., Leon, LR Skeletal growth and function in the California gull (Larus californicus). J Zool, London 1990; 222*:*375-389.
[51] Brear, K., Currey, JD, Pond, CM Ontogenetic changes in the mechanical properties of the femur of the polar bear Ursus maritimus. J Zool, London 1990; 222*:*49-58.
[52] Currey, J. D. Effects of differences in mineralization on the mechanical properties of bone. Philos Trans R Soc Lond B Biol Sci 1984; 304*:*509-18.
[53] Turner, C. H. Biomechanics of bone: determinants of skeletal fragility and bone quality. Osteoporos Int 2002; 13*:*97-104.
[54] Geusens, P., Cantatore, F., Nijs, J., Proesmans, W., Emma, F., and Dequeker, J. Heterogeneity of growth of bone in children at the spine, radius and total skeleton. Growth Dev Aging 1991; 55*:*249-56.
[55] Looker, A. C., Beck, T. J., and Orwoll, E. S. Does body size account for gender differences in femur bone density and geometry? J Bone Miner Res 2001; 16*:*1291-9.
[56] Nieves, J. W., Formica, C., Ruffing, J., Zion, M., Garrett, P., Lindsay, R., and Cosman, F. Males have larger skeletal size and bone mass than females, despite comparable body size. J Bone Miner Res 2005; 20*:*529-35.

[57] Friedl, K. E., Nuovo, J. A., Patience, T. H., and Dettori, J. R. Factors associated with stress fracture in young army women: indications for further research. Mil Med 1992; 157:334-8.
[58] Beck, T. J., Ruff, C. B., Mourtada, F. A., Shaffer, R. A., Maxwell-Williams, K., Kao, G. L., Sartoris, D. J., and Brodine, S. Dual-energy X-ray absorptiometry derived structural geometry for stress fracture prediction in male U.S. Marine Corps recruits. J Bone Miner Res 1996; 11:645-53.
[59] Taaffe, D. R., Snow-Harter, C., Connolly, D. A., Robinson, T. L., Brown, M. D., and Marcus, R. Differential effects of swimming versus weight-bearing activity on bone mineral status of eumenorrheic athletes. J Bone Miner Res 1995; 10:586-93.
[60] Petit, M. A., Beck, T. J., Shults, J., Zemel, B. S., Foster, B. J., and Leonard, M. B. Proximal femur bone geometry is appropriately adapted to lean mass in overweight children and adolescents. Bone 2005; 36:568-76.
[61] Johnson, L., Stradford, HT, Geis, RW, Dineen, JR Histogenesis of stress fractures. J Bone Joint Surg Am 1963; 45:1542.
[62] Burr, D. B., Milgrom, C., Boyd, R. D., Higgins, W. L., Robin, G., and Radin, E. L. Experimental stress fractures of the tibia. Biological and mechanical aetiology in rabbits. J Bone Joint Surg Br 1990; 72:370-5.
[63] Martin, R. Mathematical model for repair of fatigue damage and stress fracture in osteonal bone. J Orthop Res 1995; 13:309-316.
[64] Lanyon, L., and Skerry, T. Postmenopausal osteoporosis as a failure of bone's adaptation to functional loading: a hypothesis. J Bone Miner Res 2001; 16:1937-47.
[65] Milgrom, C., Simkin, A., Eldad, A., Nyska, M., and Finestone, A. Using bone's adaptation ability to lower the incidence of stress fractures. Am J Sports Med 2000; 28:245-51.
[66] Warden, S. J., Hurst, J. A., Sanders, M. S., Turner, C. H., Burr, D. B., and Li, J. Bone adaptation to a mechanical loading program significantly increases skeletal fatigue resistance. J Bone Miner Res 2005; 20:809-16.

Table 1. Monotonic mechanical properties for young-adult females and males. Data were age-adjusted and shown as mean ± standard deviation.

MECHANICAL PROPERTY	FEMALE	MALE	p-value
Modulus, GPa	17.5 ± 1.8	17.1 ± 1.7	0.5
Yield Strain	0.008 ± 0.0004	0.008 ± 0.0003	0.7
Yield Stress, MPa	106.2 ± 10.0	104.4 ± 7.8	0.6
Post-yield Strain	0.023 ± 0.006	0.025 ± 0.005	0.3
Failure Strain	0.031 ± 0.006	0.033 ± 0.005	0.3
Strength, MPa	133.8 ± 8.4	130.1 ± 4.2	0.2
Energy-to-Failure, MPa	3.1 ± 0.7	3.2 ± 0.7	0.3

Table 2. Comparison of total damage accumulation parameters for female and male cortical bone. Data were age-adjusted and shown as mean ± standard deviation.

DAMAGE PARAMETER	FEMALE	MALE	p-value
Stiffness Degradation	0.18 ± 0.04	0.17 ± 0.03	0.6
Relaxation Degradation	1.89 ± 0.08	1.91 ± 0.12	0.6

Table 3. Diaphyseal cross-sectional morphology for female and male tibiae. Data were calculated over 30-70% of the total tibial length and shown as mean ± standard deviation.

MORPHOLOGICAL TRAIT	FEMALE	MALE	p-value
TIBIA LENGTH, mm	33.9 ± 2.8	38.1 ± 1.9	0.0001
$WIDTH_{AP}$, mm	26.5 ± 2.7	31.2 ± 2.5	0.0001
$WIDTH_{ML}$, mm	20.8 ± 2.4	24.3 ± 2.3	0.0001
CtAr, mm^2	249 ± 40	356 ± 55	0.0001
J, mm^4	24776 ± 7917	51640 ± 15886	0.0001
J / r_{AP}, m^3	1836 ± 473	3279 ± 819	0.0001
J / r_{ML}, m^3	2352 ± 613	4188 ± 907	0.0001
J / L, m^3	722 ± 194	1352 ± 405	0.0001
J / A, m^2	97.1 ± 18.5	142.7 ± 24.9	0.0001
S_{AP}, $1/mm^2/kg$	14.1 ± 4.1	9.9 ± 2.0	0.002
S_{ML}, $1/mm^2/kg$	11.1 ± 3.6	7.7 ± 1.5	0.004

Table 4. Correlation matrix between morphological traits and tissue-level mechanical properties. Combined male and female data sets. First row = Pearson correlation coefficient. Second row = p-value. Damage = Stiffness degradation.

	MODULUS	STRENGTH	PY STRAIN	ENERGY	DAMAGE
$WIDTH_{AP}$	-0.13 (0.5)	-0.15 (0.4)	**0.35** **(0.05)**	0.34 (0.06)	-0.12 (0.5)
$WIDTH_{ML}$	-0.13 (0.5)	-0.17 (0.4)	0.29 (0.12)	0.28 (0.13)	-0.03 (0.8)
CtAr	-0.25 (0.2)	-0.18 (0.3)	0.31 (0.09)	0.30 (0.1)	-0.24 (0.2)
J	-0.33 (0.07)	-0.25 (0.2)	0.27 (0.14)	0.24 (0.2)	-0.24 (0.2)
J / L	**-0.35** **(0.05)**	-0.26 (0.2)	0.26 (0.2)	0.22 (0.2)	-0.26 (0.2)
J / $Width_{AP}$	**-0.36** **(0.04)**	-0.25 (0.2)	0.22 (0.2)	0.18 (0.3)	-0.27 (0.1)
J / $Width_{ML}$	**-0.36** **(0.05)**	-0.26 (0.2)	0.24 (0.2)	0.20 (0.3)	-0.30 (0.1)
S_{AP}	0.25 (0.2)	-0.05 (0.8)	-0.10 (0.6)	-0.09 (0.7)	**0.43** **(0.02)**
S_{ML}	0.27 (0.1)	-0.04 (0.8)	-0.13 (0.56)	-0.11 (0.6)	**0.44** **(0.01)**

Figure 1. Females show an age-related change in tissue-level properties that is similar to males. (A) modulus, (B) strength, (C) energy-to-failure, and (D) damageability

Figure 2. Changes in stiffness and relaxation for males and females. A plot of (A) stiffness degradation, D_{STIFF} and (B) relaxation degradation, D_{RELAX}, for each diagnostic cycle in the damage-accumulation protocol. Females and males show similar curves. Data were not age-corrected.

Figure 3. Variation in the section modulus (J / $Width_{AP}$) versus body size (body weight x tibial length) for adult female and male tibiae.

Figure 4. Variation in mechanical properties as a function of diaphyseal cross-sectional morphology. Solid lines represent the regression for the combined female and male datasets. Dashed lines represent the regressions for males and females separately.

FIGURE 1.

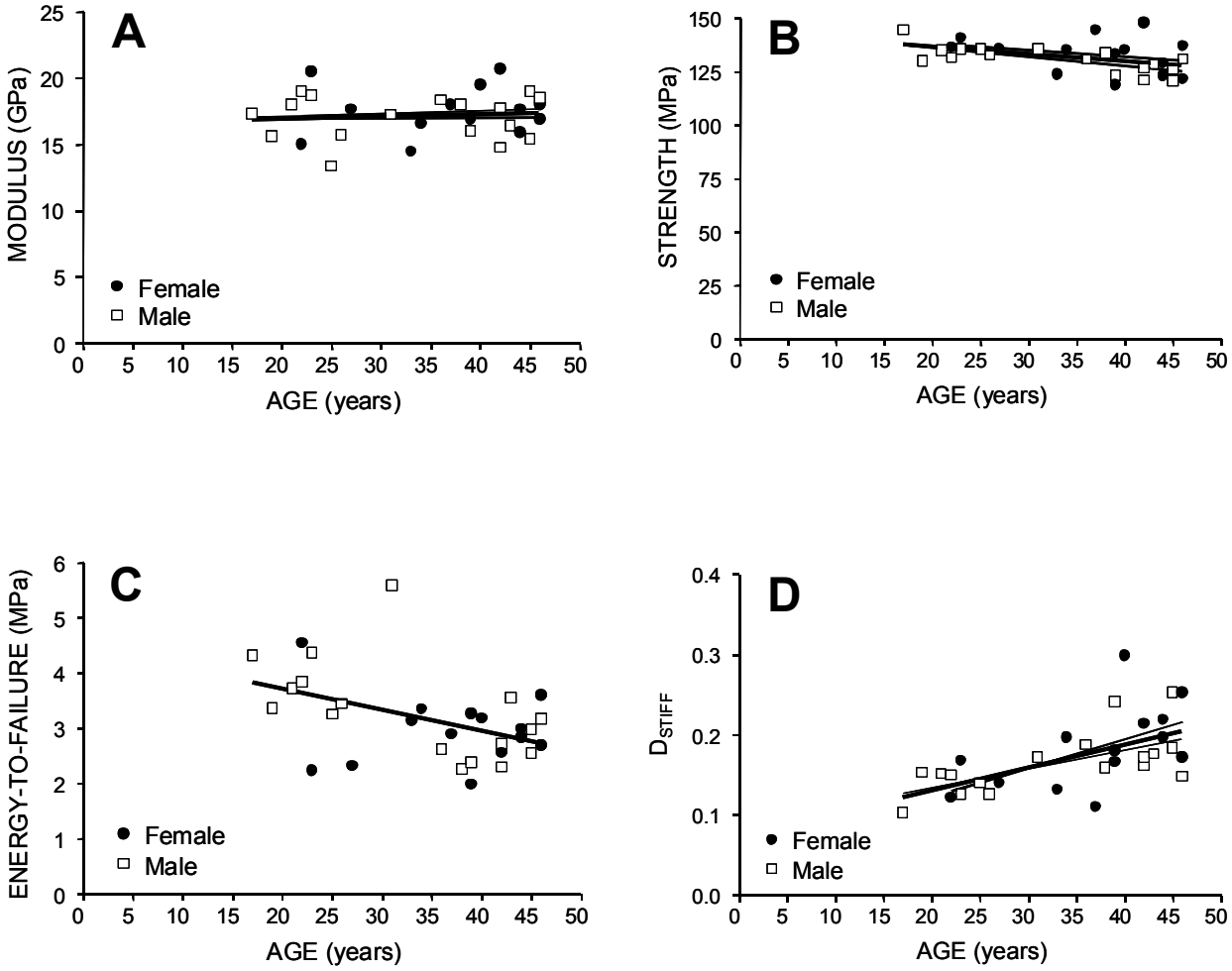
A
MODULUS (GPa)
AGE (years)
Female
Male
B
STRENGTH (MPa)
AGE (years)
Female
Male
C
ENERGY-TO-FAILURE (MPa)
AGE (years)
Female
Male
D
D_{STIFF}
AGE (years)
Female
Male

FIGURE 2.

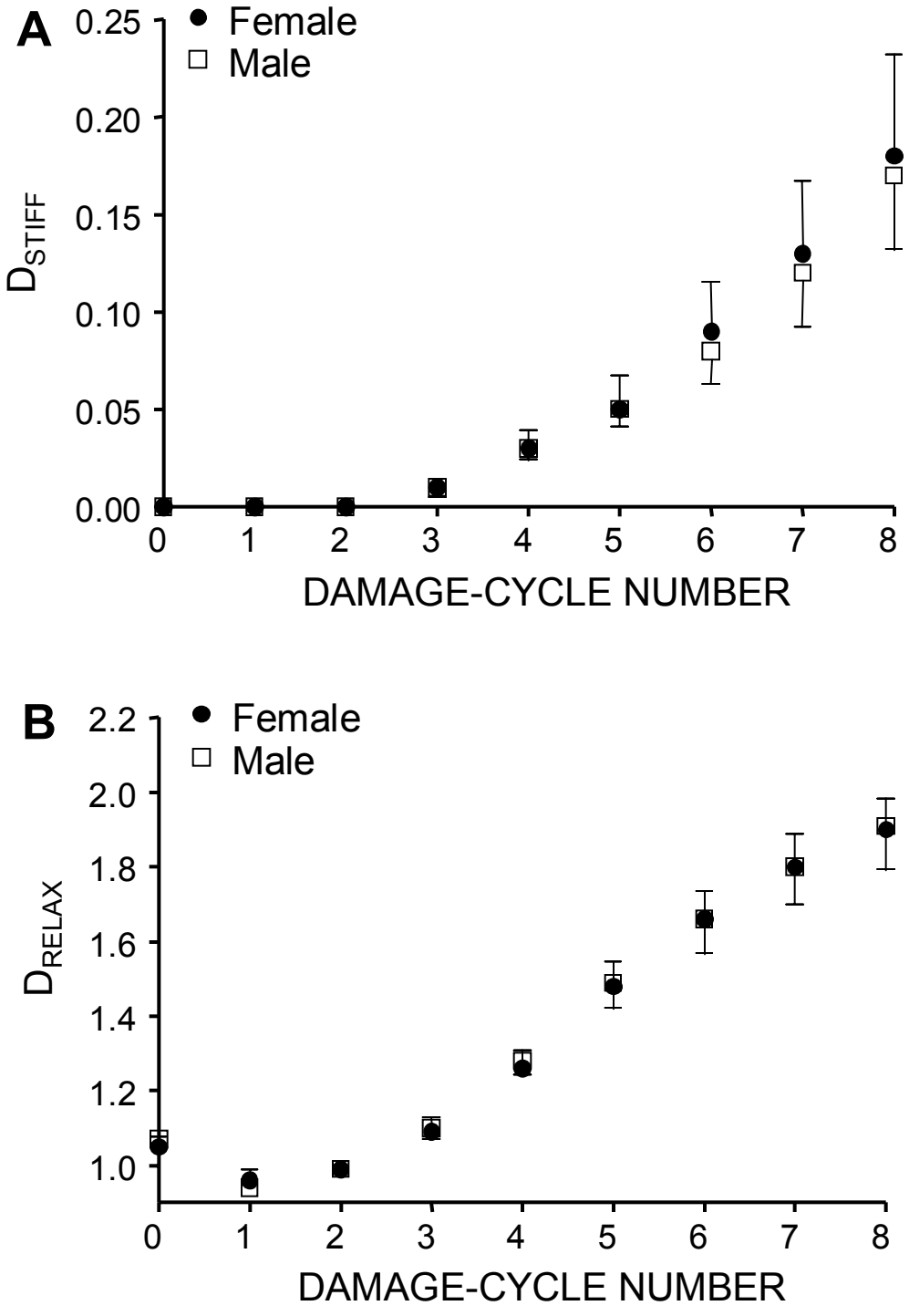
A
Female
Male
0.25
0.20
0.15
0.10
0.05
0.00
D_{STIFF}
0
1
2
3
4
5
6
7
8
DAMAGE-CYCLE NUMBER
B
Female
Male
2.2
2.0
1.8
1.6
1.4
1.2
1.0
D_{RELAX}
0
1
2
3
4
5
6
7
8
DAMAGE-CYCLE NUMBER

FIGURE 3.

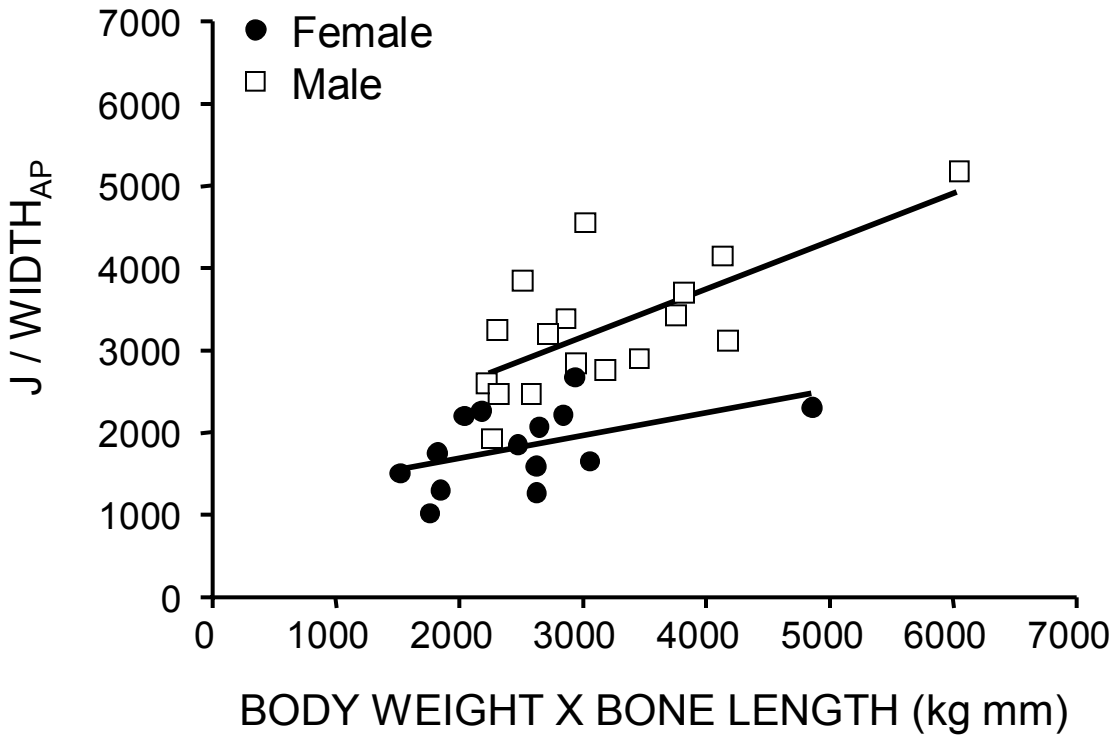
Female
Male
7000
6000
5000
4000
3000
2000
1000
0
J / WIDTH$_{AP}$
0
1000
2000
3000
4000
5000
6000
7000
BODY WEIGHT X BONE LENGTH (kg mm)

FIGURE 4.

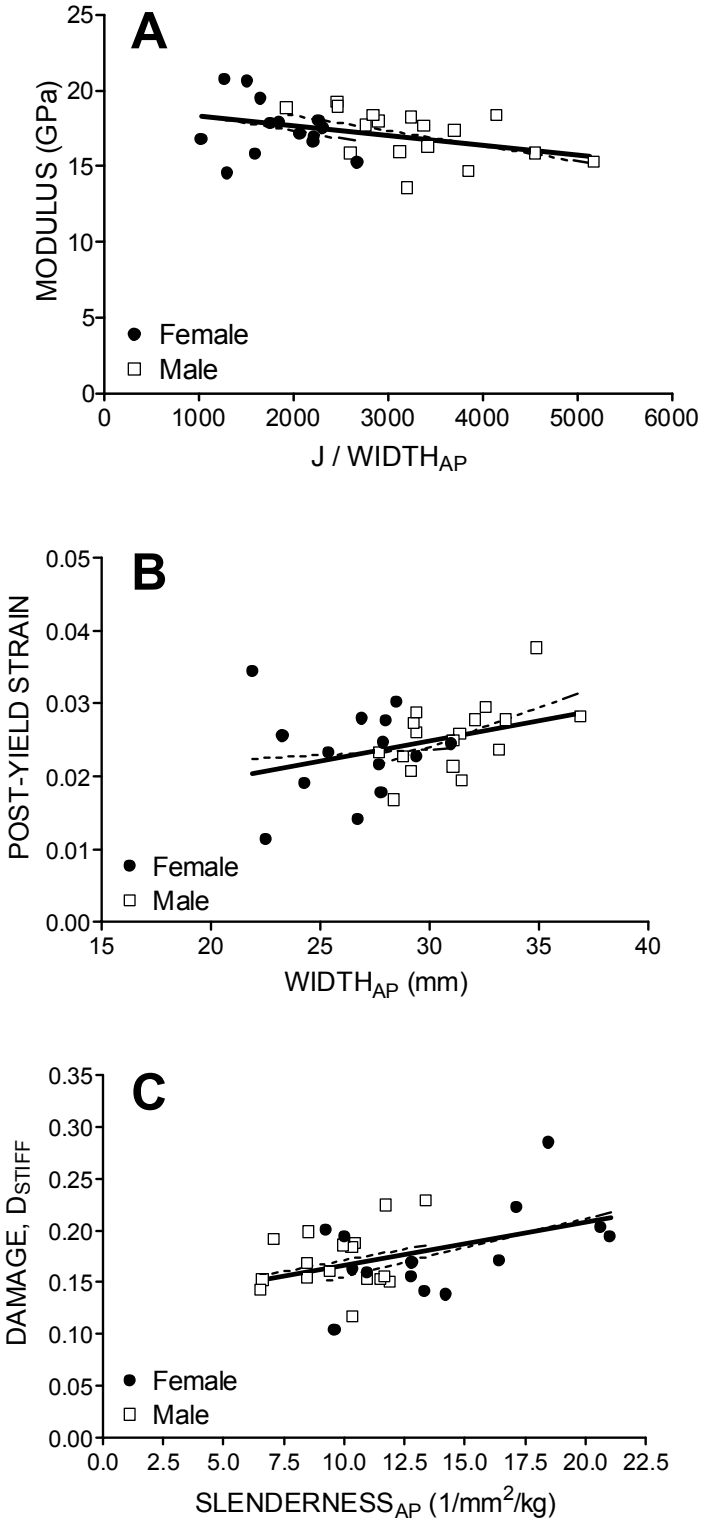
A
MODULUS (GPa)
J / WIDTH$_{AP}$
Female
Male
B
POST-YIELD STRAIN
WIDTH$_{AP}$ (mm)
Female
Male
C
DAMAGE, D$_{STIFF}$
SLENDERNESS$_{AP}$ (1/mm^2/kg)
Female
Male

OF MICE, MEN, AND WOMEN: THE RELATIONSHIP BETWEEN BONE MORPHOLOGY AND TISSUE QUALITY

*Tommasini, S M; **Nasser, P; **Hu, B; **Schaffler, M B; +**Jepsen, K J
*New York Center for Biomedical Engineering, The City College of New York/CUNY, New York, NY, USA. +**Leni & Peter W. May Department of Orthopaedics, Mount Sinai School of Medicine, New York, NY, USA
karl.jepsen@mssm.edu

INTRODUCTION: Currently, having a narrow tibia relative to body mass is one of the best predictors of stress fracture risk and fragility fractures [1]. However, the reasons are not fully understood.

Studies of bone morphology and bone quality in genetically distinct inbred mouse strains revealed mice with slender bones had increased mineral content compared to mice with more robust bones suggesting that bone morphology and quality might be biologically coupled to satisfy mechanical demands imposed by weight bearing [2]. A more strongly coordinated relationship among morphological traits, tissue-quality, and mechanical function has also been observed previously across a large range of bones from many species including bats, gulls, and polar bears [3]. Although increased mineral content may compensate for smaller morphology by increasing tissue stiffness and strength, this mineral has the adverse effect of increased bone brittleness and tissue damageability under fatigue loading. We postulate that a similar relationship between bone morphology and quality previously demonstrated in a mouse model also exists in the human skeleton. To test this hypothesis, we quantified cross-sectional morphology, tissue-level mechanical properties, tissue microstructure, and tissue composition from the tibiae of young, adult males and females. We also tested for correlations among these traits.

METHODS: Cross-sectional morphology and bone slenderness of tibiae from 14 female donors (age 22-46 yrs) and 17 male donors (age 17-46 yrs) were obtained [4,5]. Mechanical properties were measured from 8 cortical bone samples (2.5mm x 5mm x 55mm) machined from the diaphysis of each bone and split into 2 tests groups [4,5]. First, monotonic failure properties were assessed by loading to failure in 4-point bending. Mechanical properties measured were modulus (E), strength, work, and post-yield strain (PYε) as a measure of brittleness. Second, tissue damageability was assessed using a fifteen-cycle damage accumulation protocol in 4-point bending as described previously [4,5].

The density, ash content, and water content were determined for each sample retrieved from the monotonic tests. Specimen volume was determined using Archimedes' principal. Submerged weight, hydrated weight, dry weight, and ash weights were measured. To test for variation in matrix organization in males and females, bone microstructure was assessed for each sample retrieved from the damageability tests. For each specimen, digital images of three transverse sections, 100μm in thickness, were taken at 10X, stitched together, and traced using a Tablet monitor (WACOM). Parameters measured include porosity and the area fractions of osteonal, interstitial (remodeled), and circumferential lamellar (unremodeled) tissues. Both vascular canals and resorption spaces were counted as pores. Osteonal tissue was defined as a lamellar region with a Haversian canal completely surrounded by a cement line. Data from individual test samples were averaged for each donor.

To determine if males and females show a similar relationship between tibia cross-sectional morphology, bone microstructure, and tissue-level mechanical properties, linear regressions were performed while taking age into consideration and slopes and intercepts between male and female regressions were compared (ANCOVA).

RESULTS: Since no differences were found between male and female regressions, combined male and female datasets were used to compare tissue-level mechanical properties, cross-sectional morphology, composition, and bone microstructure. The only significant correlations between compositional or architectural traits and tissue-level mechanical properties were observed between ash content and tissue modulus ($p < 0.003$), strength ($p < 0.02$), and post-yield strain ($p < 0.01$; Fig. 1A). Measures of bone size (total cross-sectional area, cortical area, ML and AP width, cross-sectional polar moment of inertia) were negatively correlated with ash content ($p < 0.02$). Bone slenderness (polar moment of inertia normalized for width and polar moment of inertia normalized for tibia length) was also negatively correlated with ash content ($p < 0.02$; Fig. 1B). Bone size and slenderness were positively correlated with the area fraction of remodeled tissue ($p < 0.05$). Thus, wider (more robust) tibiae had lower mineral content and increased amount of remodeled tissue and narrow (more slender) tibiae had increased mineral content and decreased amount of remodeled tissue.

Figure 1: Correlation between ash content and (A) post-yield strain, PYε and (B) polar moment of inertia, J, normalized for tibia length, L.

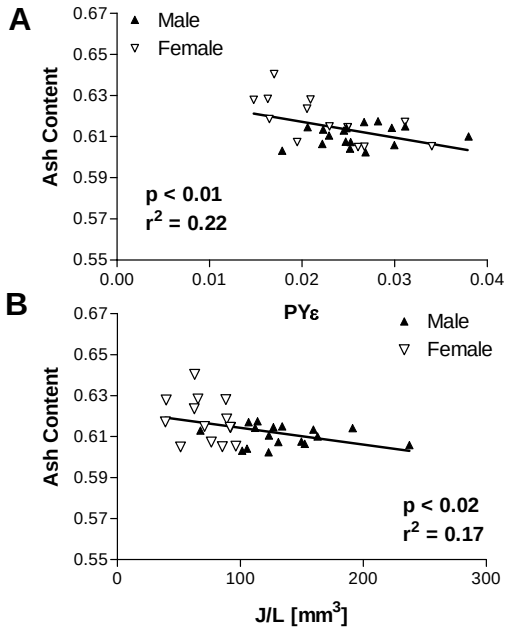

DISCUSSION: The current study confirmed that, similar to inbred mice, the tibia diaphyses of young, adult females and males show a reciprocal relationship between bone morphology and tissue quality, as hypothesized. Tissue from more slender bones (narrow relative to tibia length) was composed of material having higher mineral content and, consequently, increased tissue stiffness and strength, but reduced ductility. Unlike the mouse model, this relationship was subtle and only observed when combining male and female datasets to expand the range of data. The current study revealed a general biological phenomenon that has only been observed previously by looking across a large range of bones from many species. Here, bone from the same species with similar function showed that more slender morphology might be compensated by increased ash content. Although this coupling appears advantageous for ensuring that an adequate whole bone stiffness is achieved for day-to-day activity, the disadvantage is that the tissue-quality factors that tend to make bone stiff also tend to make bone less ductile, less tough, and more damageable.

This is an intriguing finding because, despite dimorphic growth patterns, males and females have similar tissue-level mechanical properties. Thus, both sexes may share a common underlying biological (adaptive) mechanism. This data suggest that osteoblasts and osteoclasts are capable of not only adapting bone morphology, but also modulating tissue-level mechanical properties so that the combination of traits satisfies mechanical demands [2,3]. Therefore, the phenomenon that slender bones are constructed differently with material level variation that ultimately leads to more damageable material than larger bones may help explain why individuals with more slender bones are at increased risk of stress fractures early in life and fragility fractures later in life.

REFERENCES: [1] Beck, *Bone*, 2000 [2] Jepsen, *JBMR*, 2001 [3] Currey, *J Biomech*, 1979 [4] Tommasini, *ASBMR*, 2006 [5] Tommasini, *JBMR*, 2005.

ACKNOWLEDGEMENTS: Department of Defense (DAMD17-01-1-0806), Musculoskeletal Transplant Foundation, and National Disease Research Interchange.